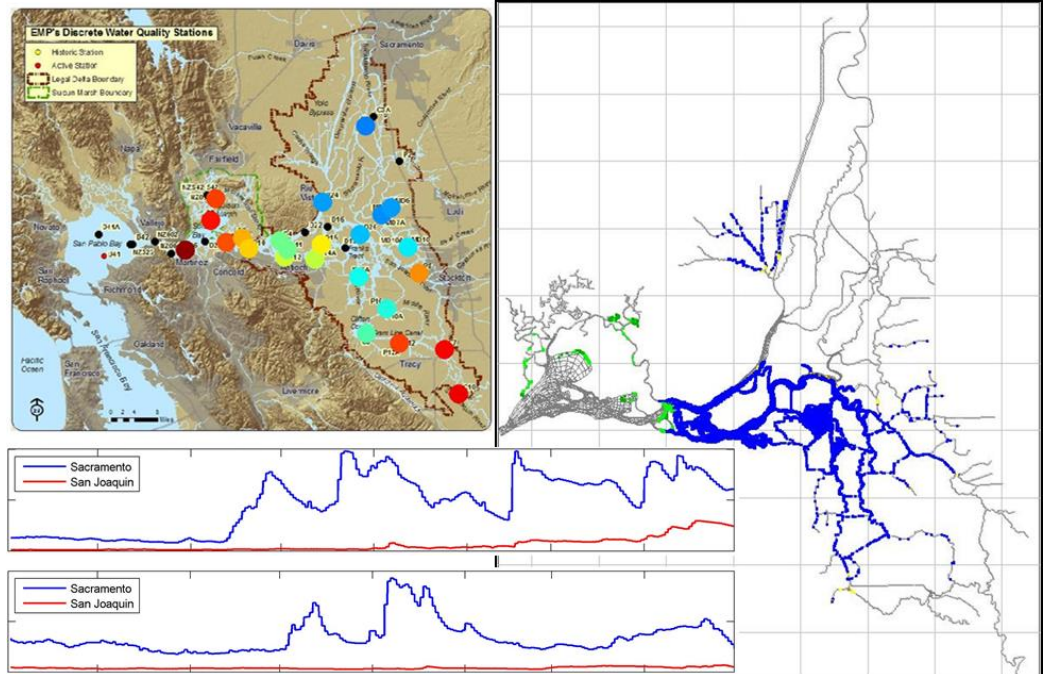


HISTORICAL VALIDATION OF ADULT DELTA SMELT BEHAVIORAL MODEL FOR WATER YEARS 1981, 1982, AND 1988

APRIL 2013



Prepared For:
Metropolitan Water District of Southern California
1121 L Street, Suite 900
Sacramento, CA 95814
Contact:
Dr. Paul Hutton
Authorized Technical Representative
916-650-2620

Prepared By:
Resource Management Associates
4171 Suisun Valley Road, Suite J
Fairfield, CA 94534
Contact:
John DeGeorge
707-864-2950

Executive Summary

The RMA delta smelt model is a predictive model simulating the upstream spawning migration of the delta smelt population in the Sacramento-San Joaquin Delta. It was originally developed to help track and predict movements of the endangered fish species in order to inform management decisions and prevent migrating smelt from becoming entrained into pumping facilities in the south Delta.

The smelt model is based on the more general RMA particle tracking model, which simulates the movement and dispersion of aquatic particles in response to ambient water currents. The smelt model includes modifications that allow these particles to exhibit certain behaviors, such as riding tidal currents, hiding, or exploring their local habitat, in response to lateral gradients in salinity and turbidity. The delta smelt behavioral model is the final step in a process that involves three prior simulations of the Delta: a hydrodynamic simulation, a salinity simulation, and a turbidity simulation. In the event that flows, salinity, or turbidities for major tributaries entering the Delta are unknown¹, a fourth model, simulating the Central Valley watershed as a whole, must also be run.

The RMA delta smelt model has previously been calibrated and validated on delta smelt salvage data collected at the southern export locations for years post-2003 (RMA 2011b). While the model predicted observed salvage patterns reasonably well, delta smelt populations during these years were only a small percentage (<5%) of their sizes during the 1980s and 1990s. Salvage patterns were also much less variable. In order to test the model over a wider range of conditions and with more significant observed data, the model was used to simulate historic water years 1981, 1982, and 1988. These specific years were chosen because each of them had unique conditions intended to test the robustness of the model. Water year 1981 (WY1981) was the highest salvage year on record, with salvage events occurring consistently throughout the fall and winter. Water year 1982 had a large turbidity pulse move through the system in the early fall, and then had sustained high flows throughout the winter. Water year 1988 experienced a large turbidity pulse from the Sacramento in December during which the Delta Cross Channel (DCC) was atypically left open.

Hydrodynamic simulations were performed for these three years using boundary conditions provided by the California Department of Water Resources (DWR) Delta Modeling Section and the US Geological Survey (USGS), along with records of historical gate and barrier operations. The model grid was created using the current Delta bathymetry, with levee sections added around Liberty Island for all runs and around Mildred Island for the 1981 and 1982 runs to represent the historical unbreached state of the islands during these earlier years. Salinity simulations were performed using the results of the hydrodynamic runs and salinity boundary conditions provided by DWR.

The delta smelt behavioral model is most sensitive to the simulated turbidity field generated by the turbidity model. This was problematic for the simulation of these historical water years for three main reasons: [1] Data from the continuous USGS turbidity monitoring stations in operation today were not available during the 1980s. While daily suspended sediment concentrations were available at the main

¹ For example, when simulating unknown future conditions or past conditions where no observed data is available.

Sacramento and San Joaquin boundary locations, these needed to be converted to turbidity using a statistical regression, and it was necessary for a calibrated watershed model to be relied upon for smaller tributary turbidity inputs. The only turbidity data available for the interior of the Delta, necessary to test the accuracy of the predictions, were point measurements taken by the California Department of Fish and Wildlife Fall Midwater Trawl (FMWT) survey and the DWR Environmental Monitoring Program (EMP). These programs sample on a monthly to bimonthly basis. [2] The RMA turbidity model utilizes decay coefficients that have been calibrated to obtain the highest model accuracy during high net Delta flows. This is usually the time of peak smelt salvage at the export locations. However, during water years 1981 and 1982 there were significant numbers of smelt salvaged during the low-flow fall period as well as during the high-flow winter period. [3] The modeling of turbidity itself is intrinsically difficult, since turbidity is not a quantity that follows strict conservation laws. Instead, it is a measure of light scattered in the backward direction as a result of suspended sediment in a water sample. It can change based on the particle size distribution as well as the material composition of the particles. While the turbidity of the water is more directly relatable to conditions experienced by migrating smelt, the physical processes leading to local changes in turbidity (for example, sediment settling, resuspension, or flocculation) are lumped together into a single decay coefficient in the turbidity model. This leads to significant model uncertainty in certain areas; for example, in large shallow areas where wind resuspension is responsible for increased turbidity. These areas are important to smelt movement through the west and central Delta areas during times of low flow, and internal turbidity boundary conditions were added at Mallard Island and Jersey Point to account for the missing resuspension.

Two sets of model runs were performed in this validation study. The first utilized the original coefficients for turbidity and smelt movement that were calibrated during high net Delta flows. The purpose of these runs was to validate the existing model with the existing model parameters. Once it became apparent that the existing high-flow calibrated model parameters were not sufficient to capture smelt movement during low-flow periods, an additional set of runs was performed in order to assess the range of applicability of the model. In these runs, turbidity model decay coefficients were allowed to vary on a monthly interval. During low flow months, a low turbidity decay coefficient was used; in high-flow months, a higher coefficient was used.

The delta smelt behavioral model was run using the results of the hydrodynamic, salinity, and turbidity models. Fifty-thousand simulated particles were released in the Suisun Bay region in early September and tracked throughout the year. Particle entrainment at the southern export locations was tracked in order to compare with historical smelt salvage records at the export facilities.

Despite the many uncertainties associated with modeling the historic turbidity fields, the smelt model with the updated model coefficients performed well in simulating observed salvage patterns for two of the three water years. Model runs using the original calibration coefficients performed well in only one of the three years. WY1988, where two well-defined winter storm pulses punctuated an otherwise dry year, was simulated with the highest accuracy. Simulated smelt salvage matched observed both in timing and relative magnitude. WY1982 was also simulated with a reasonable degree of accuracy. The periodic storms throughout January–March caused episodic smelt salvage events that were replicated

by the model. The timing of the first flush in November was also captured by one simulation. Salvage patterns in WY1981 were not simulated well by the model. Large observed fall salvage did not appear to be correlated with increases in either observed or modeled turbidity through the southern central delta. This suggests salvage data quality may be a concern or one of the hypotheses of the smelt behavioral model may need to be re-evaluated. A large salvage event occurring in January 1981, immediately prior to the first large storm pulse of the season, was also not simulated accurately. Similar to the fall salvage, this event was also uncorrelated with increases in turbidity through the southern central Delta.

Table of Contents

Executive Summary.....	ii
Table of Figures.....	vii
Objectives	1
Background	1
Adult Delta Smelt Life History.....	1
Project History	2
Water Year Information.....	3
Observed Data Sources.....	8
Environmental Monitoring Program.....	8
Fall Midwater Trawl	8
Southern Export Fish Collection Facilities'	8
Methods.....	12
RMA2 Hydrodynamic Model.....	12
RMA11 Electrical Conductivity and Turbidity Models	13
RMAPTRK Smelt Behavioral Model.....	15
Results and Discussion.....	32
Water Year 1981	33
High-Flow Calibrated Smelt and Turbidity Model Summary Results.....	35
High-Flow Calibrated Model EMP Comparison Plots.....	36
Fall Midwater Trawl Observed Smelt Distributions	40
Original Model Calibration RMA PTRK Modeled Smelt Distributions.....	43
Time Variable Decay Coefficient Smelt and Turbidity Model Summary Results	47
Time Variable Decay Coefficient Model EMP Comparison Plots	48
Time Variable Turbidity Decay Coefficient RMA PTRK Modeled Smelt Distributions	52
Water Year 1982	56
High-Flow Calibrated Smelt and Turbidity Model Summary Results.....	57
High-Flow Calibrated Model EMP Comparison Plots.....	58
FMWT Smelt Distributions	62
Original Model Calibration RMA PTRK Modeled Smelt Distributions.....	64
Time Variable Decay Coefficient Smelt and Turbidity Model Summary Results	67
Time Variable Decay Coefficient Model EMP Turbidity Comparison Plots.....	68

Time Variable Turbidity Decay RMA PTRK Modeled Smelt Distributions.....	72
Water Year 1988	75
High-Flow Calibrated Smelt and Turbidity Model Summary Results.....	76
High-Flow Calibrated Model EMP Comparison Plots.....	77
FMWT Smelt Distributions.....	81
Original Model Calibration RMA PTRK Modeled Smelt Distributions.....	83
Time Variable Decay Coefficient Smelt and Turbidity Model Summary Results	86
Time Variable Decay Coefficient Model EMP Turbidity Comparison Plots.....	87
Time Variable Turbidity Decay RMA PTRK Modeled Smelt Distributions.....	91
Conclusions	94
References	95

Table of Figures

Figure 1 Trends in delta smelt population abundance. Abundance is estimated using catch data collected from the FMWT. Declines in abundance associated with the Pelagic Organism Decline are visible in the post-2001 data.	2
Figure 2 Hydrologic, management, and salvage conditions for the Delta for WY1981. Panel A shows Sacramento River flow at Freeport and San Joaquin River flow at Vernalis. Panel B shows average flow through the Old and Middle River corridors. Negative values indicate net flow from north to south. Panel C shows timing of the DCC closure and head of Old River installation (not installed during this period). Panel D shows inflowing SSC for the Sacramento River at Freeport and the San Joaquin River at Vernalis. Panel E shows total number of delta smelt salvaged at the SWP and CVP export locations.	5
Figure 3 Hydrologic, management, and salvage conditions for the Delta for WY1982. See Figure 2 for descriptions of individual panels.	6
Figure 4 Hydrologic, management, and salvage conditions for the Delta for WY1988. See Figure 2 for descriptions of individual panels.	7
Figure 5 Location of EMP water quality sampling stations. Image obtained from EMP website.	9
Figure 6 FMWT sampling station locations. Image obtained from the CA DFW website.	10
Figure 7 Southern Delta export fish salvage facility locations. Image obtained from the CA DFW website.	10
Figure 8 RMA model grid showing major boundary condition and gate/barrier locations. Yellow points show DICU locations.	17
Figure 9 Hydrodynamic boundary conditions for WY1981. Major tributary inflows to the north, east, and south Delta are shown in the top 3 panels. The panel second from the bottom shows major export flow diversions in the south Delta. Bottom panel shows the prescribed water surface elevation at the downstream Martinez boundary.	18
Figure 10 Hydrodynamic boundary conditions for WY1982. Major tributary inflows to the north, east, and south Delta are shown in the top 3 panels. The panel second from the bottom shows major export flow diversions in the south Delta. Bottom panel shows the prescribed water surface elevation at the downstream Martinez boundary.	19
Figure 11 Hydrodynamic boundary conditions for WY1988. Major tributary inflows to the north, east, and south Delta are shown in the top 3 panels. The panel second from the bottom shows major export flow diversions in the south Delta. Bottom panel shows the prescribed water surface elevation at the downstream Martinez boundary.	20
Figure 12 WY1981 EC boundary conditions at the Sacramento River at Freeport and the San Joaquin River at Vernalis (top panel) and Martinez (bottom panel).	21
Figure 13 WY1982 EC boundary conditions at the Sacramento River at Freeport and the San Joaquin River at Vernalis (top panel) and Martinez (bottom panel).	22
Figure 14 WY1988 EC boundary conditions at the Sacramento River at Freeport and the San Joaquin River at Vernalis (top panel) and Martinez (bottom panel).	23
Figure 15 Turbidity decay coefficients calibrated for WY2007 and WY2010 high flow periods.	24
Figure 16 Measured turbidity (blue line) at Holland Cut in winter of WY2012. Large increases in turbidity are due to sediment resuspension occurring during large wind events. Elevated turbidities persist for	

several days following an event. The decay coefficient approach to modeling turbidity has difficulty accounting for these resuspension events and their subsequent effect on Delta turbidity. Figure from RMA (2012). 25

Figure 17 Relationship between USGS measured SSC at Freeport and EMP measured turbidity at Green's Landing. The least squares best fit regression was calculated as $Turbidity (NTU) = 0.201 * SSC + 2.1$ 26

Figure 18 Relationship between USGS measured SSC at Vernalis and EMP measured turbidity at Vernalis. The least squares best fit regression was calculated as $Turbidity (NTU) = 0.773 * SSC + 0.7$ 27

Figure 19 WY1981 turbidity boundary conditions. Sacramento and San Joaquin turbidities were obtained by a regression of USGS measured SSC with EMP measured turbidity values. Other tributary turbidities were generated using the WARMF watershed model..... 28

Figure 20 WY1982 turbidity boundary conditions. Sacramento and San Joaquin turbidities were obtained by a regression of USGS measured SSC with EMP measured turbidity values. Other tributary turbidities were generated using the WARMF watershed model..... 29

Figure 21 WY1988 turbidity boundary conditions. Sacramento and San Joaquin turbidities were obtained by a regression of USGS measured SSC with EMP measured turbidity values. Other tributary turbidities were generated using the WARMF watershed model..... 30

Figure 22 WY1981 modeled and observed turbidity and delta smelt salvage at the southern export locations. Original calibrated turbidity decay coefficients and smelt minimum turbidity thresholds were used. Top panel shows average modeled turbidity at the export locations along with EMP observed data. Middle panel shows RMA modeled smelt salvage (as a percent of total input particles). Bottom panel shows observed smelt salvage as number of fish divided by the water year FMWT index (a measure of the total smelt population size). 35

Figure 23 Turbidity distributions measured by the EMP (left panels) and modeled by RMA (right panels) for September (top panels) and October (bottom panels), WY1981. High-flow calibrated turbidity decay coefficients were used. 36

Figure 24 Turbidity distributions measured by the EMP (left panels) and modeled by RMA (right panels) for November (top panels) and December (bottom panels), WY1981. High-flow calibrated turbidity decay coefficients were used..... 37

Figure 25 Turbidity distributions measured by the EMP (left panels) and modeled by RMA (right panels) for January (top panels) and February (bottom panels), WY1981. Note differences in color scale between top and bottom panels. High-flow calibrated turbidity decay coefficients were used. 38

Figure 26 Turbidity distributions measured by the EMP (left panels) and modeled by RMA (right panels) for March (top panels) and April (bottom panels), WY1981. High-flow calibrated turbidity decay coefficients were used. 39

Figure 27 September and October 1980 FMWT ADS catch distributions. Dates indicate range of days catch was made over. 40

Figure 28 November and December 1980 FMWT ADS catch distributions. Dates indicate range of days catch was made over. 41

Figure 29 RMA PTRK behavioral color codes used in modeled smelt distribution figures..... 42

Figure 30 RMA PTRK modeled smelt distribution, November 1, 1980. For behavioral color codes, see Figure 29. Model results were driven using a smelt turbidity minimum threshold of 16 NTU and turbidity model results obtained with high-flow calibrated parameters. 43

Figure 31 RMA PTRK modeled smelt distribution, January 1, 1981. For behavioral color codes, see Figure 29. Model results were driven using a smelt turbidity minimum threshold of 16 NTU and turbidity model results obtained with high-flow calibrated parameters. 44

Figure 32 RMA PTRK modeled smelt distribution, February 1, 1981. For behavioral color codes, see Figure 29. Model results were driven using a smelt turbidity minimum threshold of 16 NTU and turbidity model results obtained with high-flow calibrated parameters. 45

Figure 33 RMA PTRK modeled smelt distribution, March 1, 1981. For behavioral color codes, see Figure 29. Model results were driven using a smelt turbidity minimum threshold of 16 NTU and turbidity model results obtained with high-flow calibrated parameters. 46

Figure 34 WY1981 modeled and observed turbidity and delta smelt salvage at the southern export locations. Time variable turbidity decay coefficients were used. Top panel shows average modeled turbidity at the export locations along with EMP observed data. Middle panel shows RMA modeled smelt salvage (as a percent of total input particles) using three different max turbidity threshold values. Bottom panel shows observed smelt salvage as number of fish divided by the water year FMWT index (a measure of the total smelt population size)..... 47

Figure 35 Turbidity distributions measured by the EMP (left panels) and modeled by RMA (right panels) for September (top panels) and October (bottom panels), WY1981. Time variable turbidity decay coefficients were used. 48

Figure 36 Turbidity distributions measured by the EMP (left panels) and modeled by RMA (right panels) for November (top panels) and December (bottom panels), WY1981. Time variable turbidity decay coefficients were used. 49

Figure 37 Turbidity distributions measured by the EMP (left panels) and modeled by RMA (right panels) for January (top panels) and February (bottom panels), WY1981. Note differences in color scale between top and bottom panels. Time variable turbidity decay coefficients were used. 50

Figure 38 Turbidity distributions measured by the EMP (left panels) and modeled by RMA (right panels) for March (top panels) and April (bottom panels), WY1981. Time variable turbidity decay coefficients were used..... 51

Figure 39 RMA PTRK modeled smelt distribution, November 1, 1980. For behavioral color codes, see Figure 29. Model results were driven using a smelt turbidity minimum threshold of 12 NTU and turbidity model results obtained with time variable decay coefficients. Similar distributions were produced using 10 and 14 NTU thresholds. 52

Figure 40 RMA PTRK modeled smelt distribution, January 1, 1981. For behavioral color codes, see Figure 29. Model results were driven using a smelt turbidity minimum threshold of 12 NTU and turbidity model results obtained with time variable decay coefficients. Similar distributions were produced using 10 and 14 NTU thresholds. 53

Figure 41 RMA PTRK modeled smelt distribution, February 1, 1981. For behavioral color codes, see Figure 29. Model results were driven using a smelt turbidity minimum threshold of 12 NTU and turbidity model results obtained with time variable decay coefficients. Similar distributions were produced using 10 and 14 NTU thresholds. 54

Figure 42 RMA PTRK modeled smelt distribution, March 1, 1981. For behavioral color codes, see Figure 29. Model results were driven using a smelt turbidity minimum threshold of 12 NTU and turbidity model

results obtained with time variable decay coefficients. Similar distributions were produced using 10 and 14 NTU thresholds. 55

Figure 43 WY1982 modeled and observed turbidity and delta smelt salvage at the southern export locations. Original calibrated turbidity decay coefficients and smelt minimum turbidity thresholds were used. Top panel shows average modeled turbidity at the export locations along with EMP observed data. Middle panel shows RMA modeled smelt salvage (as a percent of total input particles). Bottom panel shows observed smelt salvage as number of fish divided by the water year FMWT index (a measure of the total smelt population size). 57

Figure 44 Turbidity distributions measured by the EMP (left panels) and modeled by RMA (right panels) for September (top panels) and October (bottom panels), WY1982. High-flow calibrated turbidity decay coefficients were used. 58

Figure 45 Turbidity distributions measured by the EMP (left panels) and modeled by RMA (right panels) for November (top panels) and December (bottom panels), WY1982. High-flow calibrated turbidity decay coefficients were used. 59

Figure 46 Turbidity distributions measured by the EMP (left panels) and modeled by RMA (right panels) for January (top panels) and February (bottom panels), WY1982. High-flow calibrated turbidity decay coefficients were used. 60

Figure 47 Turbidity distributions measured by the EMP (left panels) and modeled by RMA (right panels) for March (top panels) and April (bottom panels), WY1982. High-flow calibrated turbidity decay coefficients were used. 61

Figure 48 September and October 1981 FMWT ADS catch distributions. Dates indicate range of days catch was made over. 62

Figure 49 November and December 1981 FMWT ADS catch distributions. Dates indicate range of days catch was made over. 63

Figure 50 RMA PTRK modeled smelt distribution, November 1, 1981. For behavioral color codes, see Figure 29. Model results were driven using a smelt turbidity minimum threshold of 16 NTU and turbidity model results obtained with high-flow calibrated parameters. 64

Figure 51 RMA PTRK modeled smelt distribution, January 1, 1982. For behavioral color codes, see Figure 29. Model results were driven using a smelt turbidity minimum threshold of 16 NTU and turbidity model results obtained with high-flow calibrated parameters. 65

Figure 52 RMA PTRK modeled smelt distribution, February 15, 1982. For behavioral color codes, see Figure 29. Model results were driven using a smelt turbidity minimum threshold of 16 NTU and turbidity model results obtained with high-flow calibrated parameters. 66

Figure 53 WY1982 modeled and observed turbidity and delta smelt salvage at the southern export locations. Time variable turbidity decay coefficients were used. Top panel shows average modeled turbidity at the export locations along with EMP observed data. Middle panel shows RMA modeled smelt salvage (as a percent of total input particles) using three different max turbidity threshold values. Bottom panel shows observed smelt salvage as number of fish divided by the water year FMWT index (a measure of the total smelt population size). 67

Figure 54 Turbidity distributions measured by the EMP (left panels) and modeled by RMA (right panels) for September (top panels) and October (bottom panels), WY1982. Time variable turbidity decay coefficients were used. 68

Figure 55 Turbidity distributions measured by the EMP (left panels) and modeled by RMA (right panels) for November (top panels) and December (bottom panels), WY1982. Time variable turbidity decay coefficients were used. 69

Figure 56 Turbidity distributions measured by the EMP (left panels) and modeled by RMA (right panels) for January (top panels) and February (bottom panels), WY1982. Time variable turbidity decay coefficients were used. 70

Figure 57 Turbidity distributions measured by the EMP (left panels) and modeled by RMA (right panels) for March (top panels) and April (bottom panels), WY1982. Time variable turbidity decay coefficients were used..... 71

Figure 58 RMA PTRK modeled smelt distribution, November 1, 1981. For behavioral color codes, see Figure 29. Model results were driven using a smelt turbidity minimum threshold of 12 NTU and turbidity model results obtained with time variable decay coefficients. Similar distributions were produced using 10 and 14 NTU thresholds. 72

Figure 59 RMA PTRK modeled smelt distribution, January 1, 1982. For behavioral color codes, see Figure 29. Model results were driven using a smelt turbidity minimum threshold of 12 NTU and turbidity model results obtained with time variable decay coefficients. Similar distributions were produced using 10 and 14 NTU thresholds. 73

Figure 60 RMA PTRK modeled smelt distribution, February 15, 1982. For behavioral color codes, see Figure 29. Model results were driven using a smelt turbidity minimum threshold of 12 NTU and turbidity model results obtained with time variable decay coefficients. Similar distributions were produced using 10 and 14 NTU thresholds. 74

Figure 61 WY1988 modeled and observed turbidity and delta smelt salvage at the southern export locations. Original calibrated turbidity decay coefficients and smelt minimum turbidity thresholds were used. Top panel shows average modeled turbidity at the export locations along with EMP observed data. Middle panel shows RMA modeled smelt salvage (as a percent of total input particles). Bottom panel shows observed smelt salvage as number of fish divided by the water year FMWT index (a measure of the total smelt population size)..... 76

Figure 62 Turbidity distributions measured by the EMP (left panels) and modeled by RMA (right panels) for September (top panels) and October (bottom panels), WY1988. High-flow calibrated turbidity decay coefficients were used. 77

Figure 63 Turbidity distributions measured by the EMP (left panels) and modeled by RMA (right panels) for November (top panels) and December (bottom panels), WY1988. High-flow calibrated turbidity decay coefficients were used..... 78

Figure 64 Turbidity distributions measured by the EMP (left panels) and modeled by RMA (right panels) for January (top panels) and February (bottom panels), WY1988. Note difference in color scales between top and bottom plots. High-flow calibrated turbidity decay coefficients were used..... 79

Figure 65 Turbidity distributions measured by the EMP (left panels) and modeled by RMA (right panels) for March (top panels) and April (bottom panels), WY1988. High-flow calibrated turbidity decay coefficients were used. 80

Figure 66 September and October 1987 FMWT ADS catch distributions. Dates indicate range of days catch was made over. 81

Figure 67 November and December 1987 FMWT ADS catch distributions. Dates indicate range of days catch was made over. 82

Figure 68 RMA PTRK modeled smelt distribution, November 1, 1987. For behavioral color codes, see Figure 29. Model results were driven using a smelt turbidity minimum threshold of 16 NTU and turbidity model results obtained with high-flow calibrated parameters. 83

Figure 69 RMA PTRK modeled smelt distribution, January 1, 1988. For behavioral color codes, see Figure 29. Model results were driven using a smelt turbidity minimum threshold of 16 NTU and turbidity model results obtained with high-flow calibrated parameters. 84

Figure 70 RMA PTRK modeled smelt distribution, March 1, 1988. For behavioral color codes, see Figure 29. Model results were driven using a smelt turbidity minimum threshold of 16 NTU and turbidity model results obtained with high-flow calibrated parameters. 85

Figure 71 WY1988 modeled and observed turbidity and delta smelt salvage at the southern export locations. Time variable turbidity decay coefficients were used. Top panel shows average modeled turbidity at the export locations along with EMP observed data. Middle panel shows RMA modeled smelt salvage (as a percent of total input particles) using three different max turbidity threshold values. Bottom panel shows observed smelt salvage as number of fish divided by the water year FMWT index (a measure of the total smelt population size)..... 86

Figure 72 Turbidity distributions measured by the EMP (left panels) and modeled by RMA (right panels) for September (top panels) and October (bottom panels), WY1988. Time variable turbidity decay coefficients were used. 87

Figure 73 Turbidity distributions measured by the EMP (left panels) and modeled by RMA (right panels) for November (top panels) and December (bottom panels), WY1988. Time variable turbidity decay coefficients were used. 88

Figure 74 Turbidity distributions measured by the EMP (left panels) and modeled by RMA (right panels) for January (top panels) and February (bottom panels), WY1988. Note difference in color scales between top and bottom plots. Time variable turbidity decay coefficients were used..... 89

Figure 75 Turbidity distributions measured by the EMP (left panels) and modeled by RMA (right panels) for March (top panels) and April (bottom panels), WY1988. Time variable turbidity decay coefficients were used..... 90

Figure 76 RMA PTRK modeled smelt distribution, November 1, 1987. For behavioral color codes, see Figure 29. Model results were driven using a smelt turbidity minimum threshold of 12 NTU and turbidity model results obtained with time variable decay coefficients. Similar distributions were produced using 10 and 14 NTU thresholds. 91

Figure 77 RMA PTRK modeled smelt distribution, January 1, 1988. For behavioral color codes, see Figure 29. Model results were driven using a smelt turbidity minimum threshold of 12 NTU and turbidity model results obtained with time variable decay coefficients. Similar distributions were produced using 10 and 14 NTU thresholds. 92

Figure 78 RMA PTRK modeled smelt distribution, March 1, 1988. For behavioral color codes, see Figure 29. Model results were driven using a smelt turbidity minimum threshold of 12 NTU and turbidity model results obtained with time variable decay coefficients. Similar distributions were produced using 10 and 14 NTU thresholds. 93

Objectives

This work has two main objectives. The first is to validate RMA's predictive adult delta smelt (ADS) model on historic water years in the 1980s. While the model has previously been validated using data from the 2000s, water years in the 1980s experienced much higher adult delta smelt (ADS) population numbers and variation in southern export salvage patterns. As a result they offer a much broader range of conditions over which to test the applicability and accuracy of the model. The second main objective of this work is to test hypotheses about ADS behavior based on the outcome of the model validation. Specifically, what do the successes and deficiencies of the model tell us regarding our assumption that ADS migrate in response to simple hydrodynamic and water quality cues.

Background

Adult Delta Smelt Life History

The delta smelt (*Hypomesus transpacificus*) is a small euryhaline fish endemic to the Sacramento-San Joaquin Delta. Adult delta smelt typically spawn in the late winter and early spring months as water temperatures reach the 7–15°C range (USBR 2008). Spawning takes place in shallow sloughs and in the near-bank habitat or larger channels. In recent years spawning has been concentrated in the Cache Slough Complex and Sacramento Deep Water Ship Channel areas, but has also been recorded in Suisun Marsh and at locations upstream in the Delta (USBR 2008).

Smelt larvae hatch within 9–13 days and then spend several weeks feeding near the channel bed as their fins fully develop (USBR 2008). Following this, they passively float downstream with the water currents until they reach Suisun Bay. During the summer months, smelt prefer to reside in the low salinity zone around Suisun and Grizzly Bays, where they grow rapidly, feeding on free-floating copepods, cladocerans, amphipods, and insect larvae (USBR 2008).

Once the wet season begins in late fall, smelt migration upstream to spawn is triggered by high turbidity water associated with “first flush” storms in the basin (Sommer et al. 2011). Migration can be rapid, with smelt traveling upstream as much as 3.6 km per day (Sommer et al. 2011). Many smelt exhibit a holding pattern in these upstream areas and do not spawn immediately upon reaching them (Sommer et al. 2011). Following spawning, the majority of adults die. Those that survive return downstream.

While the delta smelt was once the most abundant fish caught in routine Delta sampling surveys, it has experienced large population declines since monitoring began in the 1960s (Merz 2011). It was listed as federally endangered in 1993. Beginning around 2001, populations experienced a rapid decline associated with a concurrent broad reduction in pelagic fish populations throughout the Delta, known as the Pelagic Organism Decline (POD, see Figure 1). The delta smelt was listed as endangered under the California State Endangered Species Act in 2009.

In most water years, the Sacramento River provides the Delta with the largest loads of allochthonous sediment, and ADS follow the turbidity gradient into areas of the North Delta. However, during some

hydrologic, export volume, and gate operation conditions, the turbidity gradient can carry smelt south to the State Water Project (SWP) and Central Valley Project (CVP) export locations, where they may be killed or effectively rendered unable to spawn. Recognizing the onset of these conditions and taking management actions to prevent their occurrence has been the primary motivator of much of the work done to date on the ADS behavioral model.

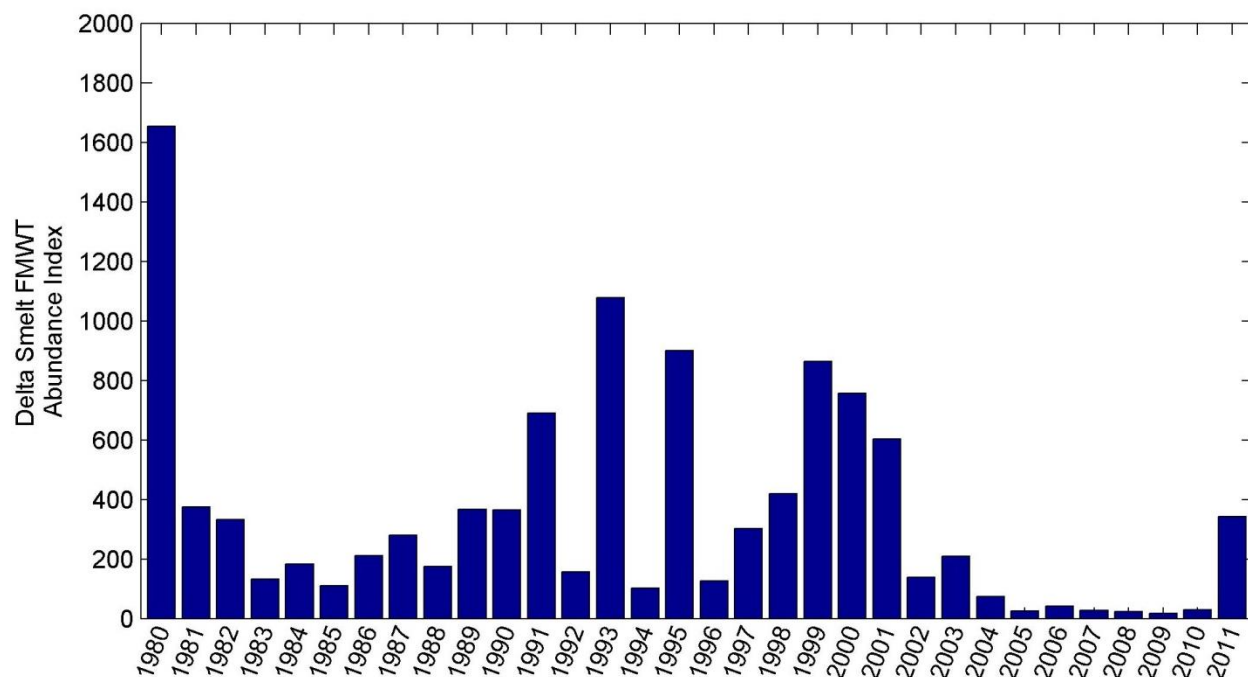


Figure 1 Trends in delta smelt population abundance. Abundance is estimated using catch data collected from the FMWT. Declines in abundance associated with the Pelagic Organism Decline are visible in the post-2001 data.

Project History

The present adult delta smelt behavioral modeling approach was developed for MWD in 2008 (RMA 2008). Initial modeling efforts were directed towards the accurate simulation of historic water years in the 2000s, in order to calibrate and validate the turbidity and smelt model parameters. The modeling approach was furthered during a study of revised export flows according to OCAP guidelines and 2-Gate Fish Protection Measures (RMA 2009). In this work, simulations were performed for the 2000, 2002, 2003, 2004 and 2008 historic periods and the turbidity model parameters were recalibrated.

In the 2009–2010, the smelt and turbidity model was first used as a forecasting tool. Up to that point, most of the Delta modeling work involved the simulation of historic conditions (RMA 2011a). While this was useful for planning work, a forecast of future conditions was necessary provide Delta managers and stakeholders information allowing them to better operate Delta infrastructure and improve water operations by reducing fish conflicts. During this forecasting project, improvements to the model grid were made, and the model parameters further refined.

Near real-time forecasting continued for the 2010–2011 and 2011–2012 smelt migratory seasons (RMA 2011a, 2012). A detailed smelt model calibration was performed on historic water years 2002, 2004,

2008, and 2009 in 2011 (RMA 2011b). The model performed overall well in comparison of simulated and observed smelt salvage patterns at the southern export locations. However, the work identified problems in the approach taken to simulate turbidity in the Delta and highlighted the sensitivity of the smelt model on the simulated turbidity fields. Near real-time forecasting of the turbidity and smelt using the RMA modeling approach was discontinued for the 2012–2013 smelt migration season and replaced with a simpler DSM2 and artificial neural network approach.

Water Year Information

Composite plots showing the major inputs affecting Delta flow and turbidity patterns, as well as smelt salvage at the southern export locations are presented in Figure 2 through Figure 4. Flow and suspended sediment concentration (SSC) were obtained from cleaned and published USGS daily data. Combined Old and Middle River flow data was obtained from RMA2 Delta model runs using historical DSM2 model² export flow as boundary conditions. DCC and southern barrier operations were obtained from data published online by DWR³ and the US Bureau of Reclamation⁴ (USBR).

For each water year, the period under consideration in this report runs from the beginning of September until the end of April of the following year. This time frame was selected in order to fully encompass the smelt migration period. This is especially necessary in years like 1981, when there were significant smelt salvage events occurring in early October. Although the water year officially begins on the first of October, for the duration of this report September will be referred to along with the next water year. E.g., September 1980 officially belongs to WY1980, but will be discussed along with October 1980–April 1981 as water year 1981.

Water year 1981 was classified by DWR as a dry water year. The fall was dry until a storm system arrived in early December 1980, bringing high turbidities to the Delta. Then after a short dry period, a series of storms from late January through April 1981 brought in higher flows and turbidities, with the largest turbidities associated with the first of these storms. The DCC was open for the storm in early December but closed when high Sacramento flows arrived in January; it remained closed until the late spring. Flow in the Old and Middle River corridor was relatively constant at around -5000 cfs for most of WY1981. However, there was a slight increase from -5000 cfs to around -7000 cfs in early January. The FMWT smelt population index for WY1981 was slightly above the average for the 1980s. Salvage at the southern exports was significant and steady throughout the fall and early winter. This may have been the result of higher than usual fall flow from the San Joaquin (>5000 cfs) carrying high (≈ 20 NTU) turbidities (Peter Smith pers. comm. 27 August 2012). A large salvage event occurred in the middle of January, before the arrival of high flow in late January, but concurrent with an increase in exports. Salvage remained high through the middle of March.

Water year 1982 was classified by DWR as a wet water year. A series of storms brought high flows and turbidities to the Delta from mid-November through the spring. The highest inflowing sediment concentrations were associated with the first storm event. The DCC was closed at the start of the first

² Delta Simulation Model II: <http://baydeltaoffice.water.ca.gov/modeling/deltamodeling/models/dsm2/dsm2.cfm>

³ http://baydeltaoffice.water.ca.gov/sdb/tbp/index_tbp.cfm

⁴ <http://www.usbr.gov/mp/cvo/vungvari/Ccgates.pdf>

storm and remained closed until the late spring. Average Old and Middle River flow for WY1982 was near the average for the 1980s at -5000 cfs. A large increase in exports occurred in February causing Old and Middle River flow to rise from approximately -2000 cfs to -7000 cfs within a short period of time. The FMWT smelt population index for WY1982 was slightly above average for the 1980s, similar to WY1981. A large salvage event occurred in late November, correlated with the arrival of the first storm. Salvage remained low until increasing during the period late January through mid-March.

Water year 1988 was classified by DWR as a critically dry water year. Two storms brought high flow and turbidities into the Delta—one in early December and one in early January. The DCC was left open for the first of these storms, but closed for the second and reopened shortly thereafter. Average Old and Middle River flows were more negative compared to the 1980s average and were around -8000 cfs. A large increase occurred in mid-December, with flows increasing from -5000 cfs to -10,000 cfs. The FMWT smelt population index for WY1988 was slightly below the average for the 1980s. Ninety percent of the salvage was recorded in December and January, correlated with the passage of the two storm systems. Although peak turbidities for both storms were approximately equal, the earlier storm was associated with greater smelt salvage even though peak flows on the Sacramento were lower. This is likely associated with the closure of the DCC during the second system.

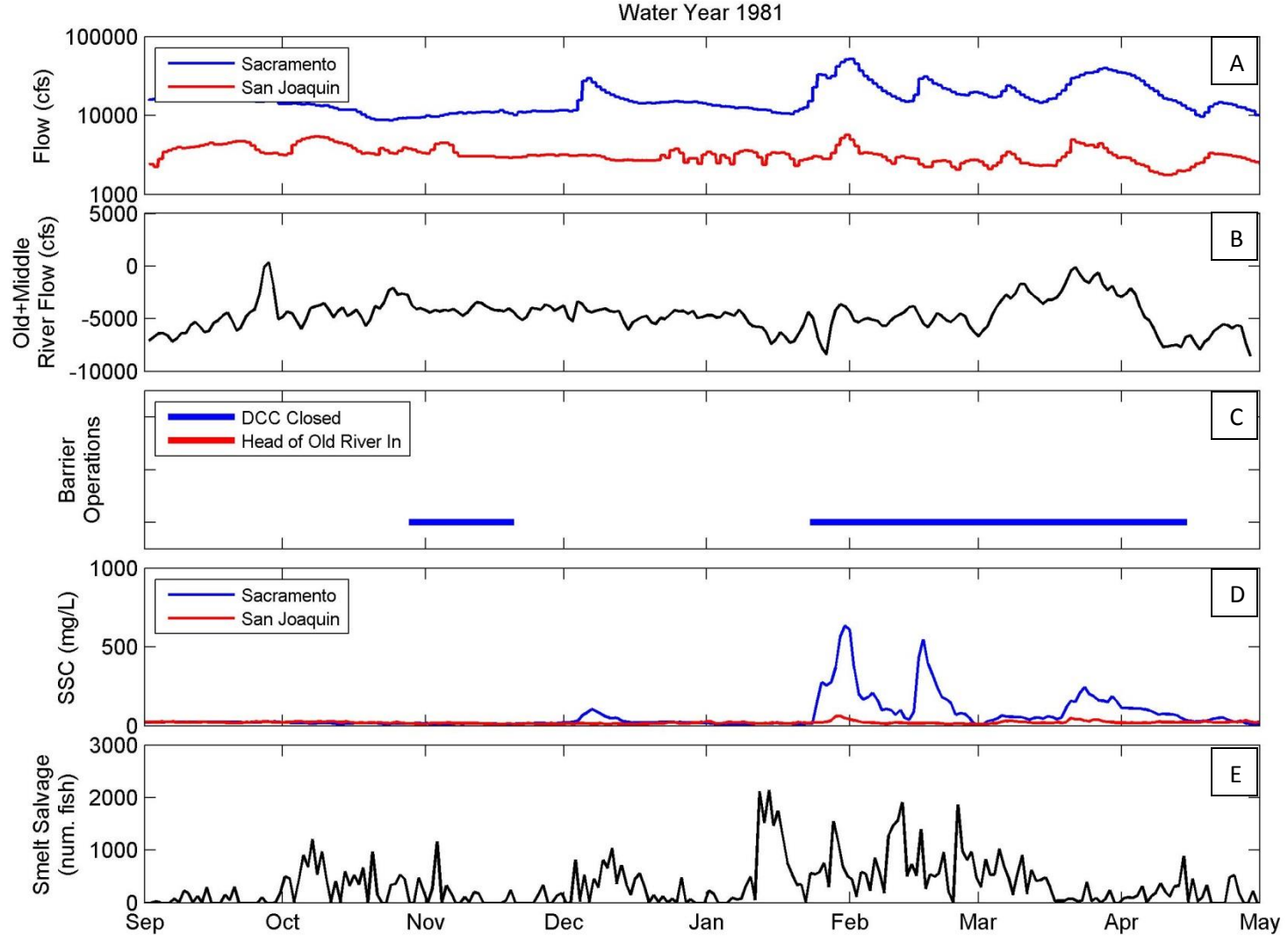


Figure 2 Hydrologic, management, and salvage conditions for the Delta for WY1981. Panel A shows Sacramento River flow at Freeport and San Joaquin River flow at Vernalis. Panel B shows average flow through the Old and Middle River corridors. Negative values indicate net flow from north to south. Panel C shows timing of the DCC closure and head of Old River installation (not installed during this period). Panel D shows inflowing SSC for the Sacramento River at Freeport and the San Joaquin River at Vernalis. Panel E shows total number of delta smelt salvaged at the SWP and CVP export locations.

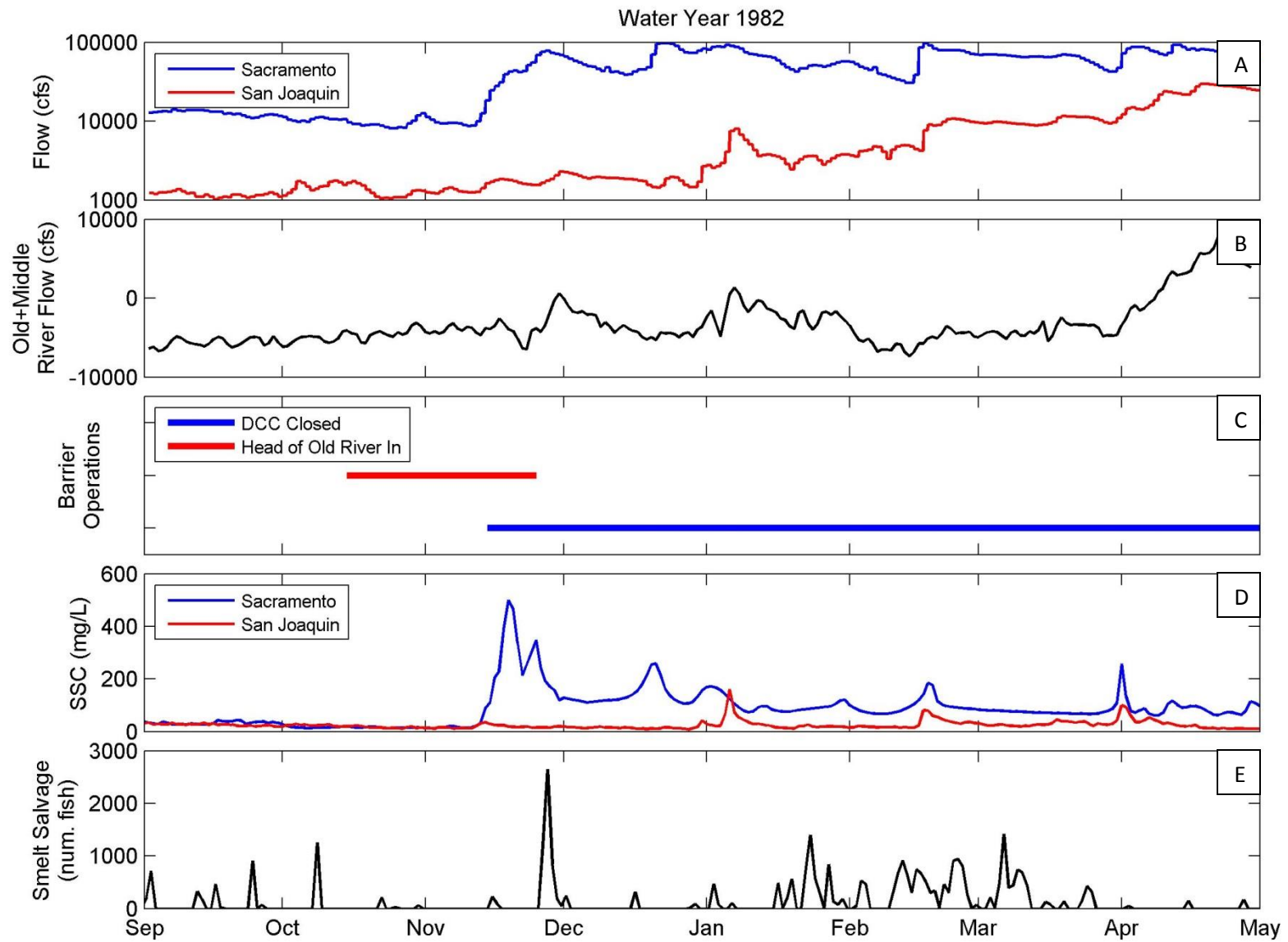


Figure 3 Hydrologic, management, and salvage conditions for the Delta for WY1982. See Figure 2 for descriptions of individual panels.

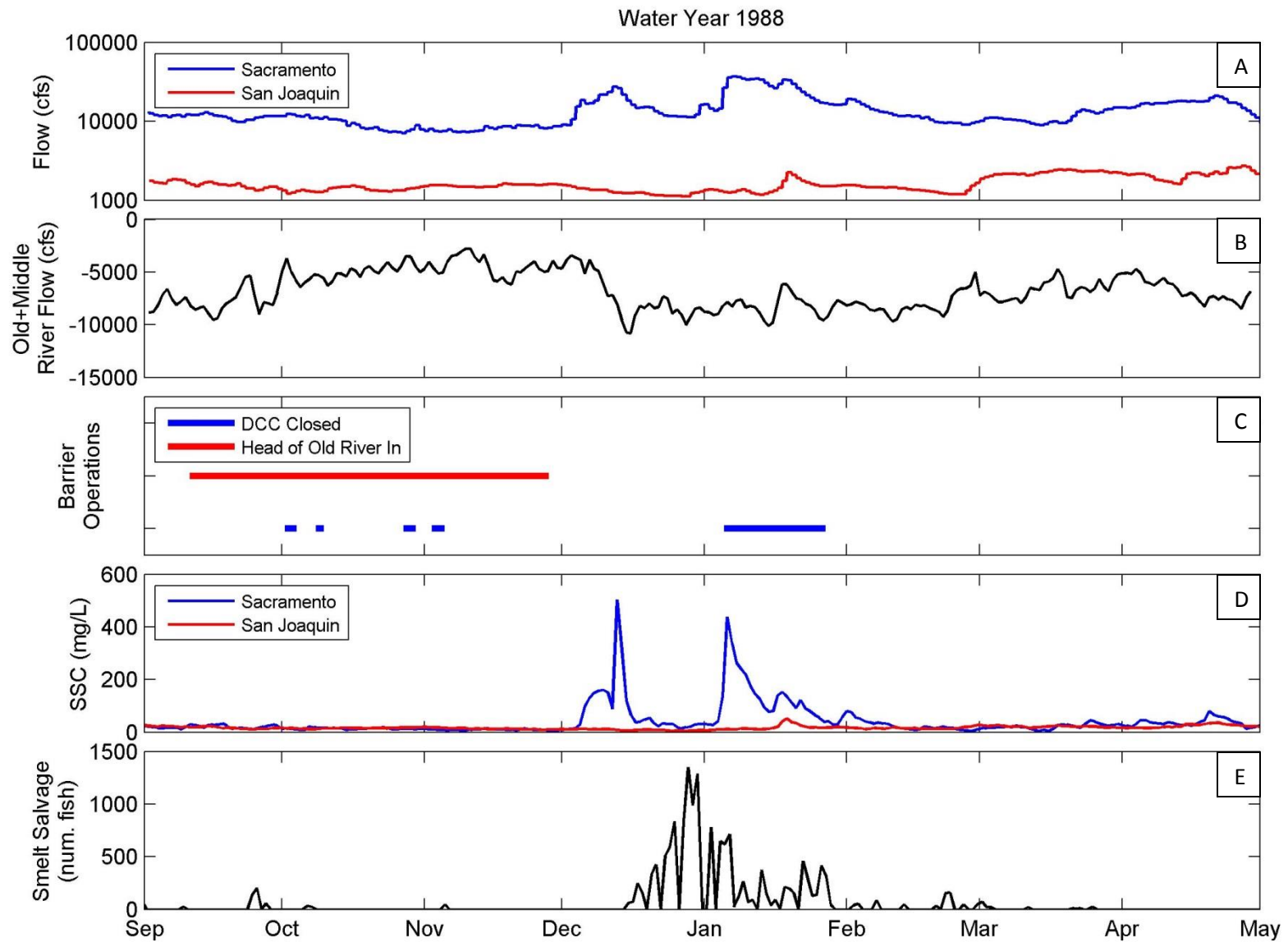


Figure 4 Hydrologic, management, and salvage conditions for the Delta for WY1988. See Figure 2 for descriptions of individual panels.

Observed Data Sources

The observed data sources used for current RMA turbidity model calibration and validation include approximately 60 continuous monitoring stations, spaced throughout the Delta and operated by the USGS. Unfortunately, none of these stations was in use during the historical water years considered here. Instead, two main sampling programs provided data used to check the accuracy of the turbidity model predictions. The first was the CA Department of Fish and Wildlife Fall Midwater Trawl (FMWT) program. Although this program's primary objective is the monthly sampling of fish populations, water quality data are taken as auxiliary measurements. The second program is the Environmental Monitoring Program (EMP), a long-term water quality sampling program with measurements taken on a monthly to bimonthly basis throughout the Delta.

Data on spatial distributions of adult delta smelt throughout the Delta were obtained from the FMWT program. Numbers of adult smelt salvaged at the southern export locations have been monitored since the late 1950s by a group of federal and state environmental agencies, and are available online.

Environmental Monitoring Program⁵

The most accurate, frequently-sampled, and wide-ranging observed turbidity data comes from the EMP. The locations of the sampling sites are shown in Figure 5. For the water years considered here, sites were sampled on a bimonthly basis throughout the fall, winter, and spring. During a typical Delta-wide sampling event, all of the stations were sampled within a 2–3 day window. Direct measurements of turbidity were taken at each station using a calibrated turbidimeter.

Fall Midwater Trawl⁶

FMWT cruises are taken monthly between September and December. Each cruises sample transects between San Pablo Bay and up the Sacramento River to Rio Vista and the San Joaquin River to Stockton, over a period of 7–10 days. Figure 6 shows the FMWT sampling station locations. Measurements of water clarity are taken at each station using a Secchi disk. For the purposes of comparing to modeled turbidity values, the Secchi depths were converted to turbidity using the lookup table (Table 1) provided by B.J. Miller (pers. comm. 2012). The relationship was calculated based on simultaneous measurements of turbidity and Secchi depth taken on Old River during 1995–2006, and are assumed to be approximately valid throughout the Delta. FMWT fish sampling is conducted using a midwater trawl net with a twelve foot square mouth. The net is towed for 12 minutes at each station, and all fish collected in the net are identified and enumerated.

Southern Export Fish Collection Facilities^{7,8}

The two major export locations in the south Delta are the Harvey Banks Pumping Plant (associated with the SWP and operated by DWR) and the C.W. Bill Jones Pumping Plant (part of the CVP and operated by USBR). Fish on their way to being entrained at the Banks Pumping Plant are salvaged at the Skinner Delta Fish Protective Facility, operated by DWR and CA DFW, which began operations in 1968. Fish

⁵ <http://www.water.ca.gov/iep/activities/emp.cfm>

⁶ <http://www.dfg.ca.gov/delta/projects.asp?ProjectID=FMWT>

⁷ http://www.usbr.gov/pmts/tech_services/tracy_research/index.html

⁸ <http://www.dfg.ca.gov/delta/data/salvage/salvageoverview.asp>

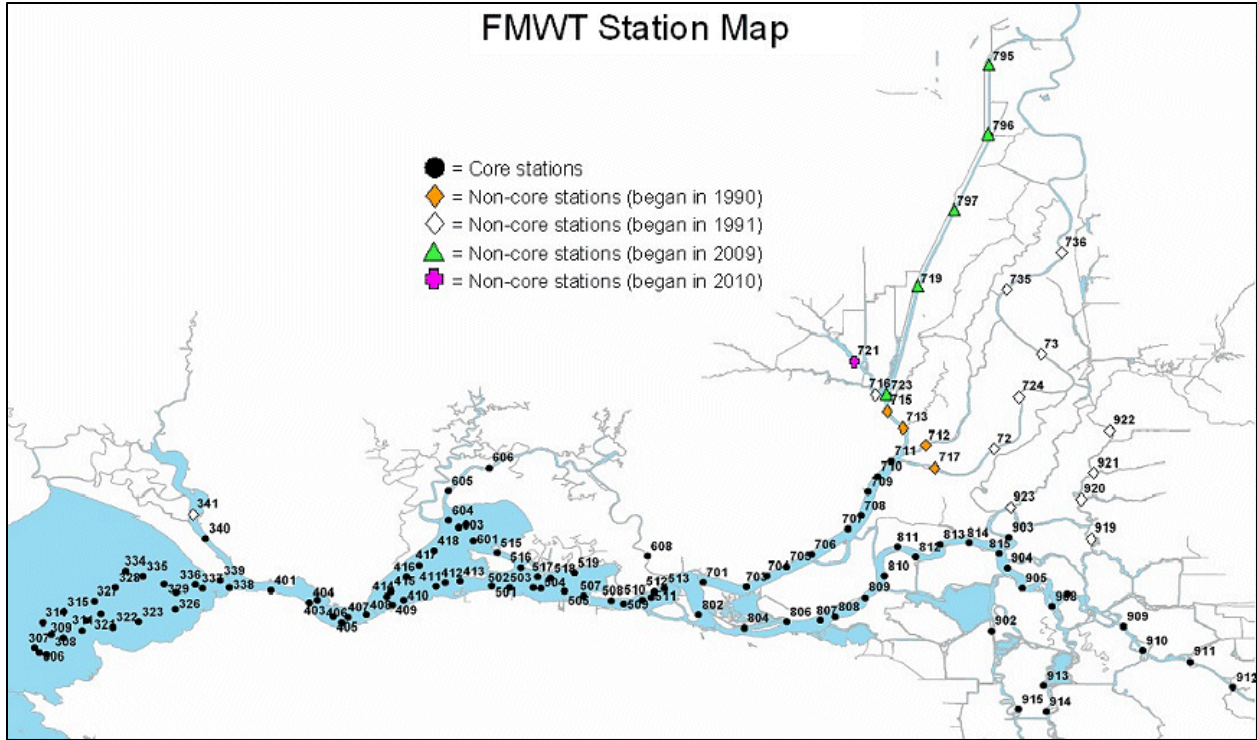


Figure 6 FMWT sampling station locations. Image obtained from the CA DFW website¹⁰.



Figure 7 Southern Delta export fish salvage facility locations. Image obtained from the CA DFW website¹¹.

¹⁰ <http://www.dfg.ca.gov/delta/data/fmwt/stations.asp>

Table 1 Turbidity - Secchi Depth relationship for Delta.

Turbidity	Secchi Depth	Turbidity	Secchi Depth	Turbidity	Secchi Depth
(NTU)	(cm)	(NTU)	(cm)	(NTU)	(cm)
5	150	27	24	49	13
6	122	28	24	50	13
7	102	29	23	51	13
8	88	30	22	52	13
9	78	31	21	53	12
10	69	32	21	54	12
11	62	33	20	55	12
12	57	34	19	56	12
13	52	35	19	57	11
14	48	36	18	58	11
15	45	37	18	59	11
16	42	38	17	60	11
17	39	39	17	61	11
18	37	40	16	62	10
19	35	41	16	63	10
20	33	42	16	64	10
21	32	43	15	65	10
22	30	44	15	66	10
23	29	45	15	67	10
24	28	46	14	68	10
25	26	47	14		
26	25	48	14		

¹¹ <http://www.dfg.ca.gov/delta/data/salvage/salvagemap.asp>

Methods

The adult delta smelt behavioral model is driven by RMA's two-dimensional hydrodynamic and water quality models for the Delta. These models have been iteratively developed, calibrated, and validated over several years, including a few times specifically for the purpose of use with the delta smelt model. These models produce highly accurate predictions of flow patterns throughout the Delta, given appropriate boundary conditions, for a wide range of hydrologic forcing conditions. A brief overview of the models, along with the boundary conditions that were used, is given here. For more detailed information, please refer to the technical reports detailing prior smelt modeling efforts (RMA 2008, 2009, 2010, 2011a, 2011b, 2012) and the most recent full model calibration document (RMA 2005).

RMA2 Hydrodynamic Model

The RMA2 hydrodynamic model is a two-dimensional, depth-averaged, finite-element model of the Delta. Upstream channels are represented with trapezoidal cross sections and connect with two-dimensional elements in the more complex flow areas of the central and western Delta, as well as Suisun Bay. The model is driven by water movement into and out of the Delta area, including flow in at major Delta tributaries, Delta Island Consumptive Use (DICU), major water exports (e.g., SWP, CVP), and tidal flow at the downstream boundary. The major inflow boundary conditions are located on the Sacramento River near Freeport and the San Joaquin River near Vernalis. Smaller tributary inflows are specified for the Yolo Bypass, the Calaveras River, the Mokelumne River, and the Cosumnes River at their approximate intersection with the legal Delta boundaries. Exports are removed from the system at Clifton Court Forebay (SWP), the Harvey Banks Pumping Plant (CVP), the North Bay Aqueduct at Barker Slough Pumping Plant, and smaller Contra Costa Water District withdrawals at Rock Slough, Victoria Canal, and Old River. A downstream water surface boundary condition is applied at Martinez. Gate operations are taken into account to restrict flow at the Delta Cross Channel (DCC), the Suisun Marsh Salinity Control Gates (SMSCG), and temporary barriers that are periodically placed at locations on Old and Middle Rivers. DICU withdrawals and return flows are included at approximately 200 separate locations throughout Delta interior. Figure 8 shows the RMA model grid along with the locations of major boundary conditions, gates, and DICU.

Boundary condition data were available for measured flows on the Sacramento and San Joaquin Rivers from USGS stations 11447650 and 11303500 and for measured stage at Martinez from DWR via the California Data Exchange Center (CDEC, station code: MRZ). Flows for the smaller tributary inputs as well as export flows and DICU were obtained from data compiled by DWR for historical DSM2 runs. Historic gate operation conditions were downloaded from the DWR and USBR websites specified in the Water Year Information section. For the water years under consideration here, the temporary barriers for the Old River at Tracy, the spring head of Old River, and Grant Line canal were not yet in use. Export pumping from the Contra Costa Water District withdrawals at Old River and Victoria Canal had also not yet begun. Flow and stage boundary conditions for WY1981, 1982, and 1988 are shown in Figure 9 through Figure 11.

The Delta geometry for the modeling periods considered here was complicated by a lack of detailed historic bathymetry data and the many island breaches that occurred throughout the 1980s. For the

purposes of this modeling effort, it was assumed that the majority of the Delta geometry in the 1980s was similar to (and could be modeled accurately with) the current RMA model geometry after a few major changes were made: [1] For water years 1981 and 1982, Mildred Island and Liberty Island had not yet been breached and left flooded, as they are presently. The model geometry was therefore modified in order to make these areas hydrologically unconnected from the adjacent channel. [2] Since Mildred Island breached in January of 1983, its flooded area was added back into the model grid for the WY1988 run.

During water years 1981 and 1982, several levees failed within the simulation time period of September to April. However, the full simulation of the fine scale levee break and subsequent dewatering event was beyond the scope of this project and was not performed. These levee break events should be considered as uncertainties in the hydrodynamic model accuracy. They include specifically:

- Lower Jones Tract failure in September 1980 (DWR 2009)
- Prospect Island failure in the fall of 1981 (DWR 2009)
- Little Franks Tract failure in December 1981 (DWR 2009)
- Private levees on the Cosumnes River near Galt failed in January and February 1982 (DWR 2009)

RMA11 Electrical Conductivity and Turbidity Models

The resultant RMA2 flow modeling results were used to drive the RMA11 water quality models for electrical conductivity¹² (EC) and turbidity. EC boundary conditions are necessary for all major model inflow boundaries. These data were obtained for the Sacramento River at Freeport, the San Joaquin River at Vernalis, and the downstream Martinez boundary from historical DSM2 runs performed by DWR (see Figure 12 through Figure 14). WY1981 included a long period of time with presumably missing or corrupted EC data at the Vernalis boundary which had been replaced by DWR using linear interpolated. In order to improve model accuracy, EC values for this period of time (from approximately mid-December until late March) were removed and replaced with a more realistic, flow-based estimate. EC values were calculated from Vernalis flow based on the equation $EC = 120,000 * \text{flow}^{-0.703}$ (where flow values are in cfs), which was obtained from a best fit regression of flow and EC for the remainder of WY1981.

DICU return flows were also set to values provided by DSM2. The Yolo Bypass EC value was set to mirror the EC for the Sacramento boundary. Cosumnes, Mokelumne, and Calaveras River inflow EC values were set to a constant value of 125 $\mu\text{mhos/cm}$, consistent with observed data measured at CDEC stations near these sites.

The delta smelt behavioral model is relatively insensitive to the calculated EC field. Smelt are sensitive to a maximum EC beyond which they become physiologically stressed. So the calculated EC field typically sets their westernmost position near Suisun and Grizzly Bays in the early fall before any turbidity pulses

¹² Salinity is a measure of the dissolved salts in a parcel of water. Electrical conductivity is a measure of the ability of that water to conduct electricity. The two characteristics are closely related, but electrical conductivity is easier to measure and is thus more available for model boundary condition and calibration/validation data. Relationships for converting between the two quantities are available for the Delta and are highly accurate in most cases.

enter the Delta. Upstream turbidity, however, is their main driver for movement into the Delta, and the EC model results will not be discussed or presented in detail in this report.

Turbidity is modeled in the RMA turbidity model as a non-conservative constituent using prescribed decay coefficients. These decay coefficients are spatially variable and were calibrated to match model results with observed turbidities at interior Delta sites for the high flow period of water years 2007 and 2010 (RMA 2011a, see Figure 15). While this approach is useful and effective during the high flow winter periods when smelt typically migrate, it has several important drawbacks that require some background explanation on turbidity and its relationship with suspended sediment.

Turbidity is a measure of light backscattered from particles suspended in the water column. It is typically described as the cloudiness of a parcel of water and is probably a more accurate description of what migrating smelt respond to than is the suspended sediment concentration (SSC) of the water. SSC is typically measured in units of mg/L. Because small particles scatter greater light than larger ones given the same total particles mass, two samples of water with the same SSC may have dramatically different turbidities. For example, imagine the cloudiness of a glass of water with a whole piece of blackboard chalk dropped into it versus the cloudiness of a glass of water with the chalk crumbled into powder first before being dropped in. Turbidity and SSC are linked, however, in that increases in SSC generally lead to increases in turbidity. If the particle size distribution and particle composition remain relatively constant, the two vary linearly with one another, and a regression can be calculated to relate one quantity to the other.

Since suspended sediment concentration is a measure of the mass of particles per unit volume, mass conservation equations can be written which take into account all of the physical processes acting to increase or decrease mass in the water column. The processes include removal due to settling, increases due to entrainment or resuspension, and flocculation/floc breakup. Since turbidity is only an observable effect of particles in suspension it is itself not strictly conserved, all of the formulas detailing the processes leading to increases and decreases of sediment in suspension cannot be applied to turbidity, and these processes must be lumped into a single decay coefficient.

As mentioned previously, the use of a decay coefficient is easily implemented and produces accurate results during times of high flow for which the coefficients were calibrated. At those times, turbidities within the Delta are high as a result of inflowing turbid water and rapidly decrease as material drops out of suspension. However during times of low flow, tidal and wind-driven resuspension (see for example, Figure 16) acts to increase suspended sediment locally, and the use of the high-flow decay coefficients serves to attenuate much more turbidity than observed, producing a poor model fit.

For these reasons, two sets of turbidity model runs were performed. The first set used the high-flow decay coefficients previously calibrated over water years 2007 and 2010 (Figure 15). These model runs served to address the original intent of the modeling study—to examine the performance of the RMA adult delta smelt model on historical water years in the 1980s. An examination of preliminary results from WY1981 and WY1982, where there was significant smelt salvage during low-flow months, indicated poor model agreement with observed data. To further explore the applicability of the smelt

model, an additional set of model runs was performed by relaxing the restriction to use the previously calibrated decay coefficient set.

The second set of model runs were performed with a time varying decay coefficient. This allowed for the simulation of low decay rates during the low-flow period and higher decay rates during high flow. For the sake of simplicity, only 3 model decay coefficients were considered: 0.01/day [low], 0.05/day [medium], and 0.10/day [high]. These coefficients were assumed to apply over the entire Delta. The low decay coefficient was applied to modeled months when the Sacramento River was flowing at a relatively low flow rate (generally below 20,000 cfs). After running the turbidity model using both the high and the medium decay coefficients, the medium coefficient was found to provide a better match to the observed turbidity data during the high flow months. Table 2 shows the decay coefficients used for each month of each water year.

Boundary conditions for turbidity on the Sacramento River at Freeport and the San Joaquin River at Vernalis were generated using USGS measured suspended sediment concentration. These concentrations were regressed against observed data measured for the EMP sampling program in order to obtain turbidity time series at those boundaries (Figure 17 and Figure 18). All other inflow turbidity boundary conditions were produced by the WARMF¹³ watershed model, calibrated to the Central Valley Watershed and run by Systec Water Resources, Inc. For more information about the WARMF model, please refer to the 2012 RMA Turbidity and Smelt Forecast document.

The downstream boundary at Martinez was held at a constant 20 NTU, consistent with observed data at that location. In order to account for sediment resuspension in the fall low-flow period coming from Suisun and Grizzly Bays, internal boundary conditions were prescribed at Mallard Island and Jersey Point. These boundary conditions were based on observed EMP data and were only set to apply until the beginning of the first major storm event of the season. Boundary conditions for each of the water years are shown in Figure 19 through Figure 21.

RMAPTRK Smelt Behavioral Model

The hydrodynamic, EC, and turbidity model results were used to drive the adult delta smelt particle tracking-behavioral model. Fifty thousand particles were dropped into the Suisun Bay region on the first of September of each run. The particles move in response to the local flow field around their current location, but can choose whether to surf the current to get to a more preferable habitat or hide near the channel bed to remain stationary. The decision to either surf or hide is based on a set of simple rules, taking into account EC and turbidity values as well as lateral gradients in these variables. These rules can be summarized as follows:

1. If $EC > EC_{max}$ and a significant gradient in the EC at that location is present, ride the current if it's moving in the direction of decreasing EC; otherwise hide and wait for the tide to turn
2. If $turbidity < turbidity_{min}$, and a significant gradient in the turbidity at that location is present, ride the current if it's moving in the direction of increasing turbidity; otherwise hide and wait for the tide to turn

¹³ Watershed Analysis Risk Management Framework: <http://www.epa.gov/athens/wwqtsc/html/warmf.html>

3. If $EC < EC_{max}$ and $turbidity > turbidity_{min}$, explore the local habitat by randomly riding the current and hiding

For these model runs, the value for EC_{max} was set at 3000 $\mu\text{mhos/cm}$ (a salinity of approximately 1.5 parts per thousand).

As with the turbidity modeling, two sets of smelt particle tracking model runs were performed. The first set used turbidity model results obtained with the original, high-flow-calibrated decay coefficients. These smelt model runs used the $turbidity_{min}$ value of 16 NTU, which was similarly previously calibrated (RMA 2011b). The intent here was to address the original intent of the modeling study—to validate the RMA adult delta smelt model on historical water years. In the following Results sections, these runs will be referred to as the “high-flow calibrated runs” or the “original model calibration runs.”

The second set of smelt model runs used turbidity model results obtained with the time-varying decay coefficients, accounting for decay in both low-flow and high-flow periods. These smelt model runs additionally examined $turbidity_{min}$ values of 10, 12, and 14 NTU in order to examine the sensitivity of model results to this parameter. The intent with these runs was to further explore the applicability of the smelt model under conditions for which it was not calibrated against. In the Results sections, these runs will be referred to as the “time variable decay coefficient runs.”

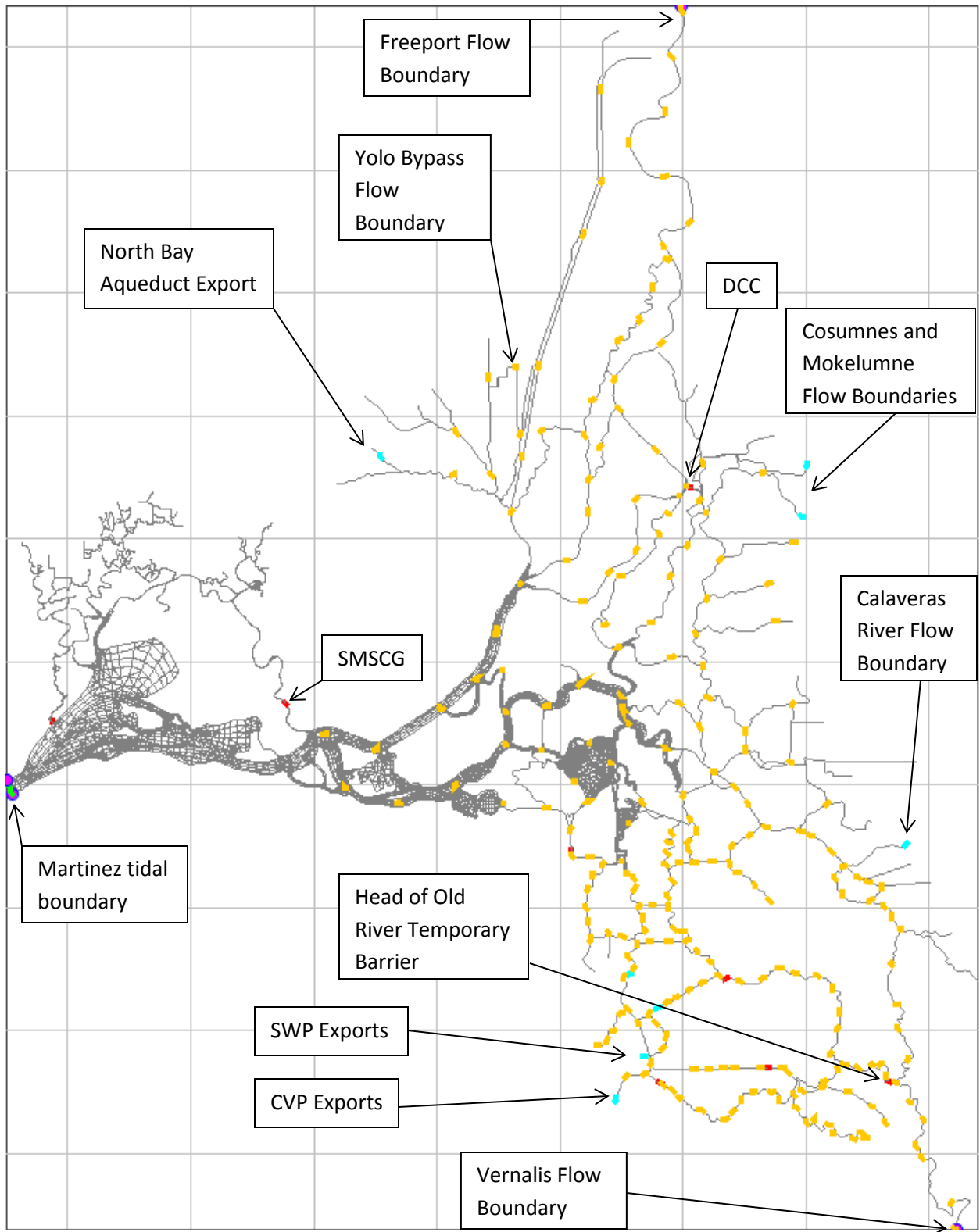


Figure 8 RMA model grid showing major boundary condition and gate/barrier locations. Yellow points show DICU locations.

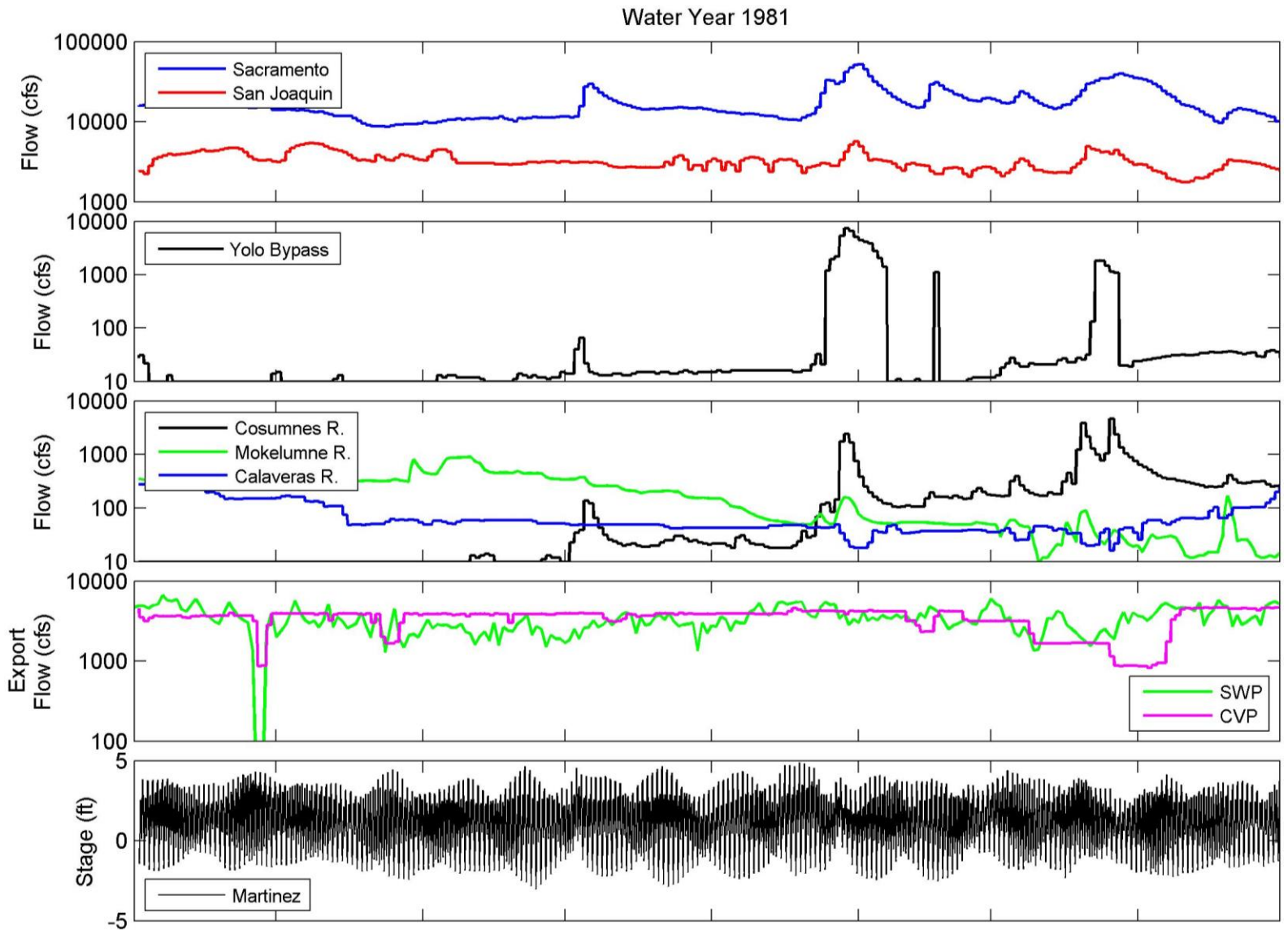


Figure 9 Hydrodynamic boundary conditions for WY1981. Major tributary inflows to the north, east, and south Delta are shown in the top 3 panels. The panel second from the bottom shows major export flow diversions in the south Delta. Bottom panel shows the prescribed water surface elevation at the downstream Martinez boundary.

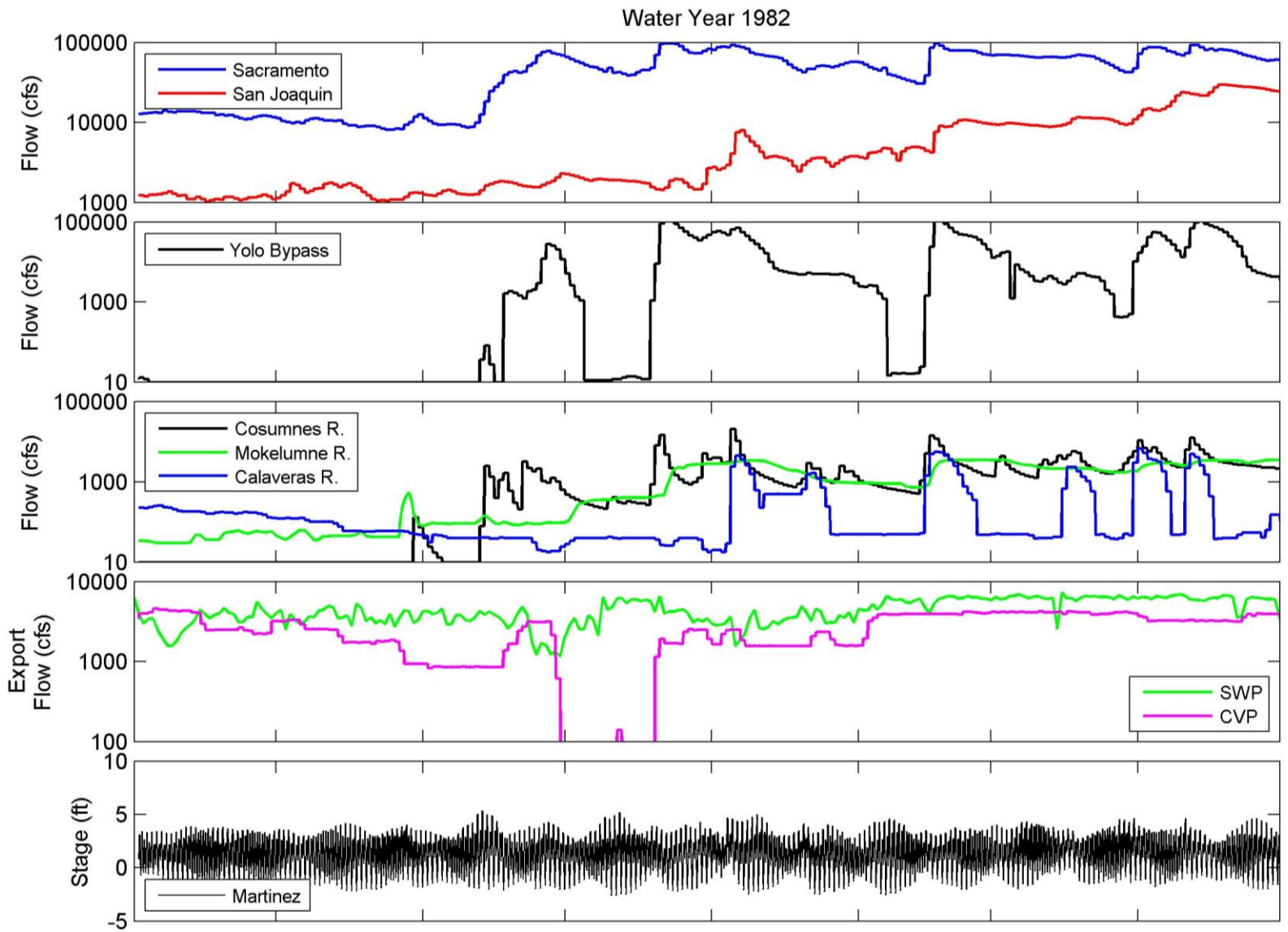


Figure 10 Hydrodynamic boundary conditions for WY1982. Major tributary inflows to the north, east, and south Delta are shown in the top 3 panels. The panel second from the bottom shows major export flow diversions in the south Delta. Bottom panel shows the prescribed water surface elevation at the downstream Martinez boundary.

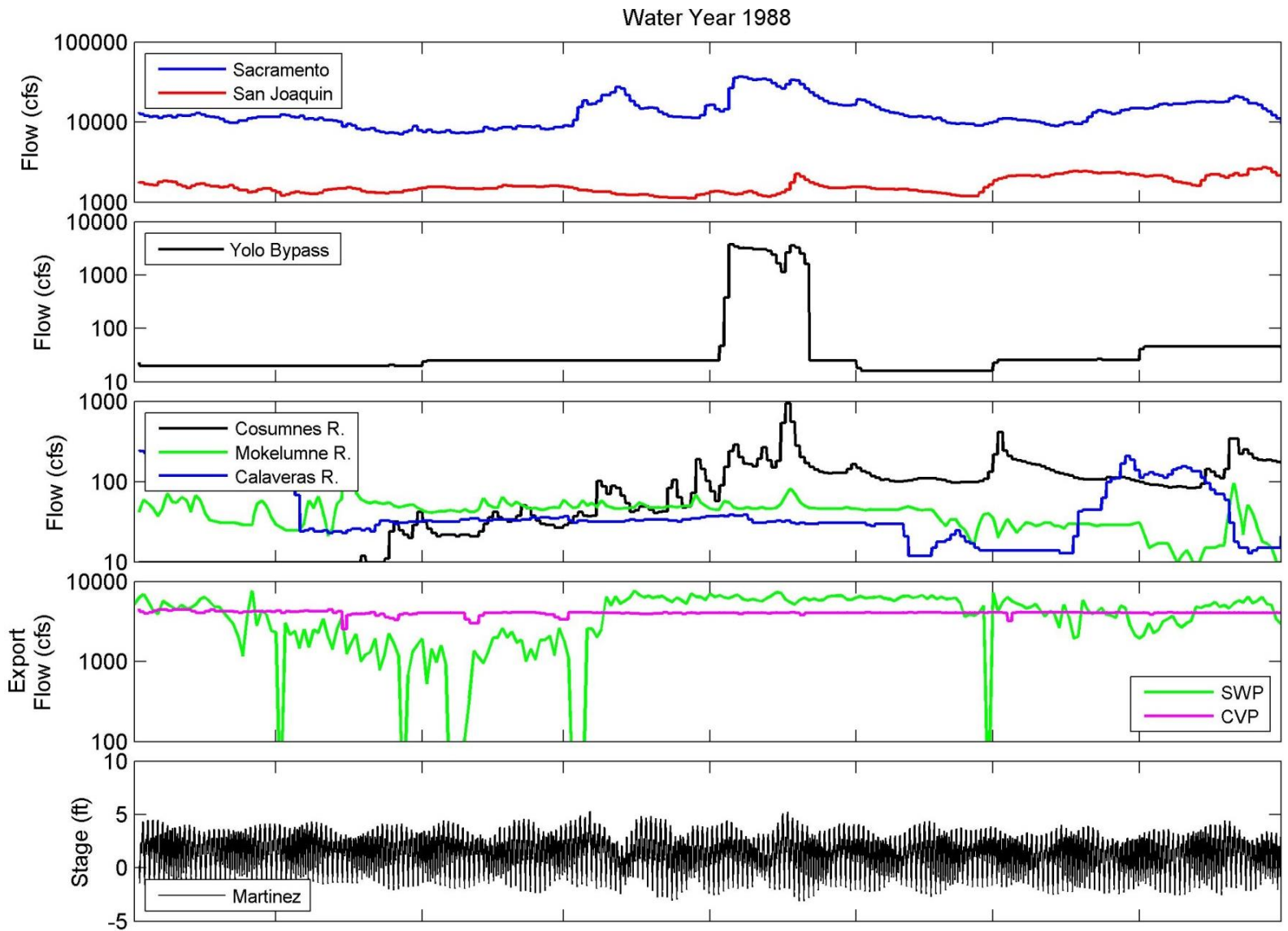


Figure 11 Hydrodynamic boundary conditions for WY1988. Major tributary inflows to the north, east, and south Delta are shown in the top 3 panels. The panel second from the bottom shows major export flow diversions in the south Delta. Bottom panel shows the prescribed water surface elevation at the downstream Martinez boundary.

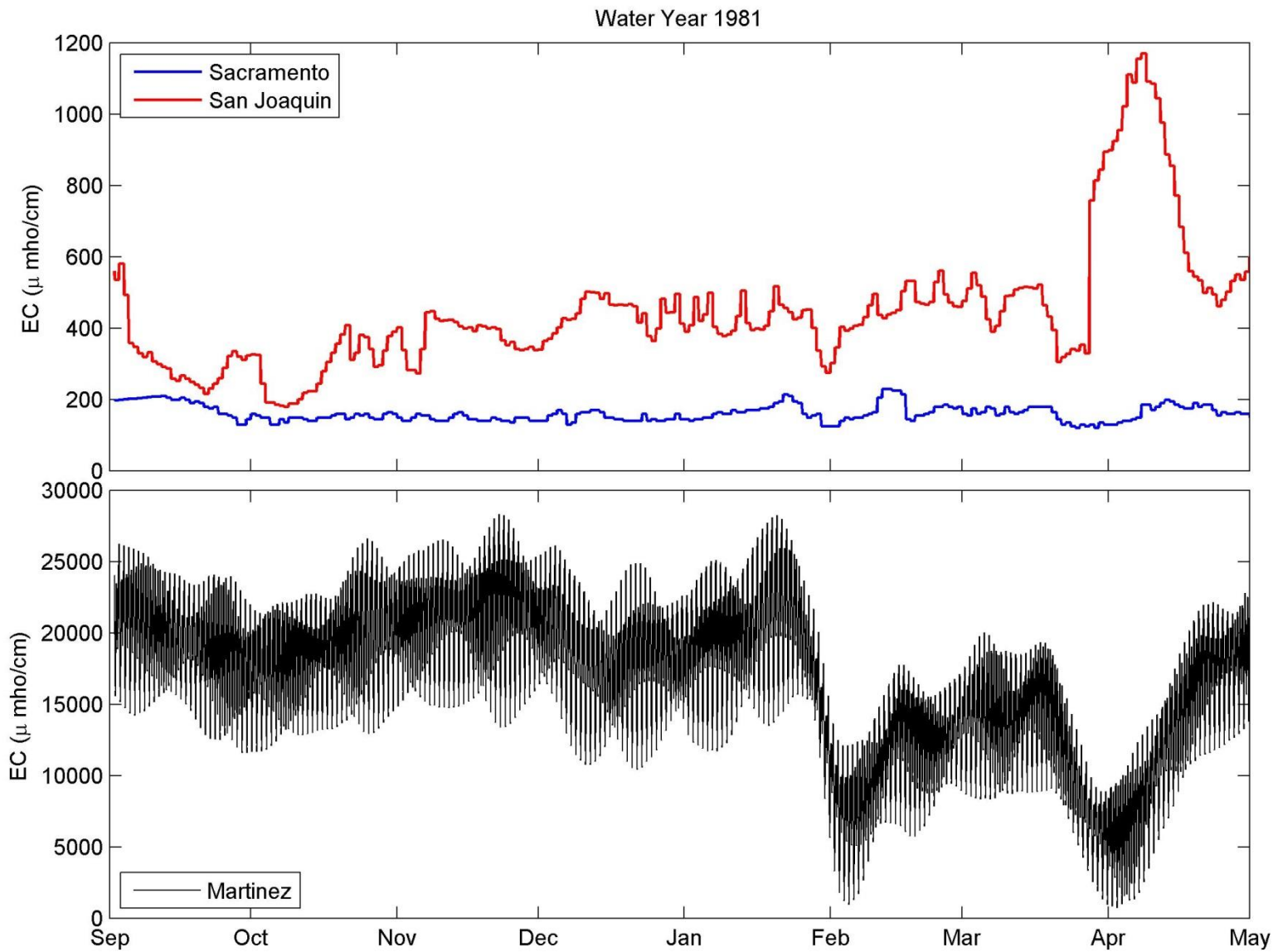


Figure 12 WY1981 EC boundary conditions at the Sacramento River at Freeport and the San Joaquin River at Vernalis (top panel) and Martinez (bottom panel).

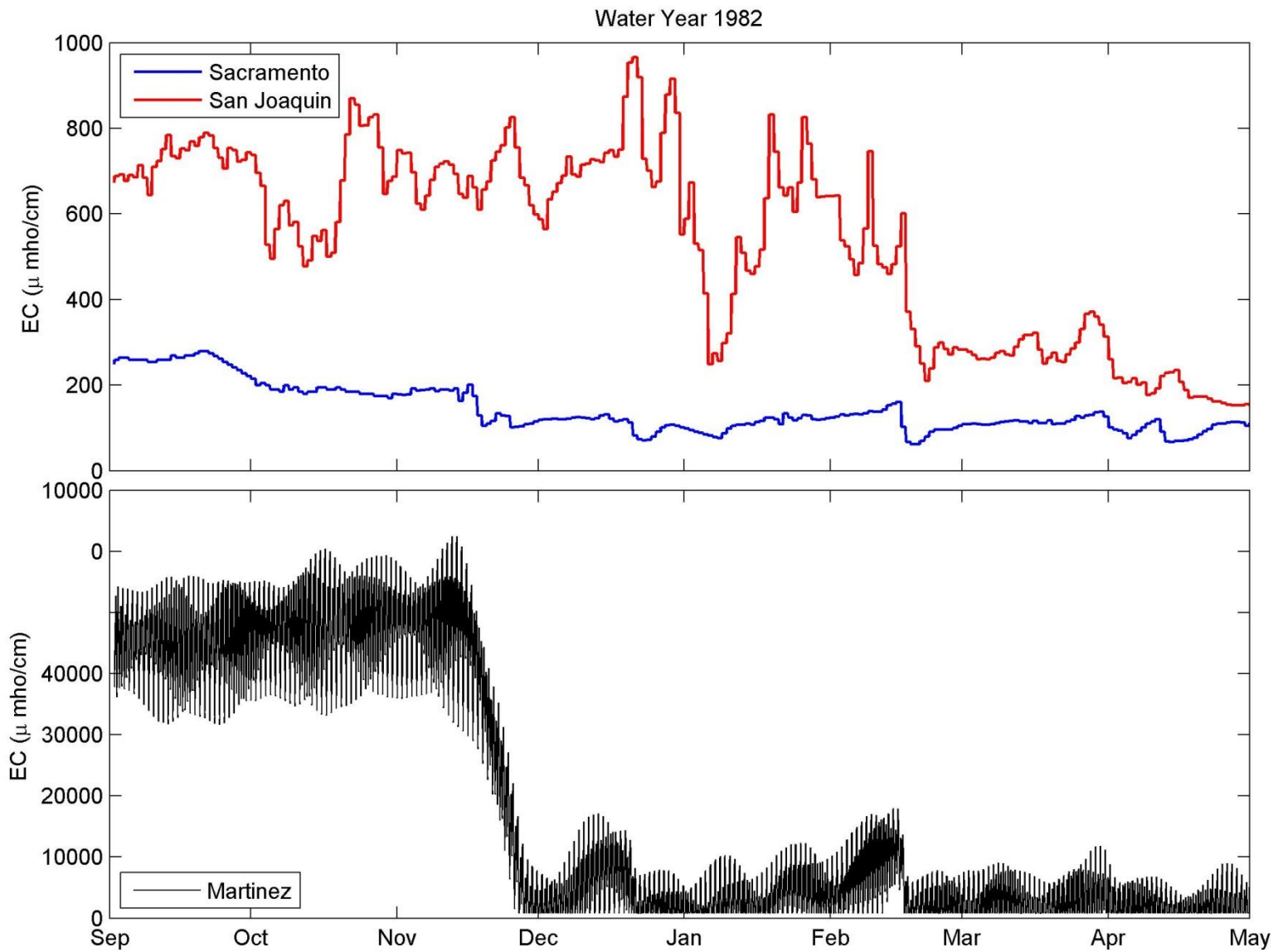


Figure 13 WY1982 EC boundary conditions at the Sacramento River at Freeport and the San Joaquin River at Vernalis (top panel) and Martinez (bottom panel).

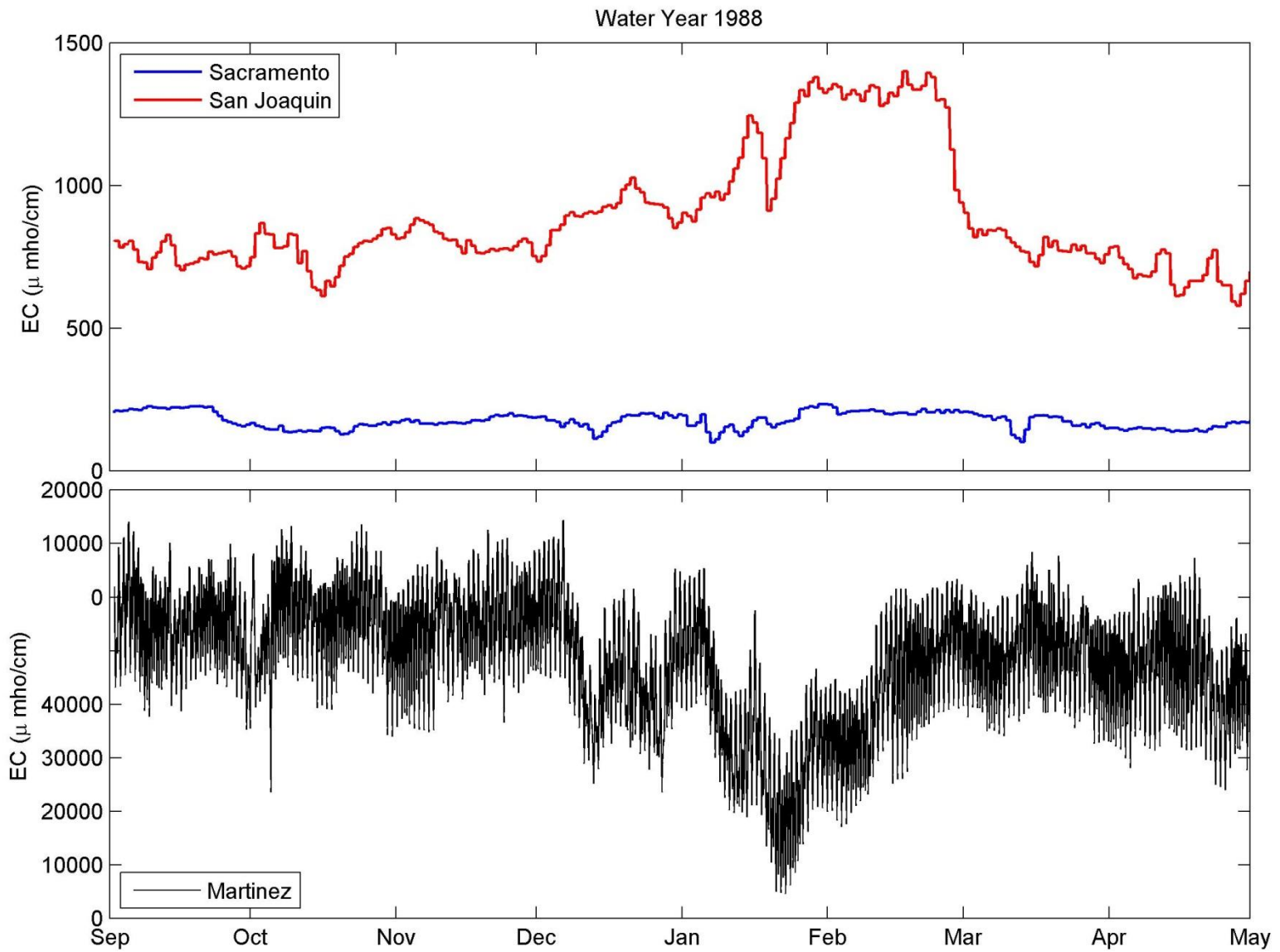


Figure 14 WY1988 EC boundary conditions at the Sacramento River at Freeport and the San Joaquin River at Vernalis (top panel) and Martinez (bottom panel).

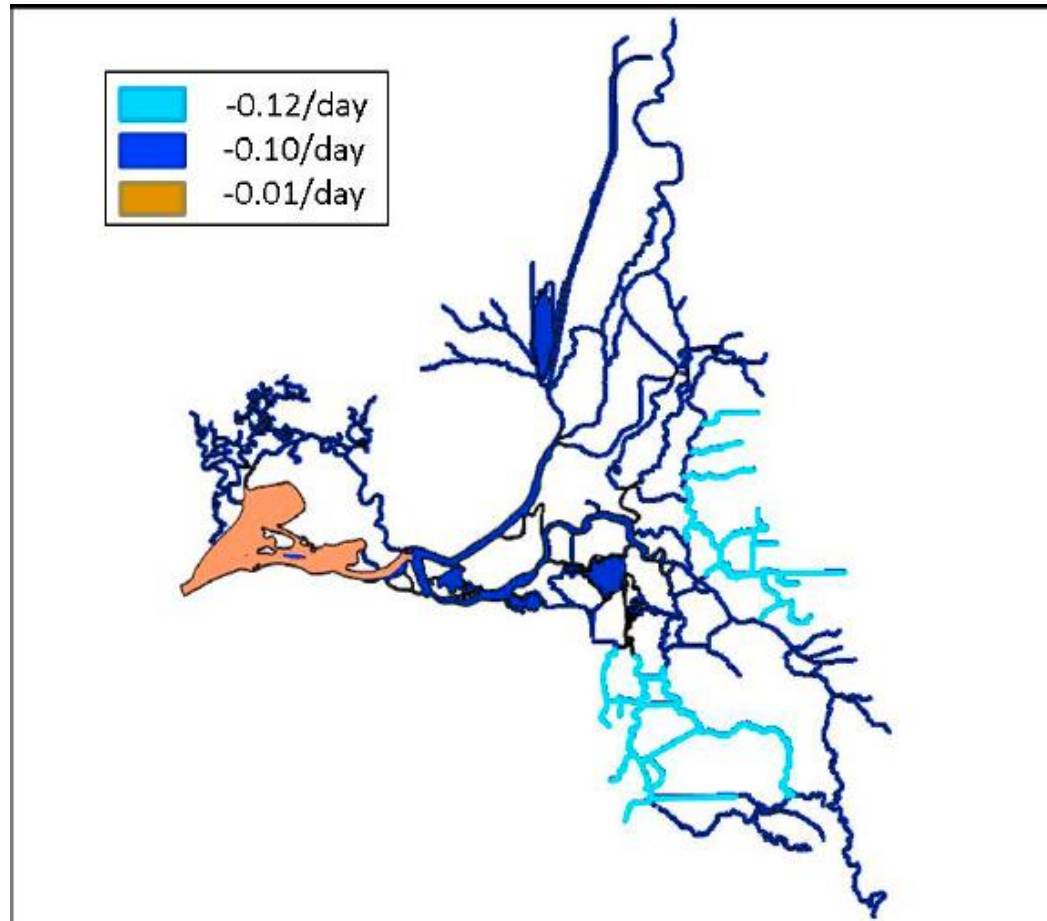


Figure 15 Turbidity decay coefficients calibrated for WY2007 and WY2010 high flow periods.

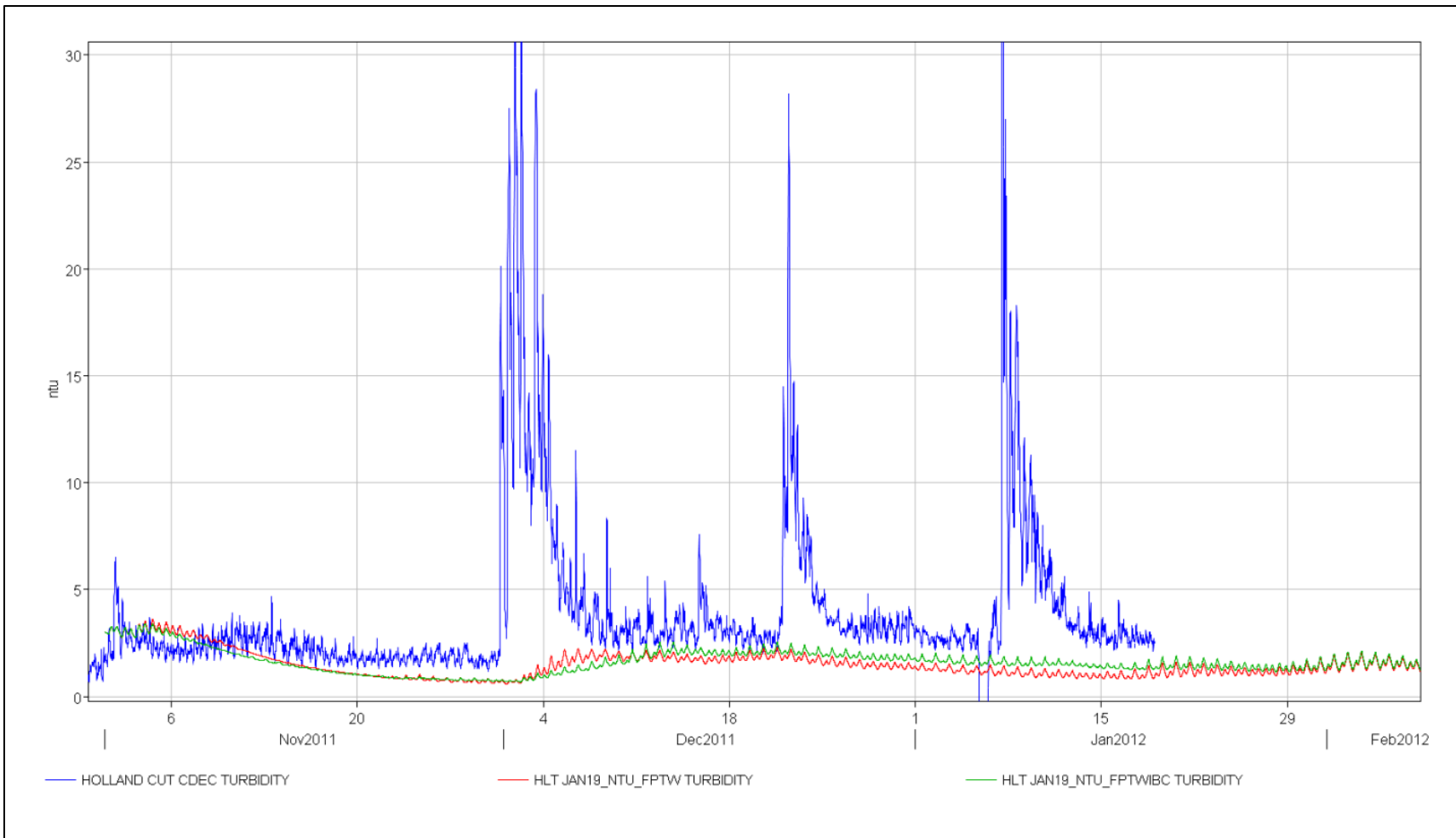


Figure 16 Measured turbidity (blue line) at Holland Cut in winter of WY2012. Large increases in turbidity are due to sediment resuspension occurring during large wind events. Elevated turbidities persist for several days following an event. The decay coefficient approach to modeling turbidity has difficulty accounting for these resuspension events and their subsequent effect on Delta turbidity. Figure from RMA (2012).

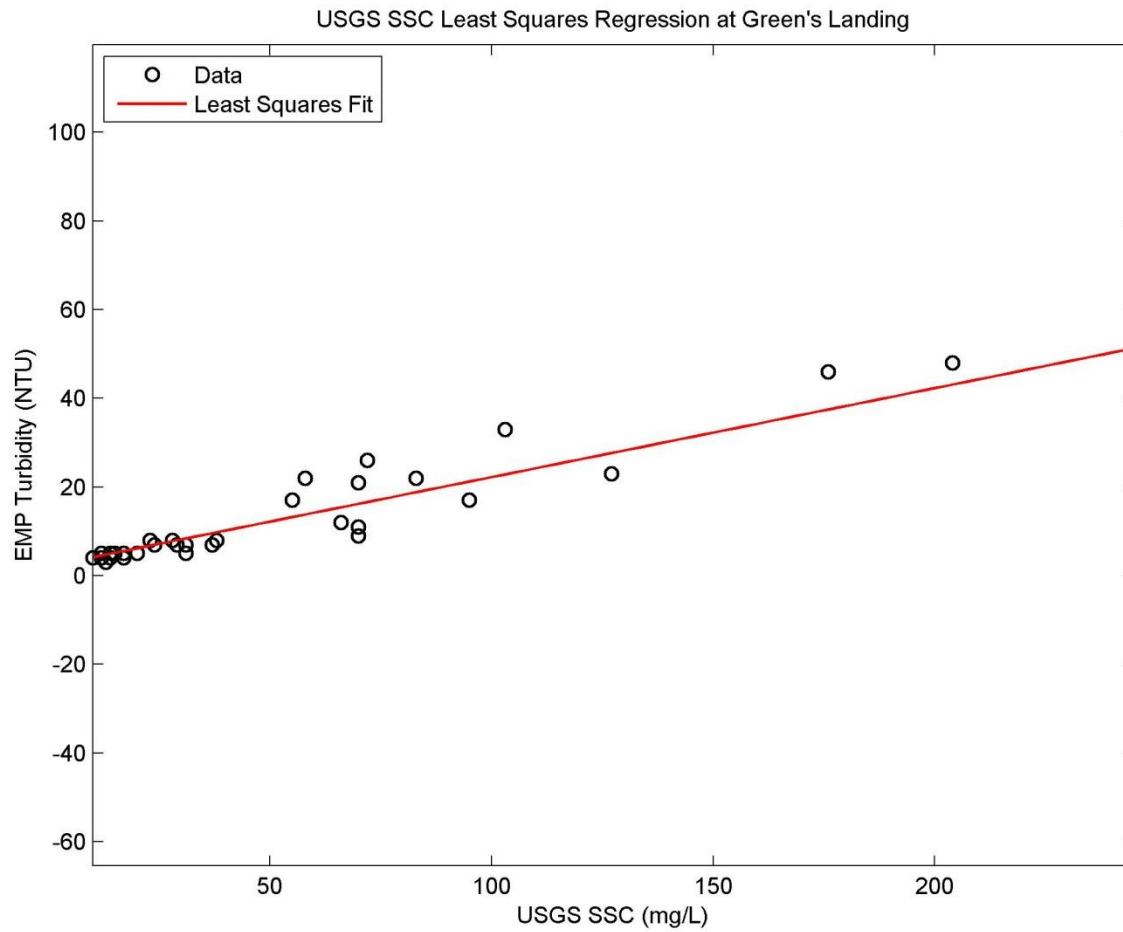


Figure 17 Relationship between USGS measured SSC at Freeport and EMP measured turbidity at Green's Landing. The least squares best fit regression was calculated as $\text{Turbidity (NTU)} = 0.201 * \text{SSC} + 2.1$.

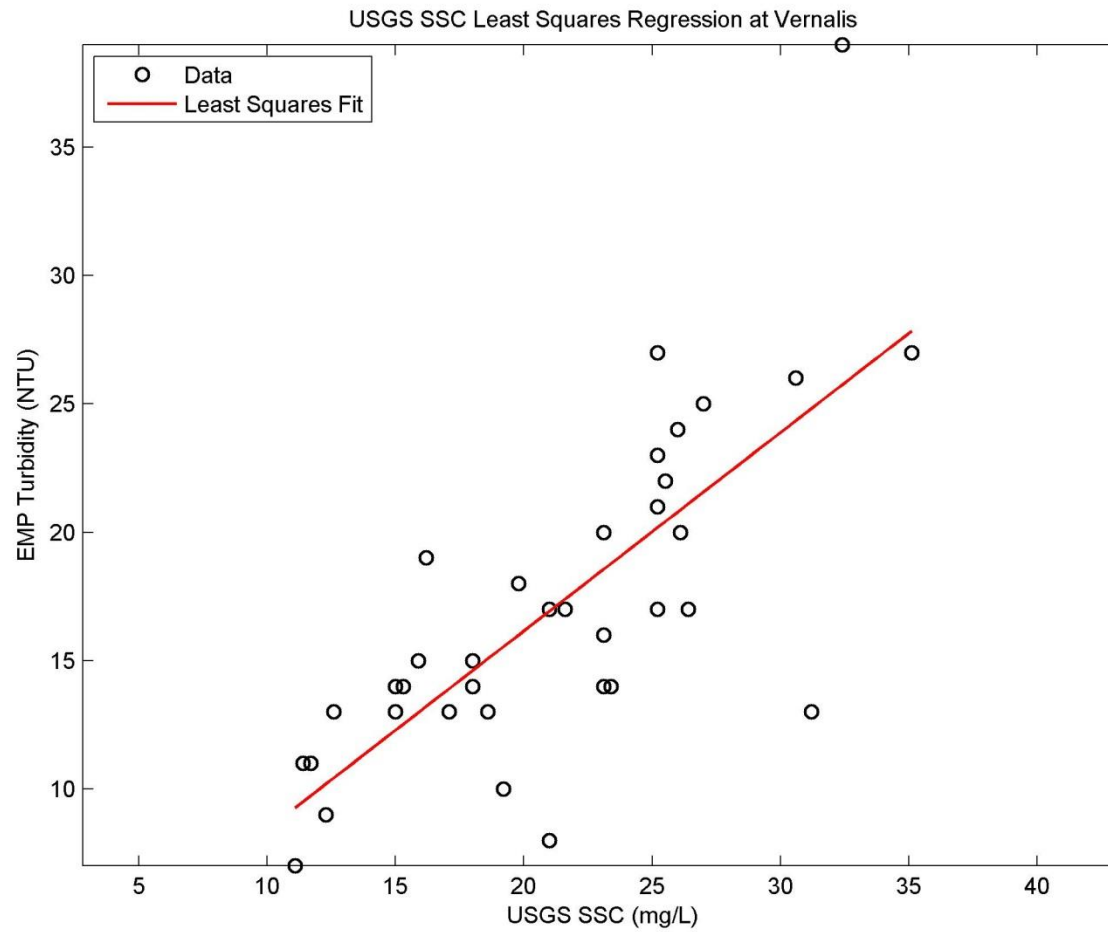


Figure 18 Relationship between USGS measured SSC at Vernalis and EMP measured turbidity at Vernalis. The least squares best fit regression was calculated as $\text{Turbidity (NTU)} = 0.773 * \text{SSC} + 0.7$.

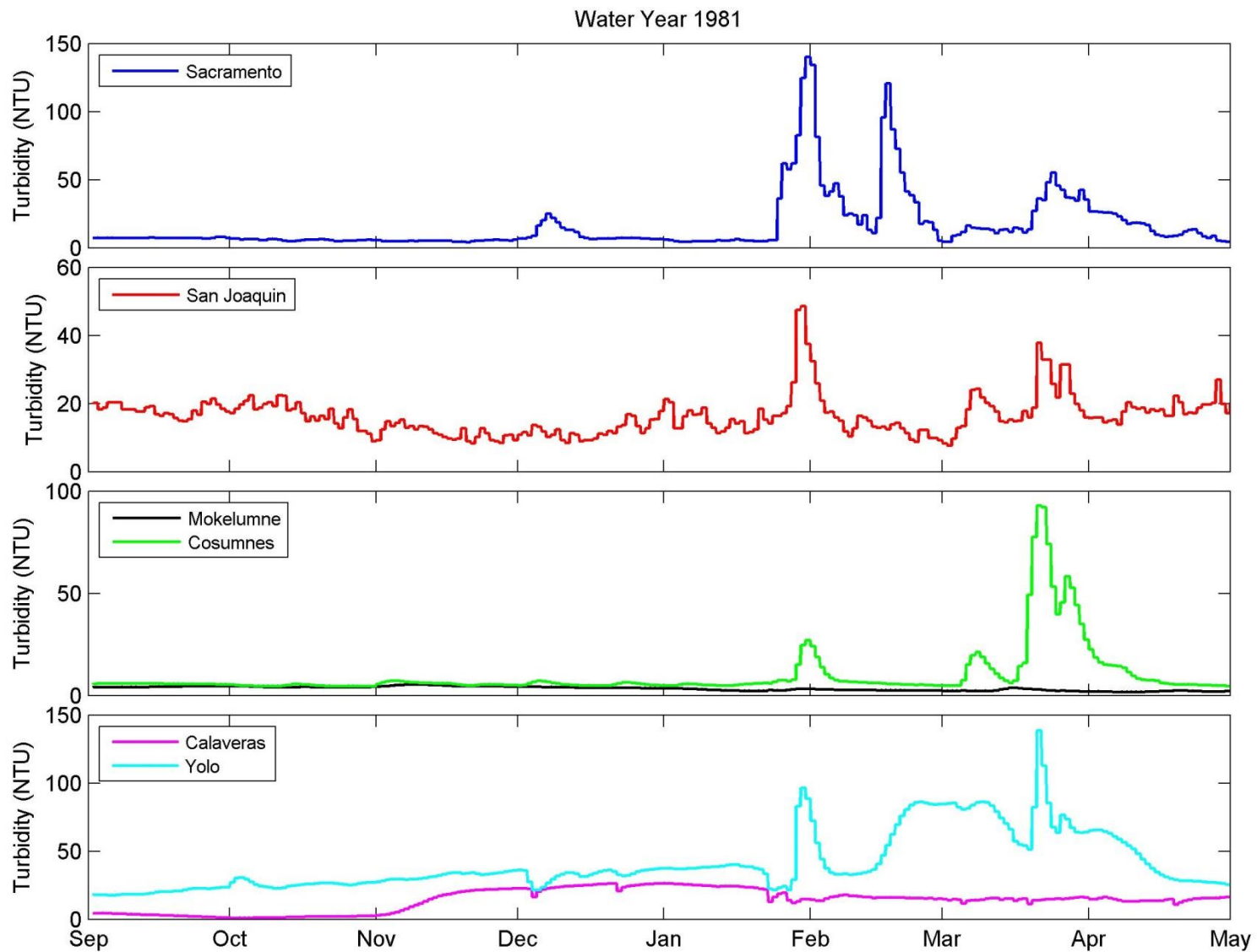


Figure 19 WY1981 turbidity boundary conditions. Sacramento and San Joaquin turbidities were obtained by a regression of USGS measured SSC with EMP measured turbidity values. Other tributary turbidities were generated using the WARMF watershed model.

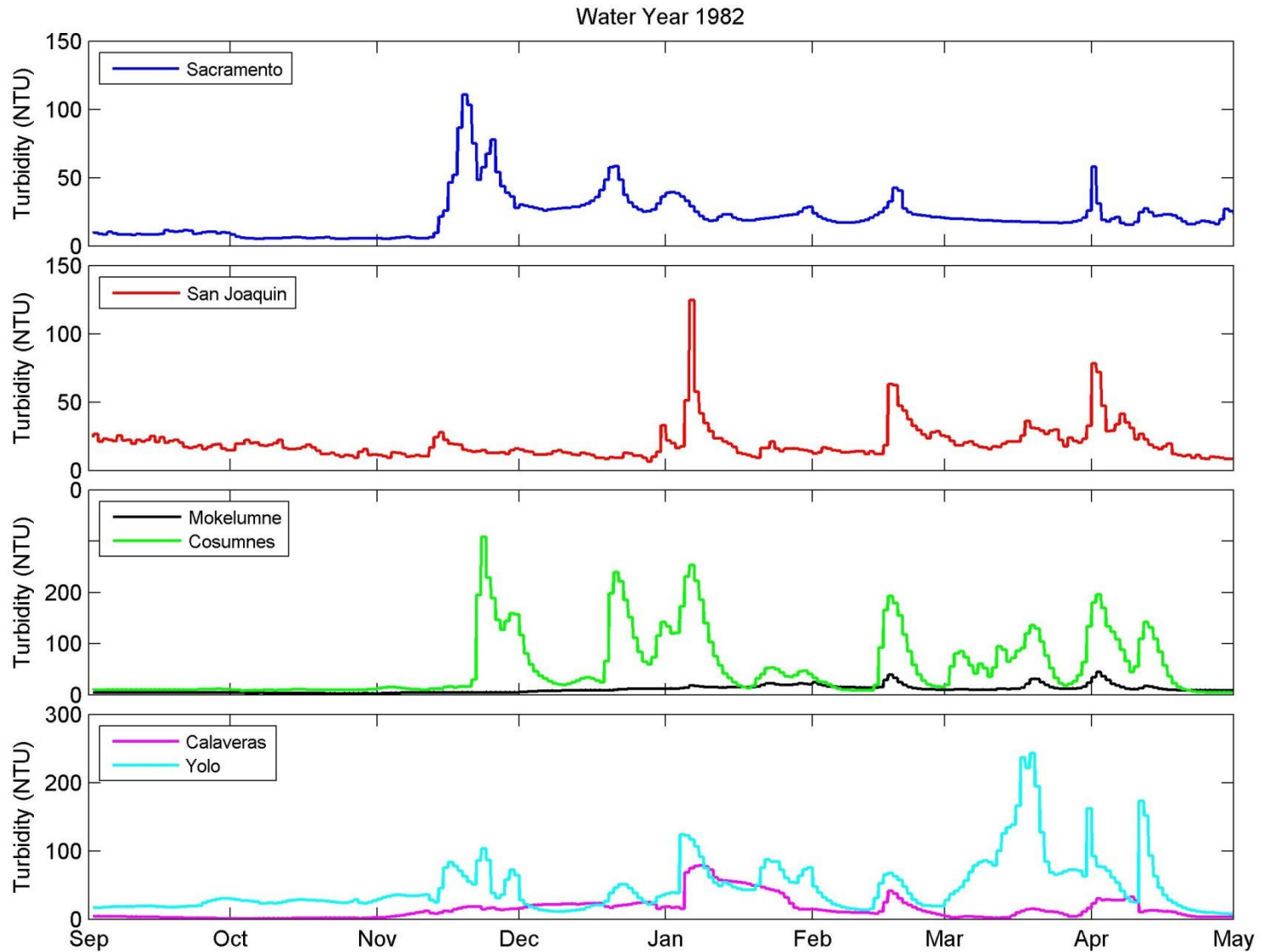


Figure 20 WY1982 turbidity boundary conditions. Sacramento and San Joaquin turbidities were obtained by a regression of USGS measured SSC with EMP measured turbidity values. Other tributary turbidities were generated using the WARMF watershed model.

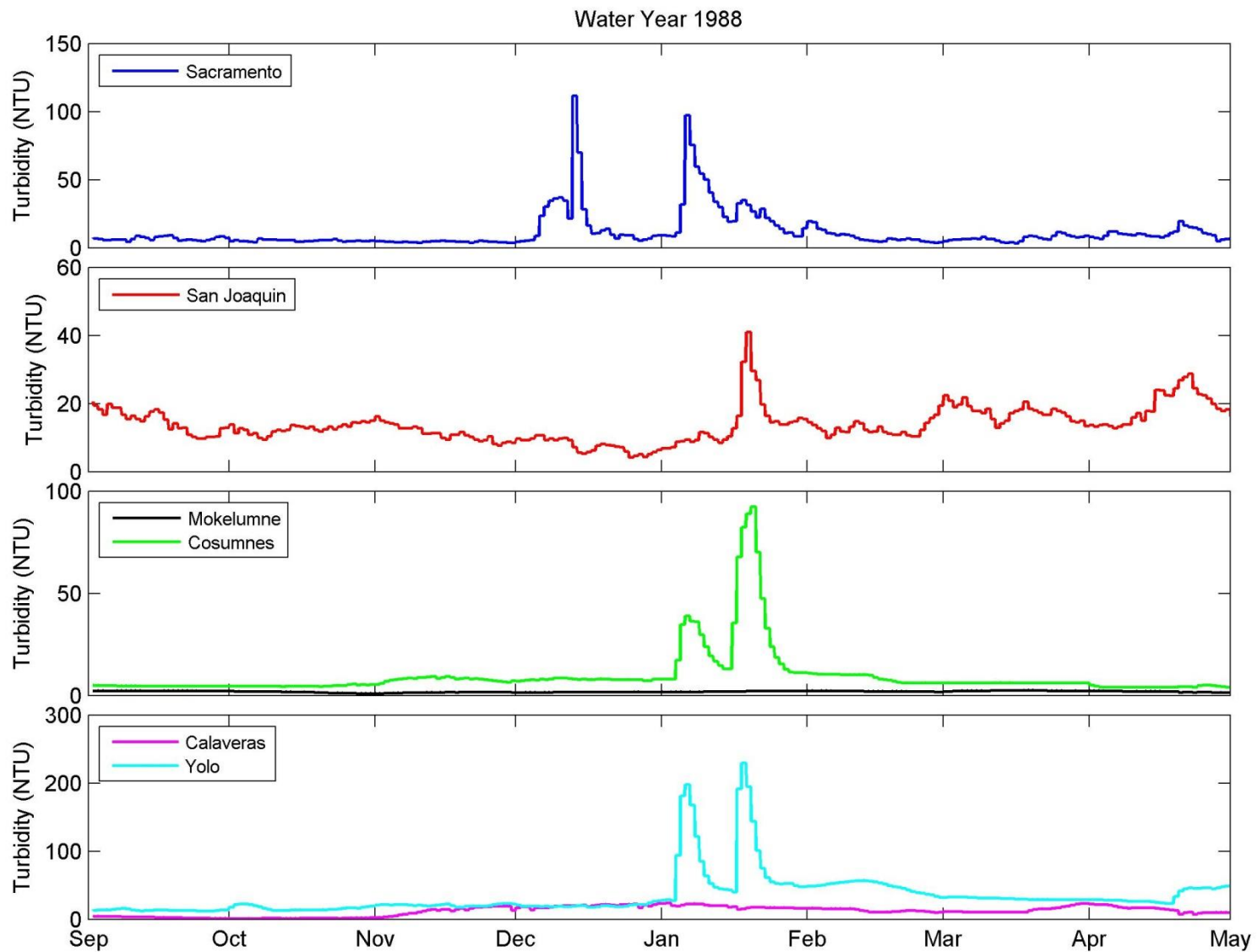


Figure 21 WY1988 turbidity boundary conditions. Sacramento and San Joaquin turbidities were obtained by a regression of USGS measured SSC with EMP measured turbidity values. Other tributary turbidities were generated using the WARMF watershed model.

Table 2 Turbidity decay coefficients used for model runs with time variable coefficients. Low = 0.01/day, Medium = 0.05/day.

	Sep	Oct	Nov	Dec	Jan	Feb	Mar	Apr
WY1981	Low	Low	Low	Low	Low	Medium	Medium	Medium
WY1982	Low	Low	Low	Medium	Medium	Medium	Medium	Medium
WY1988	Low	Low	Low	Low	Medium	Low	Low	Low

Results and Discussion

For each water year, three sets of comparison graphics are presented in order to compare model results with observed data. The first set presents time series data collected at the export locations. Included are observed and modeled data for both turbidity at the exports and smelt salvage. These graphics represent the true test of how well the model performed in its main objective: predicting smelt salvage. However, only examining time series at one location does not give the full story of how the model performed the way it did. Accordingly, the second set of comparison graphics shows spatial distributions of modeled and observed turbidity at several snapshot days throughout the water year. These days were chosen to align with turbidity data measured as part of the EMP and are given at a frequency of once per month. The third and final set of comparison graphics show modeled and observed smelt distributions in the Delta. Measured smelt distributions from the FMWT monitoring program are shown monthly for September through December, the autumn months when trawls were performed. Unfortunately, these plots mostly show smelt concentrated near the Sacramento-San Joaquin confluence area before any upstream migration occurred. Snapshots of modeled smelt distributions are shown for the fall and representative periods thereafter during which significant fish movement occurred.

The three sets of comparison graphics are presented for each water year for two different model runs:

1. Turbidity model simulations run using the original, high-flow calibrated turbidity decay coefficients from previous RMA modeling efforts. Smelt behavioral model simulations were run using these turbidity results and a minimum turbidity threshold of 16 NTU, similarly calibrated during previous RMA modeling work. These runs represent a true model validation study for the historical water years.
2. Turbidity model simulations run using new, time-variable decay coefficients. Smelt behavioral model simulations were run using these turbidity results and three different minimum turbidity thresholds: 10, 12, and 14 NTU. These runs represent efforts to examine the applicability of the model on conditions over which it was not originally calibrated to handle. Time variable decay coefficients were an attempt to improve turbidity model fit during periods of low flow. Lower minimum turbidity thresholds in the smelt model were an attempt to explore the sensitivity of the model to this parameter and potentially better replicate early season salvage in WYs 1981 and 1982.

Model runs using the original calibration coefficients performed poorly in replicating observed smelt salvage patterns for WY1981 and WY1982, but performed very well in WY1988. The likely reason for this is that WY1988 had a well-defined first-flush turbidity pulse, whereas WYs 1981 and 1982 had weak or multi-storm first-flush events. Since WY1988 better represented the conditions for which the turbidity and smelt model were originally developed, it performed better.

Changes to the turbidity decay coefficients (the second set of model runs) to better model low flow turbidity in the system allowed the model to better predict mid- and late-season salvage for all of the water years. However, early fall salvage was still absent from model predictions.

Descriptions of model performance and a discussion of smelt migratory patterns and forcing factors are given below for each individual water year.

Water Year 1981

Observed smelt salvage was high throughout the months of September to November. This has been hypothesized to be due to higher than average turbid San Joaquin flows (Pete Smith pers. comm. 27 Aug 2012). However, the observed and modeled turbidity patterns do not indicate a full bridge forming to link high turbidities between the confluence and the southern export areas during these months; a band of low (8–10 NTU) turbidities persists through the southern central Delta (see Figure 35 and Figure 36). Smelt distribution data do not include measurements in the Old and Middle River corridor, but of the locations that are shown, there is nothing to indicate a distribution shifted more towards the southern Delta than usual (Figure 27 and Figure 28). Smelt distributions modeled using the improved low-flow coefficients during this time (Figure 39) also show smelt located near the confluence area, in response to the calculated EC and turbidity fields. The discrepancy in fall observed versus modeled salvage patterns may be due to uncertainties in fish counting or identification practices at the salvage facilities during this time. They may also be the result of incorrect assumptions about the parameters that govern smelt migration; e.g., turbidity threshold values or what gradients in turbidity smelt are able to detect. The low turbidity values found in both the observed and modeled data through the southern central data, however, suggest that uncertainty in model boundary conditions are not responsible for the discrepancy.

Following the fall low-flow season, a storm in early December coupled with an open DCC brought high turbidities into the South Delta (Figure 24). This led to a broad peak in observed salvage in mid-December. The RMA turbidity model run using the original calibration coefficients greatly underpredicted values through the central Delta (Figure 24), and the model run with improved calibration coefficients (Figure 36) still slightly underpredicted values. This led to a disparity in observed versus modeled salvage. The original model coefficient runs completely missed this salvage peak. Modeled smelt salvage using the improved coefficients peaked later in January, as turbidities diffused into the central and south Delta and smelt were passively transported down to the export locations without following a well-defined turbidity gradient (Figure 40). The disparity between the central Delta modeled and observed turbidities during this period may be due to general model inaccuracy for the conditions, or may be due to the increased central Delta turbidities due to wind resuspension associated with the winter storm. This process would not have been accounted for in the model.

A spike in the observed salvage in mid-January (before the arrival of the first large storm pulse on the Sacramento River) has been hypothesized to be due to an increase in export pumping at that time (Pete Smith pers. comm. 27 Aug 2012). However, EMP measured turbidity distributions corresponding to this time period do not show the turbidity increases through the Old and Middle River corridor that would be expected with this scenario (Figure 37).

Following January, storms in the basin bring increased turbidities to the central and south Delta regions, causing smelt to follow and leading to broad peaks in observed salvage in February and March (Figure 34). In the RMA particle smelt model run using improved calibration coefficients, particles begin moving

into Franks Tract on Feb 1 (Figure 41) and are at the pumps by Mar 1 (Figure 42). This leads to increased salvage beginning slightly later than observed. Model runs using the original calibration coefficients produce a salvage peak in late March (Figure 22). This peak, however, represented only a very small fraction of the simulated particles (0.02%).

High-Flow Calibrated Smelt and Turbidity Model Summary Results

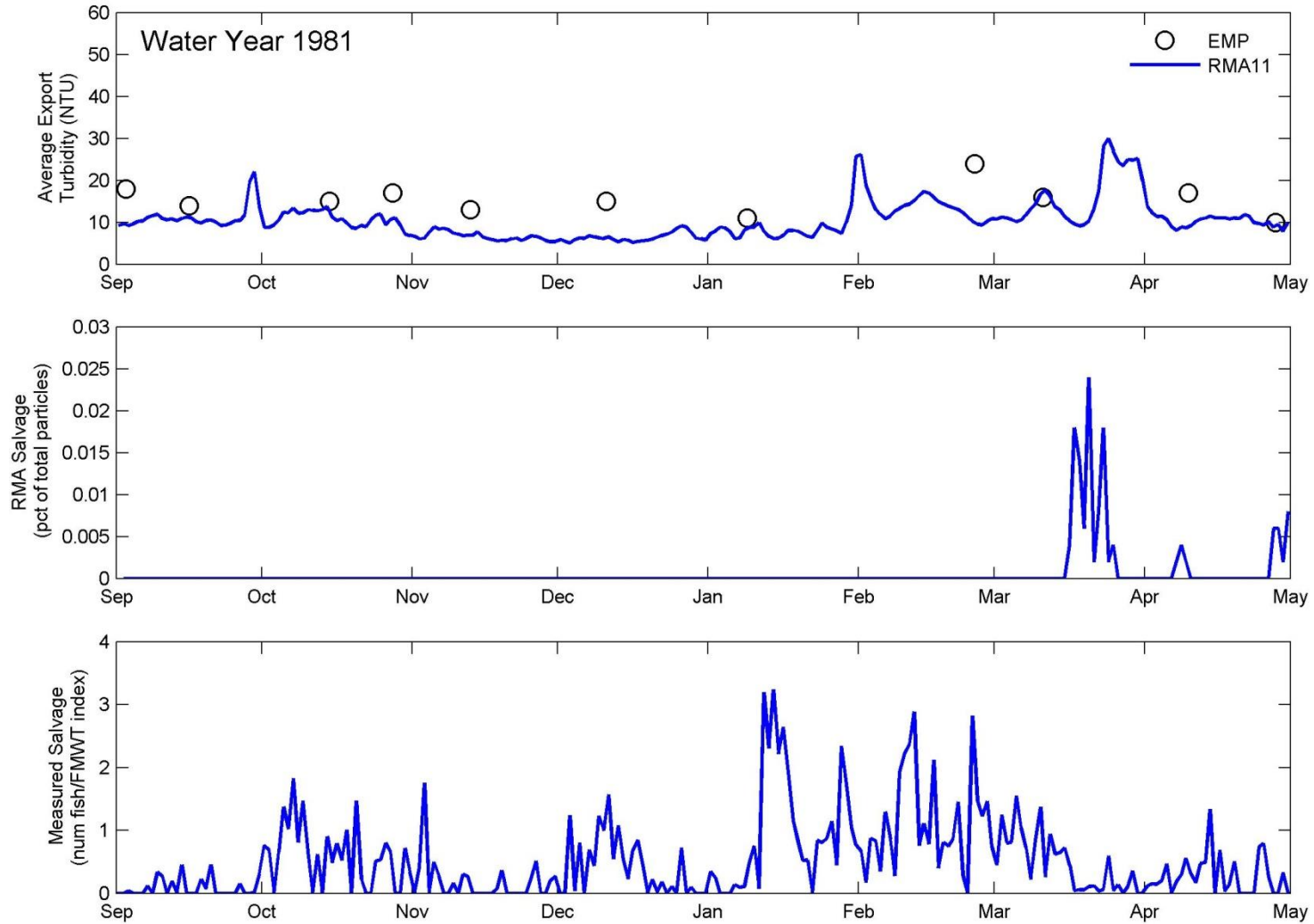
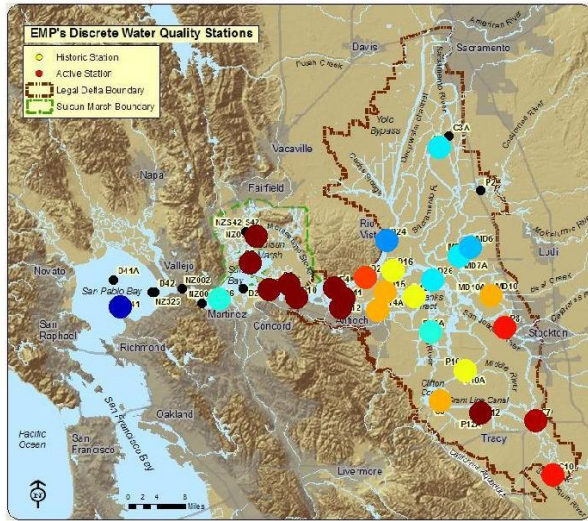


Figure 22 WY1981 modeled and observed turbidity and delta smelt salvage at the southern export locations. Original calibrated turbidity decay coefficients and smelt minimum turbidity thresholds were used. Top panel shows average modeled turbidity at the export locations along with EMP observed data. Middle panel shows RMA modeled smelt salvage (as a percent of total input particles). Bottom panel shows observed smelt salvage as number of fish divided by the water year FMWT index (a measure of the total smelt population size).

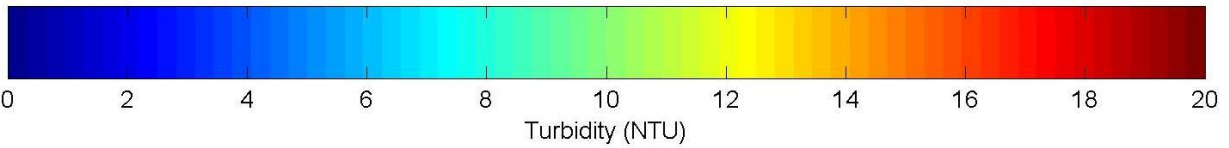
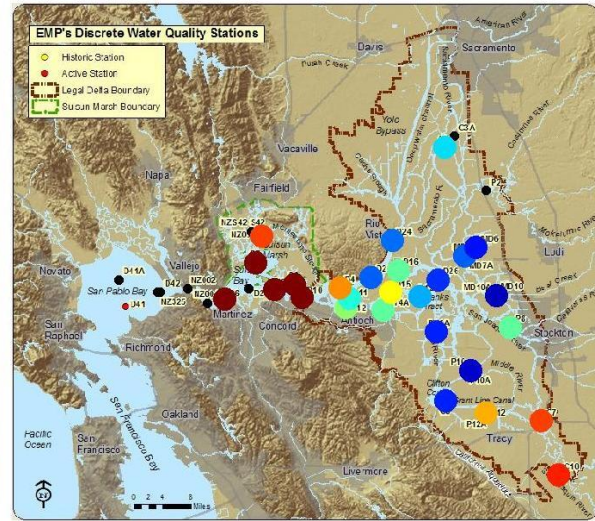
High-Flow Calibrated Model EMP Comparison Plots

17 Sep 1980

EMP Data

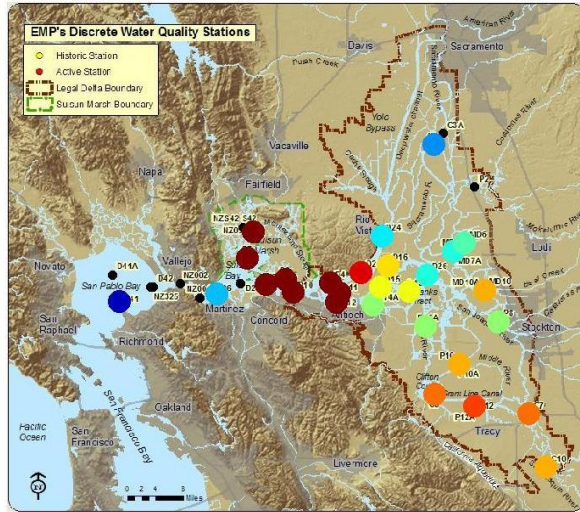


RMA11 Data



16 Oct 1980

EMP Data



RMA11 Data

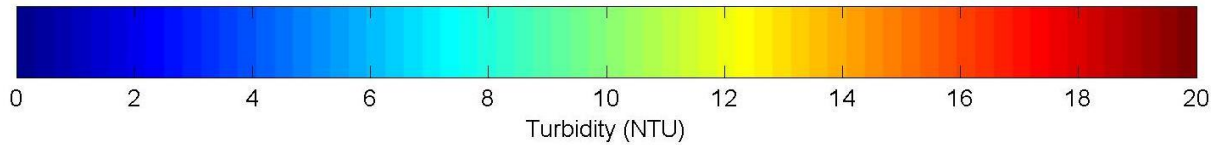
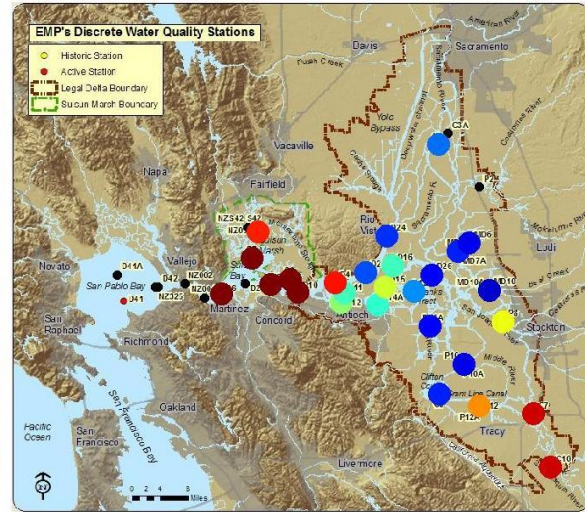
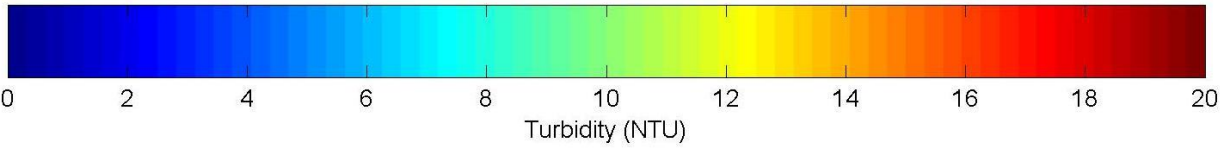
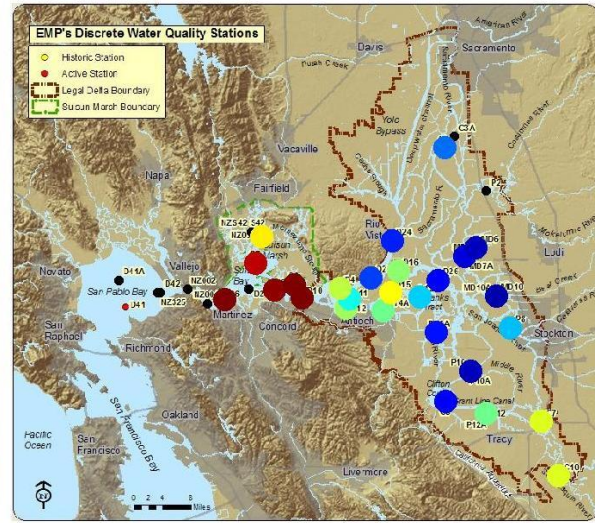
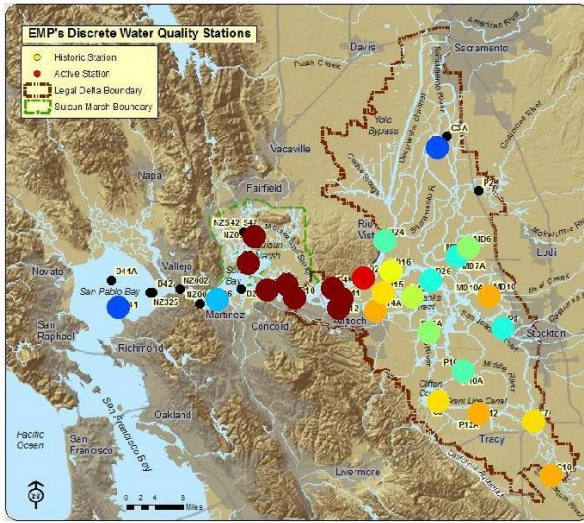


Figure 23 Turbidity distributions measured by the EMP (left panels) and modeled by RMA (right panels) for September (top panels) and October (bottom panels), WY1981. High-flow calibrated turbidity decay coefficients were used.

13 Nov 1980

EMP Data

RMA11 Data



11 Dec 1980

EMP Data

RMA11 Data

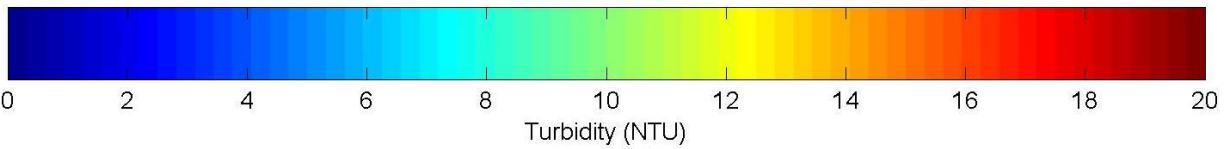
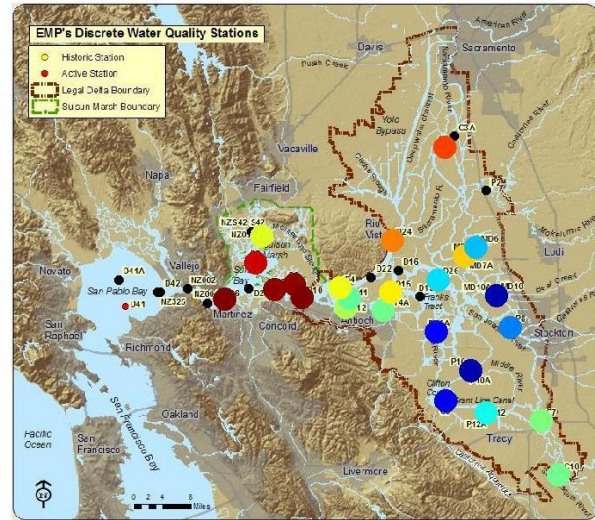
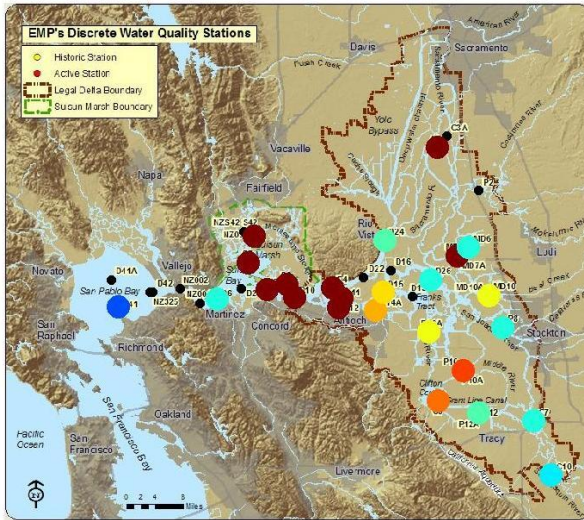
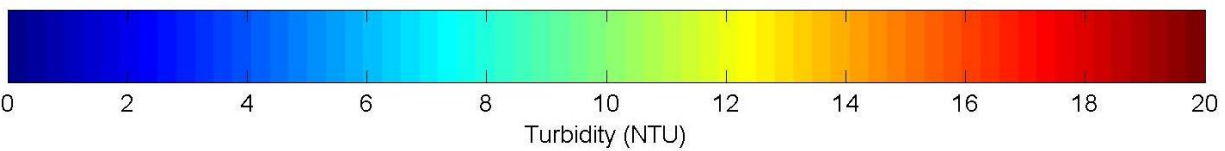
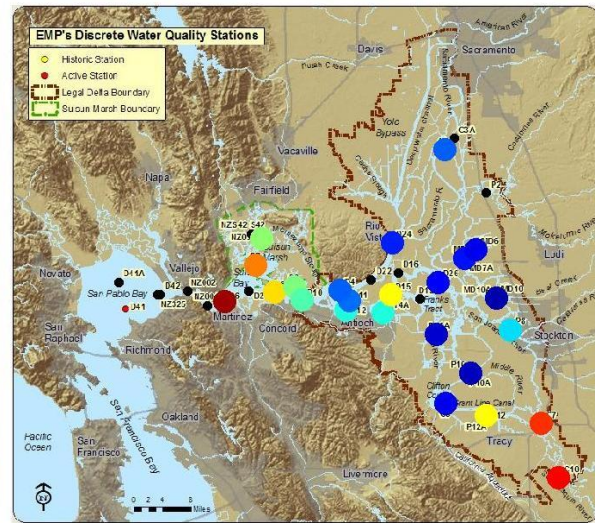
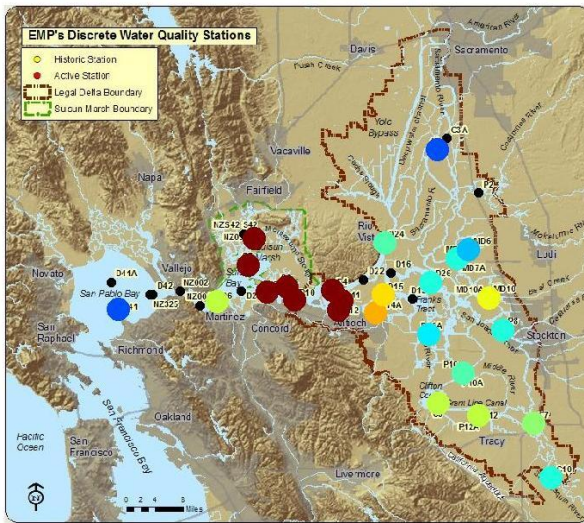


Figure 24 Turbidity distributions measured by the EMP (left panels) and modeled by RMA (right panels) for November (top panels) and December (bottom panels), WY1981. High-flow calibrated turbidity decay coefficients were used.

09 Jan 1981

EMP Data

RMA11 Data



26 Feb 1981

EMP Data

RMA11 Data

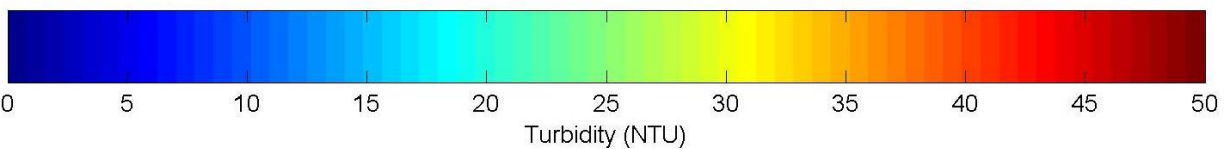
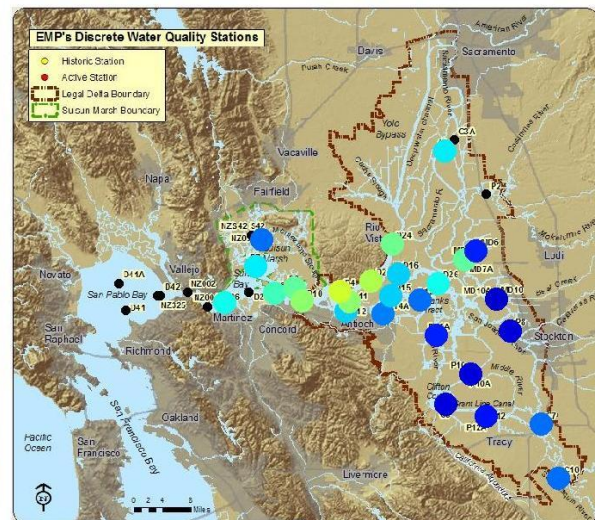
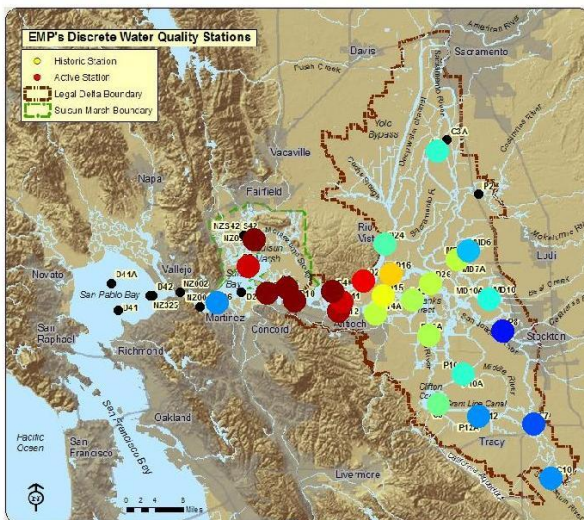
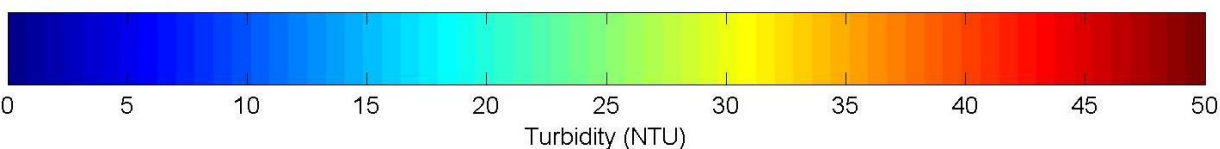
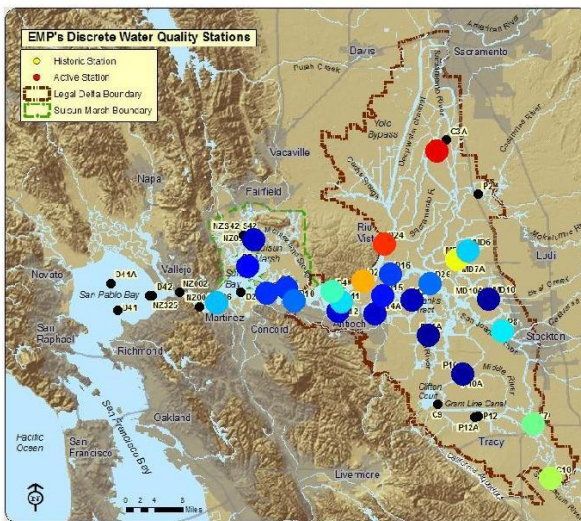
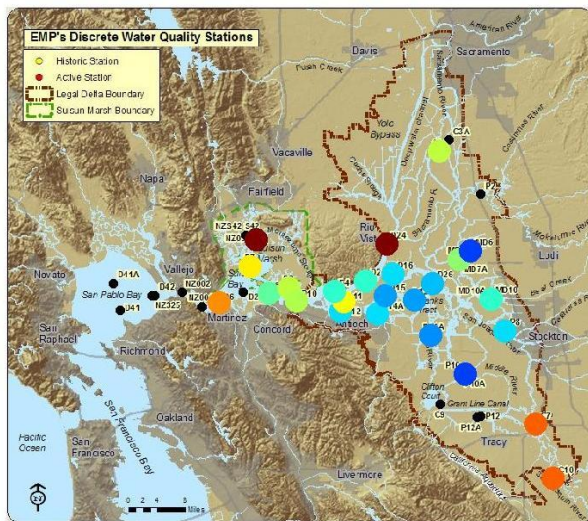


Figure 25 Turbidity distributions measured by the EMP (left panels) and modeled by RMA (right panels) for January (top panels) and February (bottom panels), WY1981. Note differences in color scale between top and bottom panels. High-flow calibrated turbidity decay coefficients were used.

26 Mar 1981

EMP Data

RMA11 Data



29 Apr 1981

EMP Data

RMA11 Data

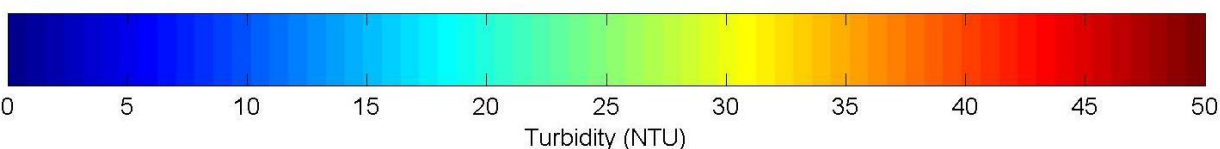
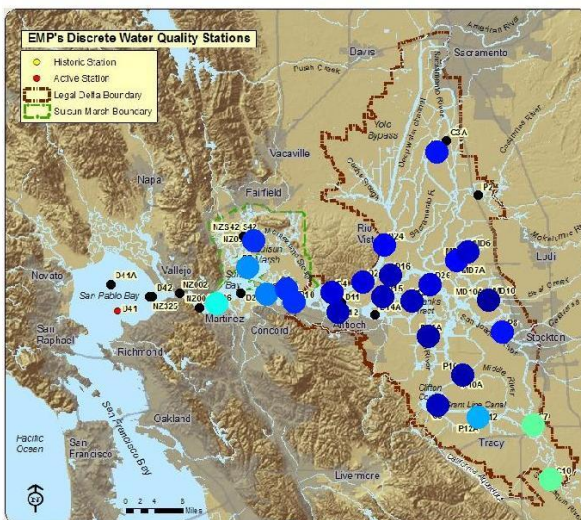
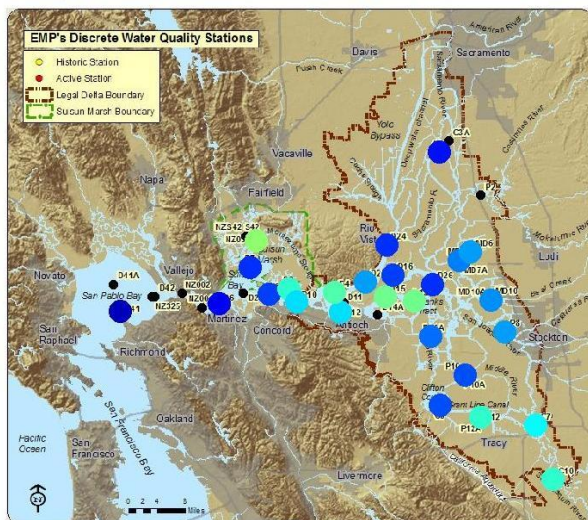


Figure 26 Turbidity distributions measured by the EMP (left panels) and modeled by RMA (right panels) for March (top panels) and April (bottom panels), WY1981. High-flow calibrated turbidity decay coefficients were used.

Fall Midwater Trawl Observed Smelt Distributions

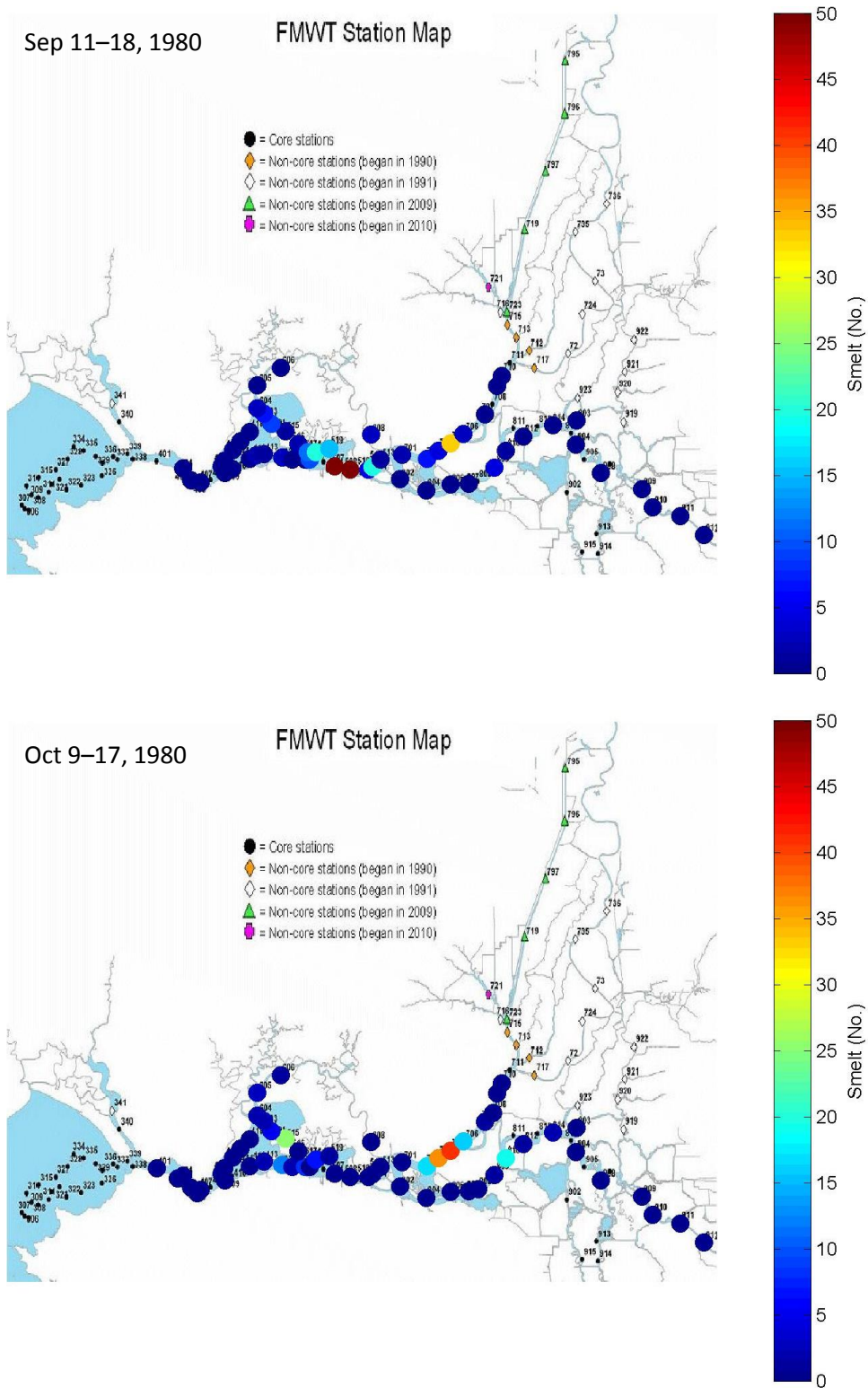


Figure 27 September and October 1980 FMWT ADS catch distributions. Dates indicate range of days catch was made over.

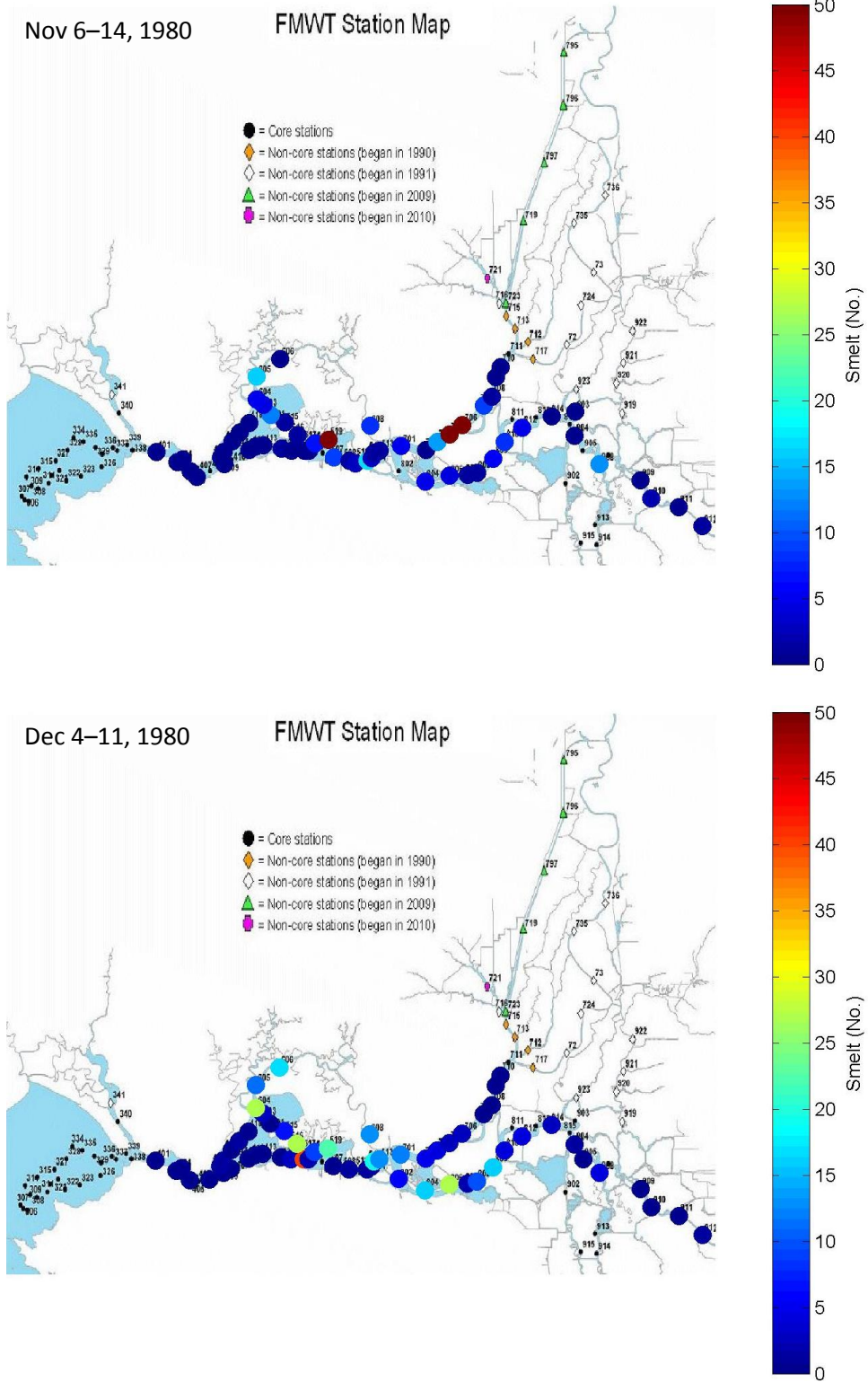


Figure 28 November and December 1980 FMWT ADS catch distributions. Dates indicate range of days catch was made over.

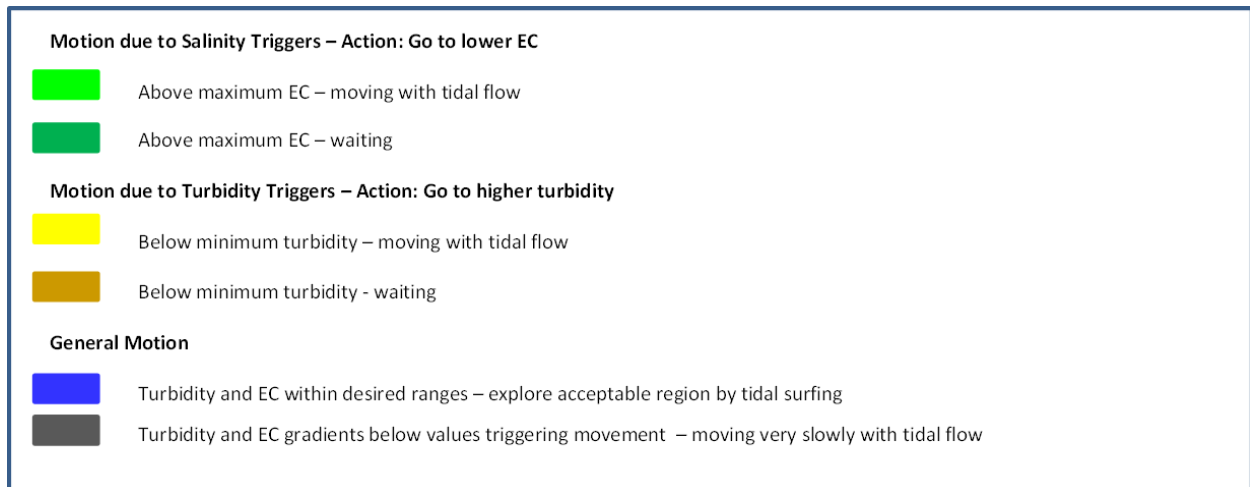


Figure 29 RMA PTRK behavioral color codes used in modeled smelt distribution figures.

Original Model Calibration RMA PTRK Modeled Smelt Distributions

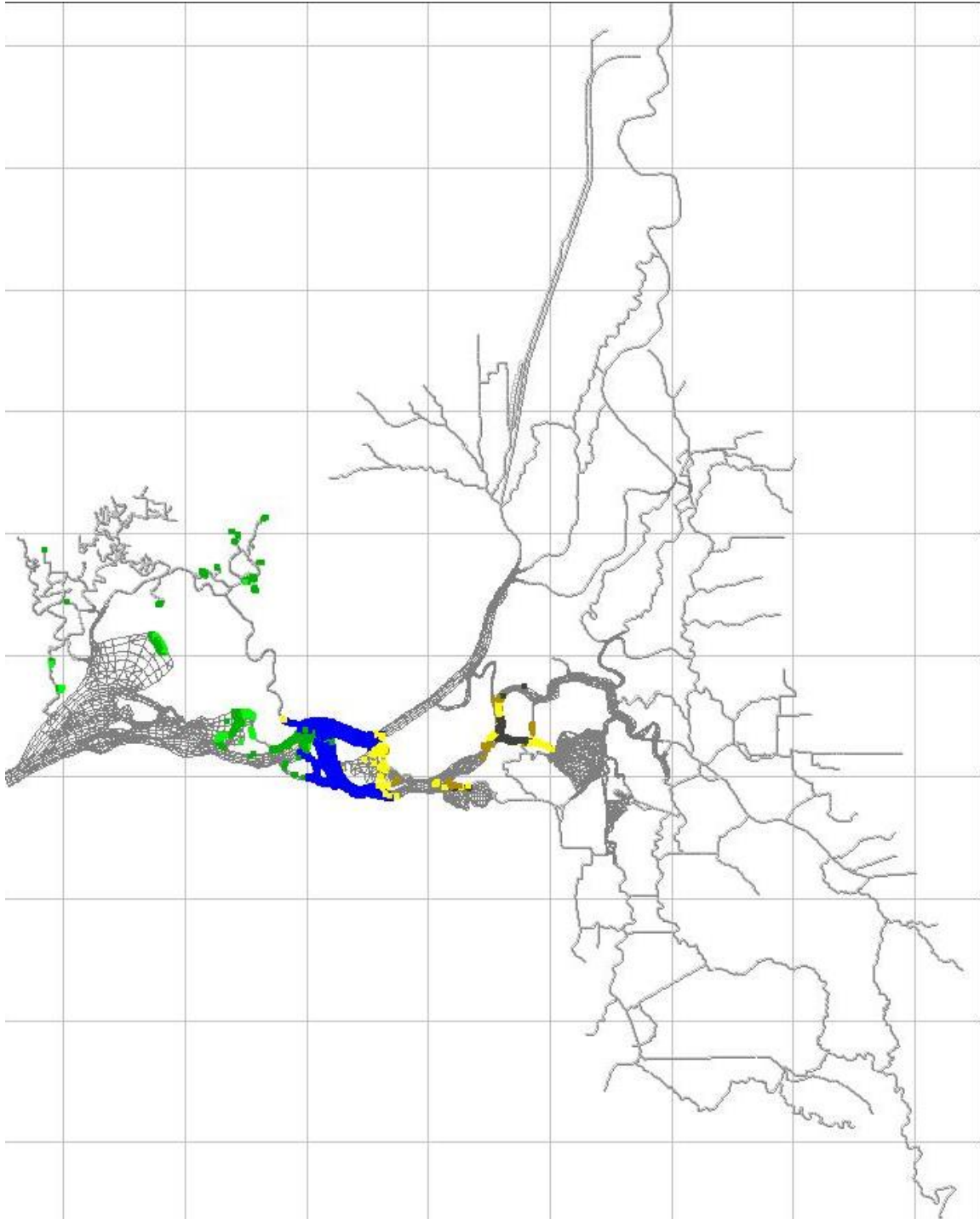


Figure 30 RMA PTRK modeled smelt distribution, November 1, 1980. For behavioral color codes, see Figure 29. Model results were driven using a smelt turbidity minimum threshold of 16 NTU and turbidity model results obtained with high-flow calibrated parameters.

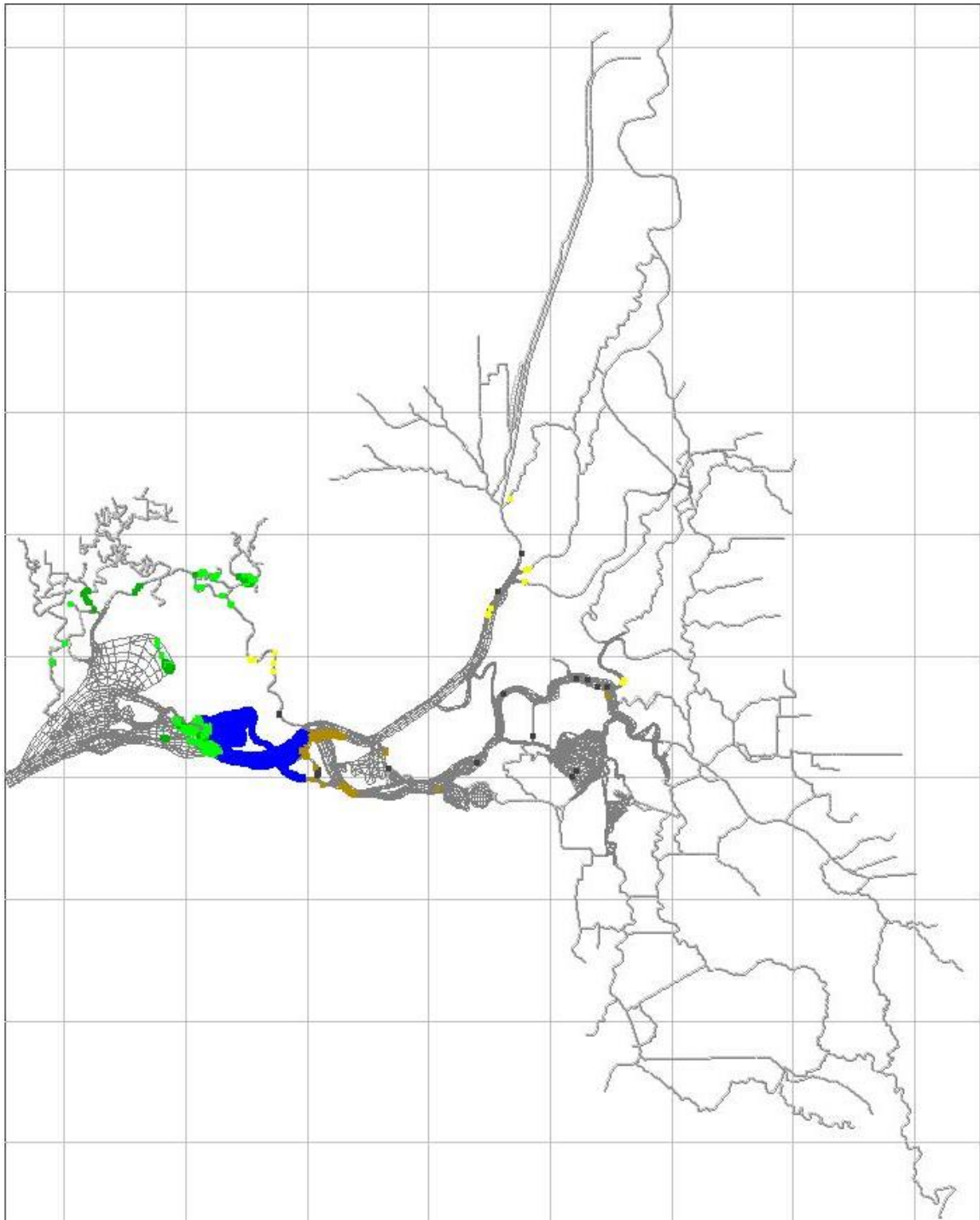


Figure 31 RMA PTRK modeled smelt distribution, January 1, 1981. For behavioral color codes, see Figure 29. Model results were driven using a smelt turbidity minimum threshold of 16 NTU and turbidity model results obtained with high-flow calibrated parameters.

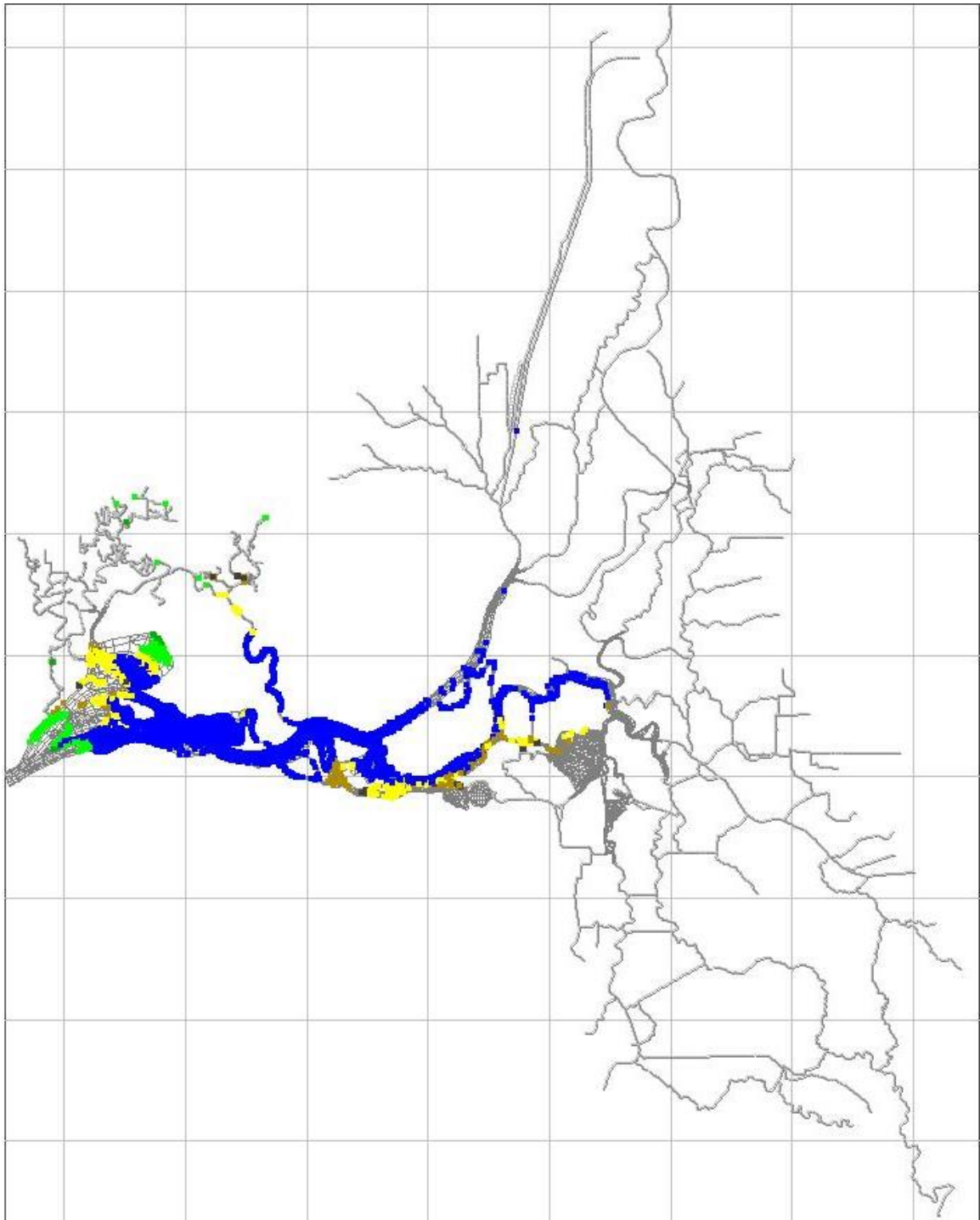


Figure 32 RMA PTRK modeled smelt distribution, February 1, 1981. For behavioral color codes, see Figure 29. Model results were driven using a smelt turbidity minimum threshold of 16 NTU and turbidity model results obtained with high-flow calibrated parameters.

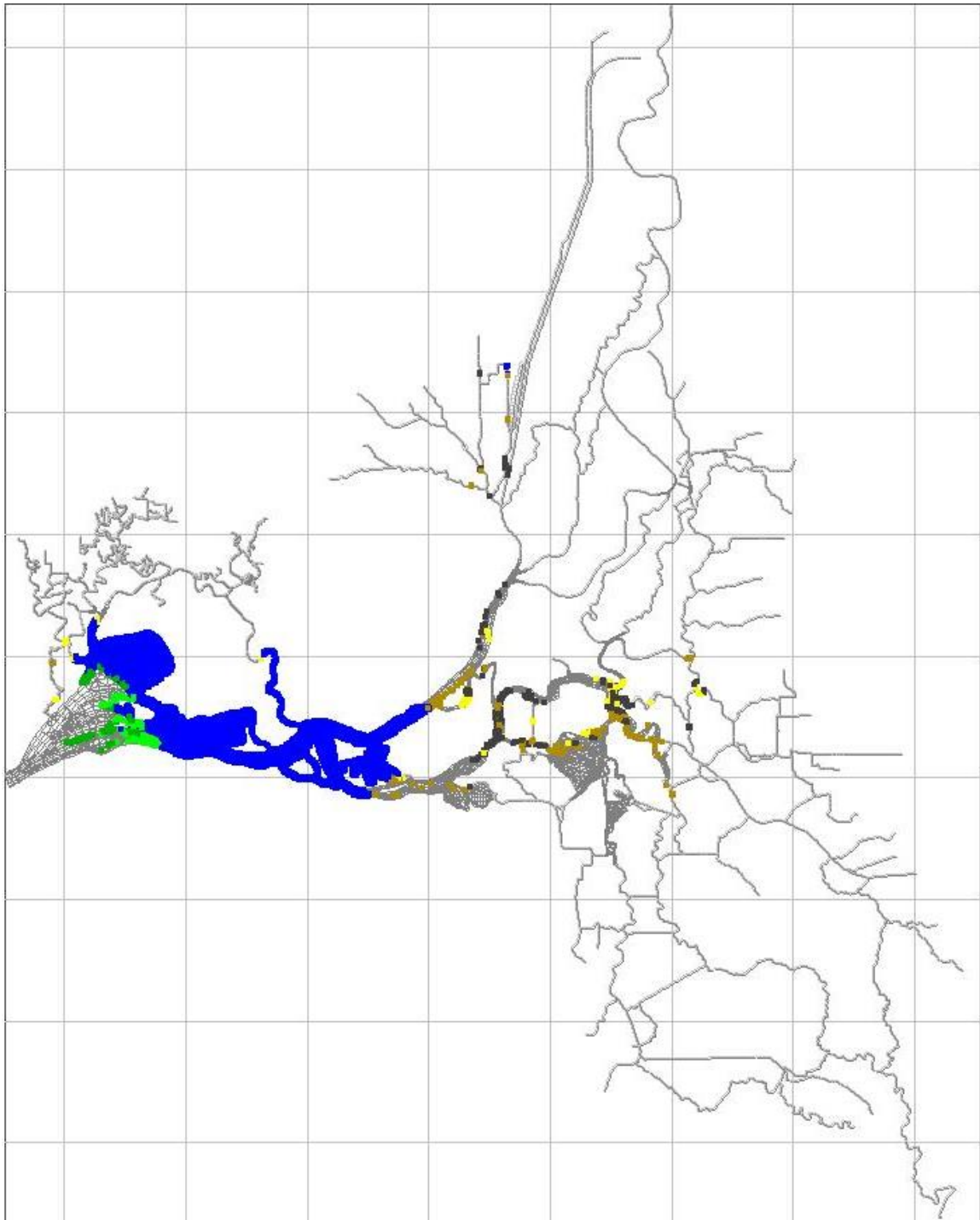


Figure 33 RMA PTRK modeled smelt distribution, March 1, 1981. For behavioral color codes, see Figure 29. Model results were driven using a smelt turbidity minimum threshold of 16 NTU and turbidity model results obtained with high-flow calibrated parameters.

Time Variable Decay Coefficient Smelt and Turbidity Model Summary Results

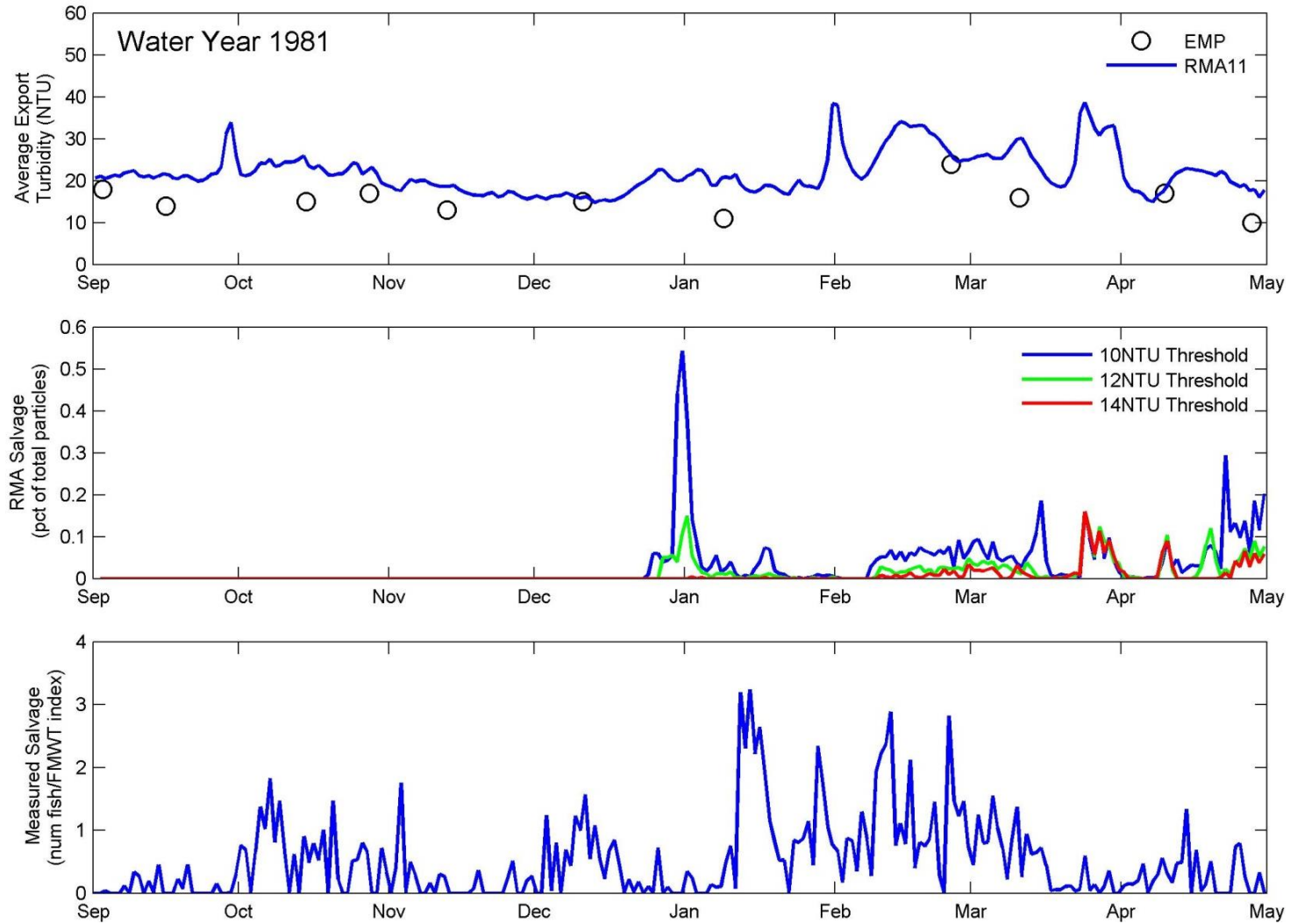
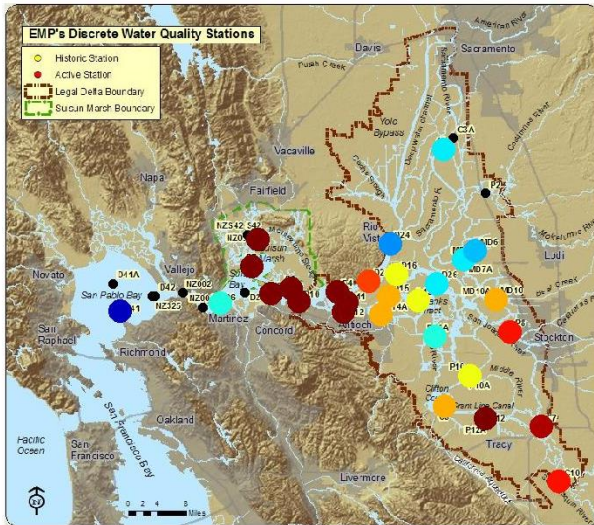


Figure 34 WY1981 modeled and observed turbidity and delta smelt salvage at the southern export locations. Time variable turbidity decay coefficients were used. Top panel shows average modeled turbidity at the export locations along with EMP observed data. Middle panel shows RMA modeled smelt salvage (as a percent of total input particles) using three different max turbidity threshold values. Bottom panel shows observed smelt salvage as number of fish divided by the water year FMWT index (a measure of the total smelt population size).

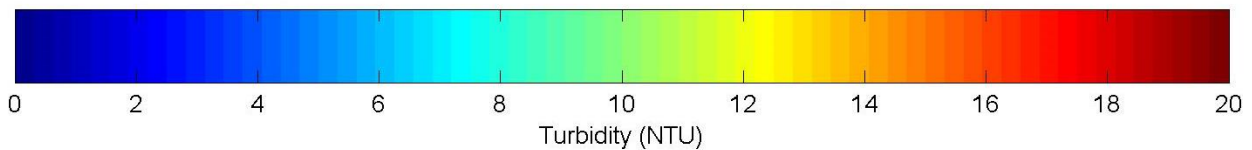
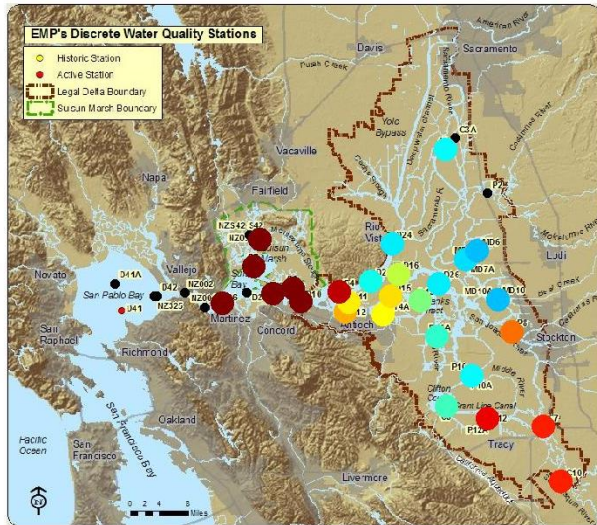
Time Variable Decay Coefficient Model EMP Comparison Plots

17 Sep 1980

EMP Data

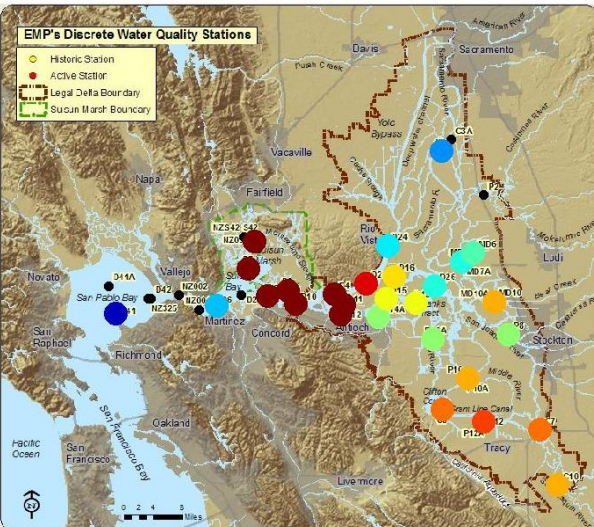


RMA11 Data



16 Oct 1980

EMP Data



RMA11 Data

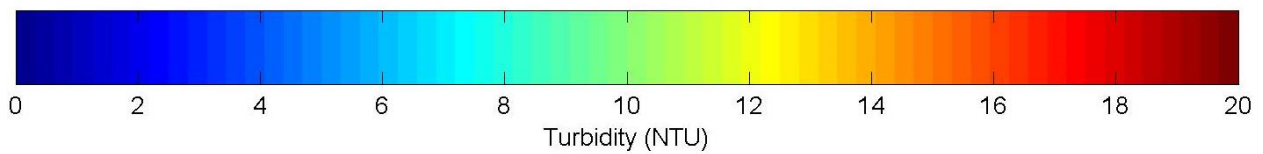
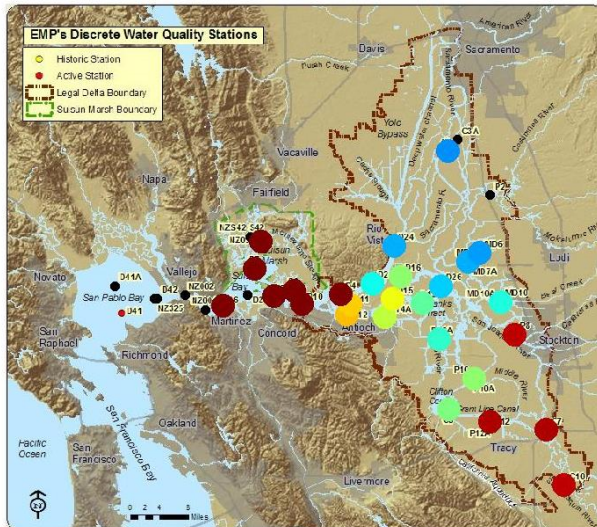
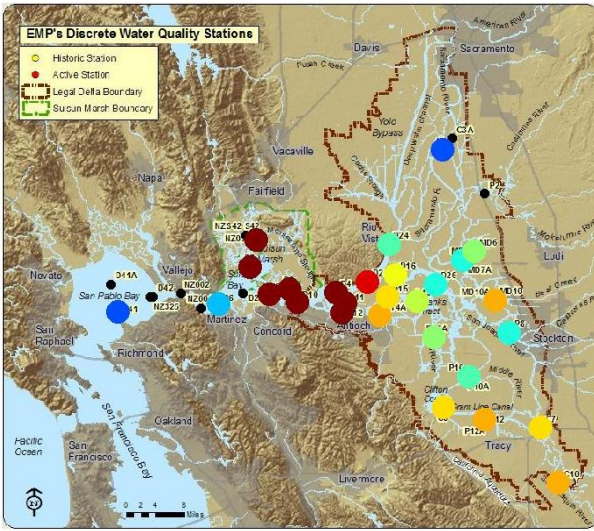


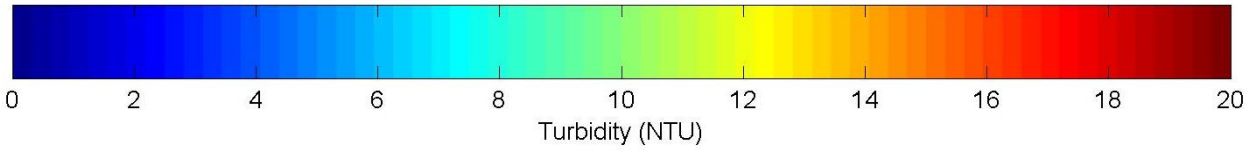
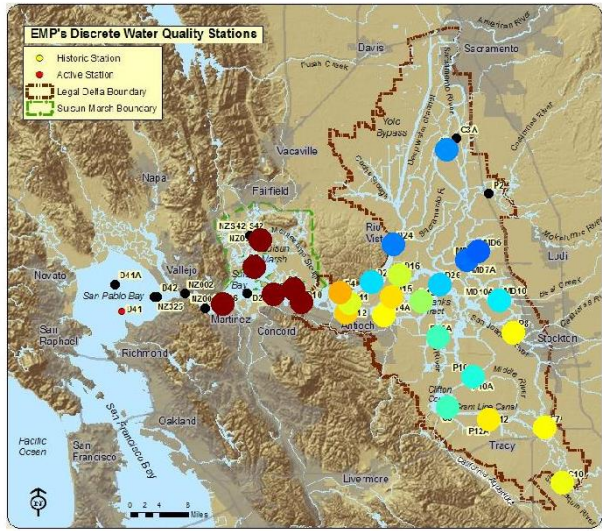
Figure 35 Turbidity distributions measured by the EMP (left panels) and modeled by RMA (right panels) for September (top panels) and October (bottom panels), WY1981. Time variable turbidity decay coefficients were used.

13 Nov 1980

EMP Data

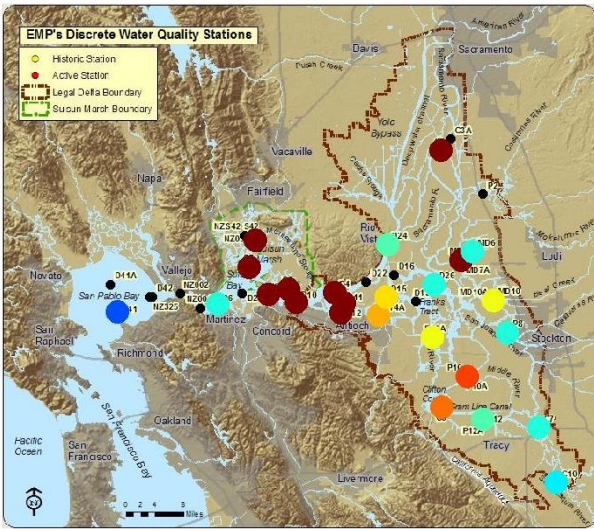


RMA11 Data



11 Dec 1980

EMP Data



RMA11 Data

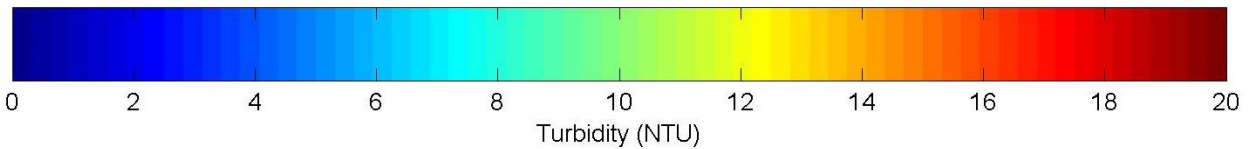
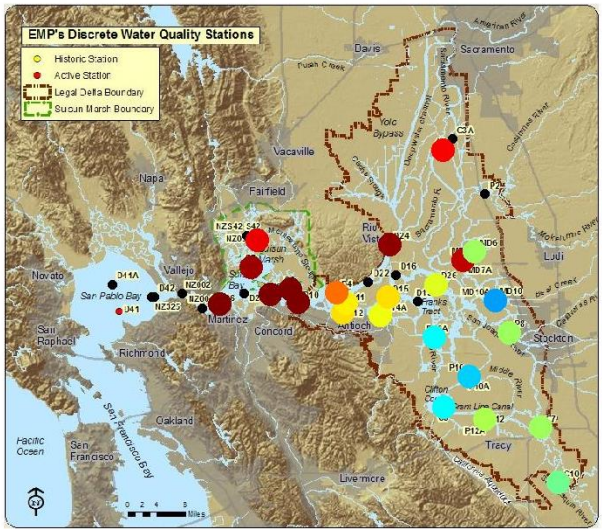
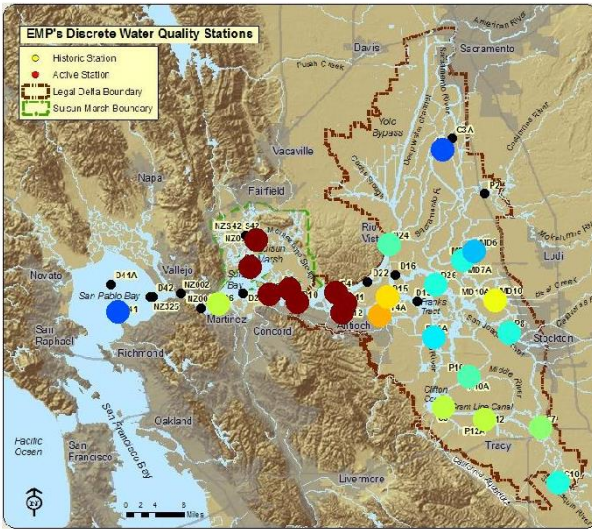


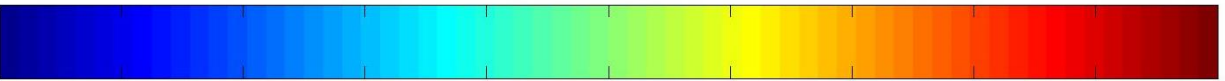
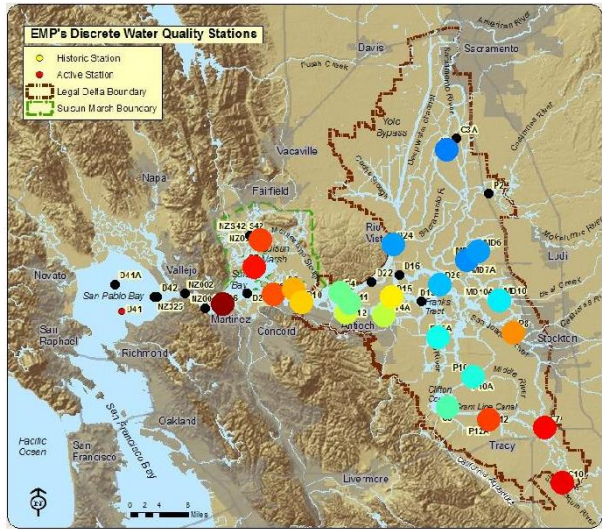
Figure 36 Turbidity distributions measured by the EMP (left panels) and modeled by RMA (right panels) for November (top panels) and December (bottom panels), WY1981. Time variable turbidity decay coefficients were used.

09 Jan 1981

EMP Data



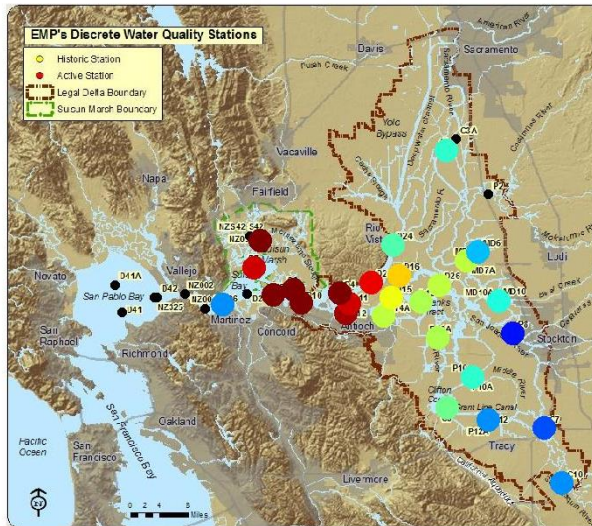
RMA11 Data



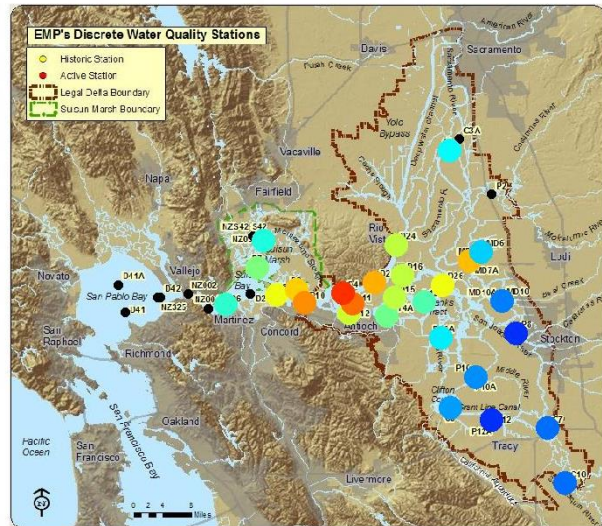
Turbidity (NTU)

26 Feb 1981

EMP Data



RMA11 Data

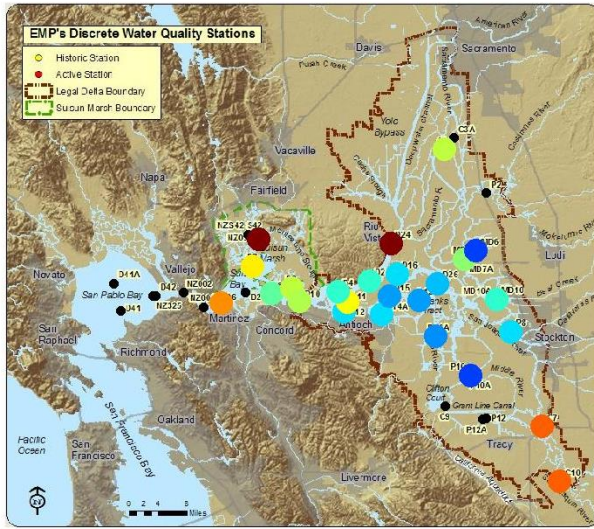


Turbidity (NTU)

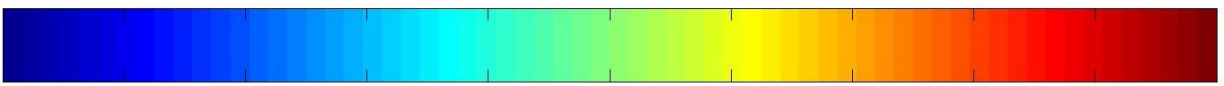
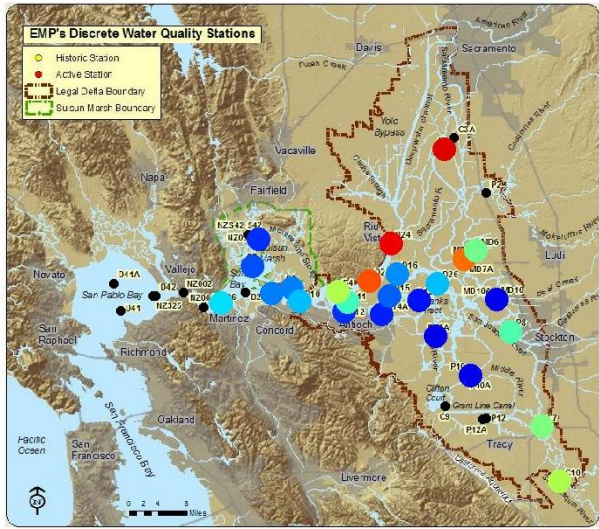
Figure 37 Turbidity distributions measured by the EMP (left panels) and modeled by RMA (right panels) for January (top panels) and February (bottom panels), WY1981. Note differences in color scale between top and bottom panels. Time variable turbidity decay coefficients were used.

26 Mar 1981

EMP Data



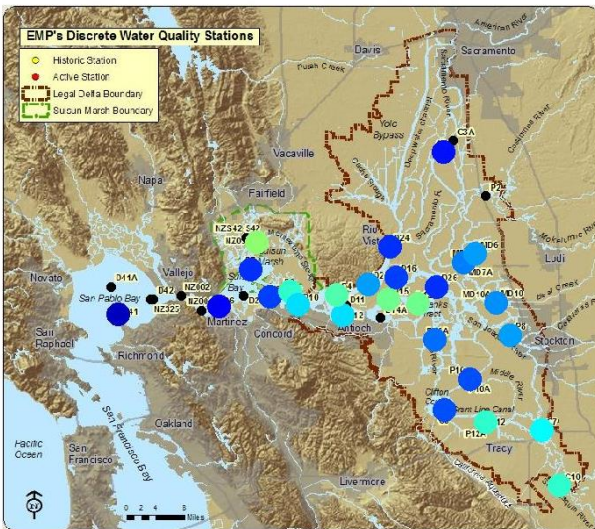
RMA11 Data



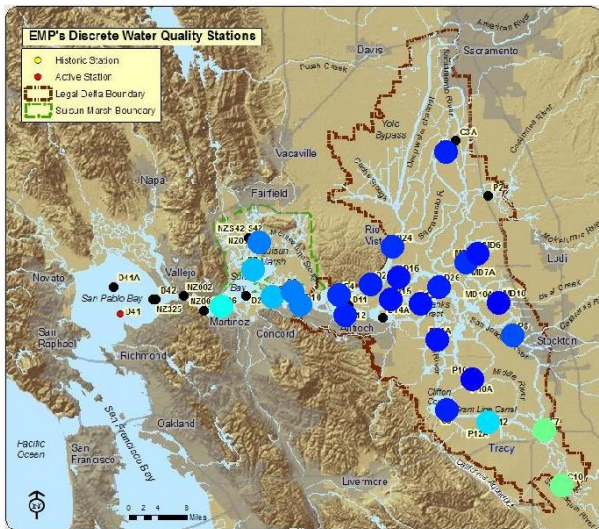
0 5 10 15 20 25 30 35 40 45 50
Turbidity (NTU)

29 Apr 1981

EMP Data



RMA11 Data



0 5 10 15 20 25 30 35 40 45 50
Turbidity (NTU)

Figure 38 Turbidity distributions measured by the EMP (left panels) and modeled by RMA (right panels) for March (top panels) and April (bottom panels), WY1981. Time variable turbidity decay coefficients were used.

Time Variable Turbidity Decay Coefficient RMA PTRK Modeled Smelt Distributions

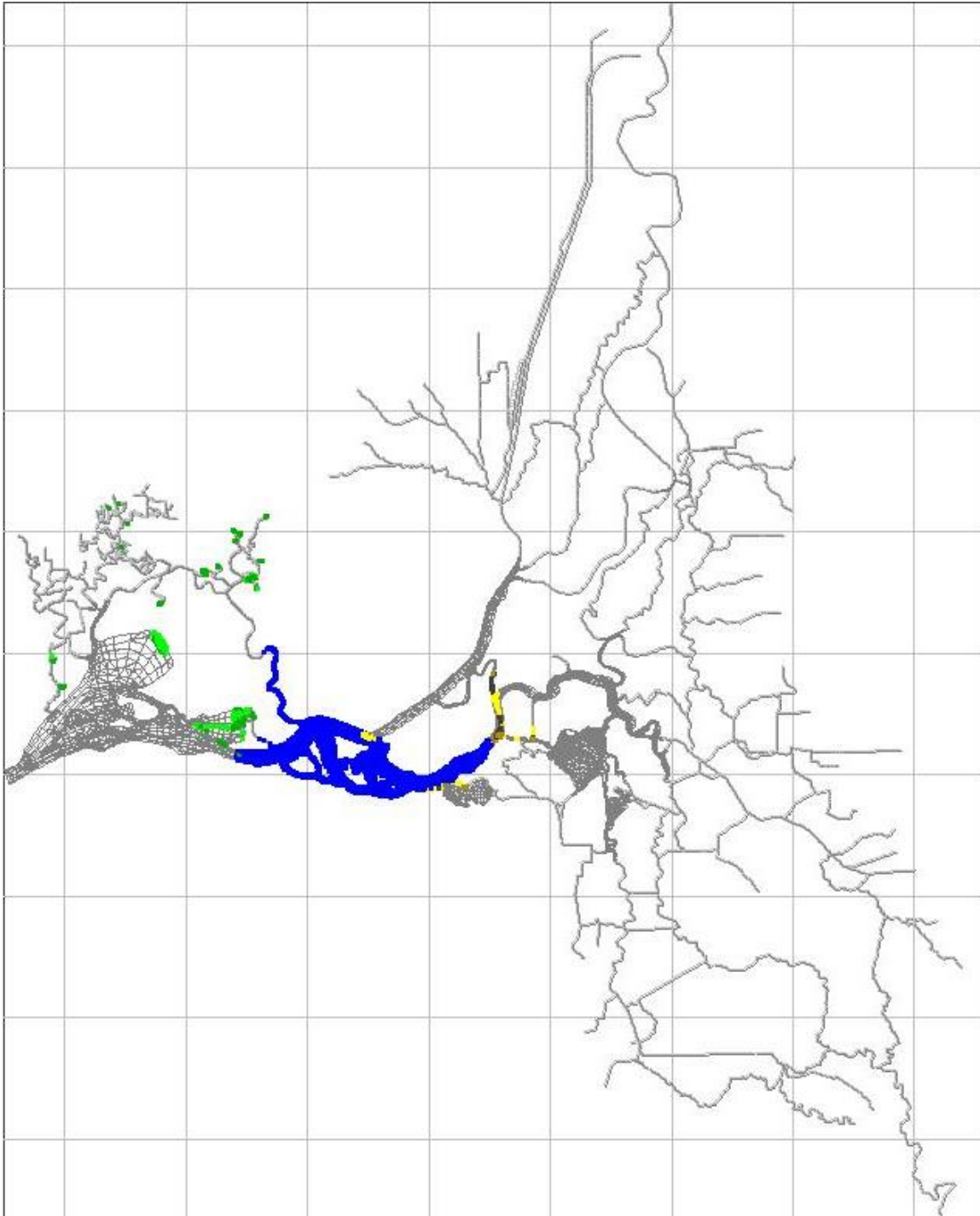


Figure 39 RMA PTRK modeled smelt distribution, November 1, 1980. For behavioral color codes, see Figure 29. Model results were driven using a smelt turbidity minimum threshold of 12 NTU and turbidity model results obtained with time variable decay coefficients. Similar distributions were produced using 10 and 14 NTU thresholds.

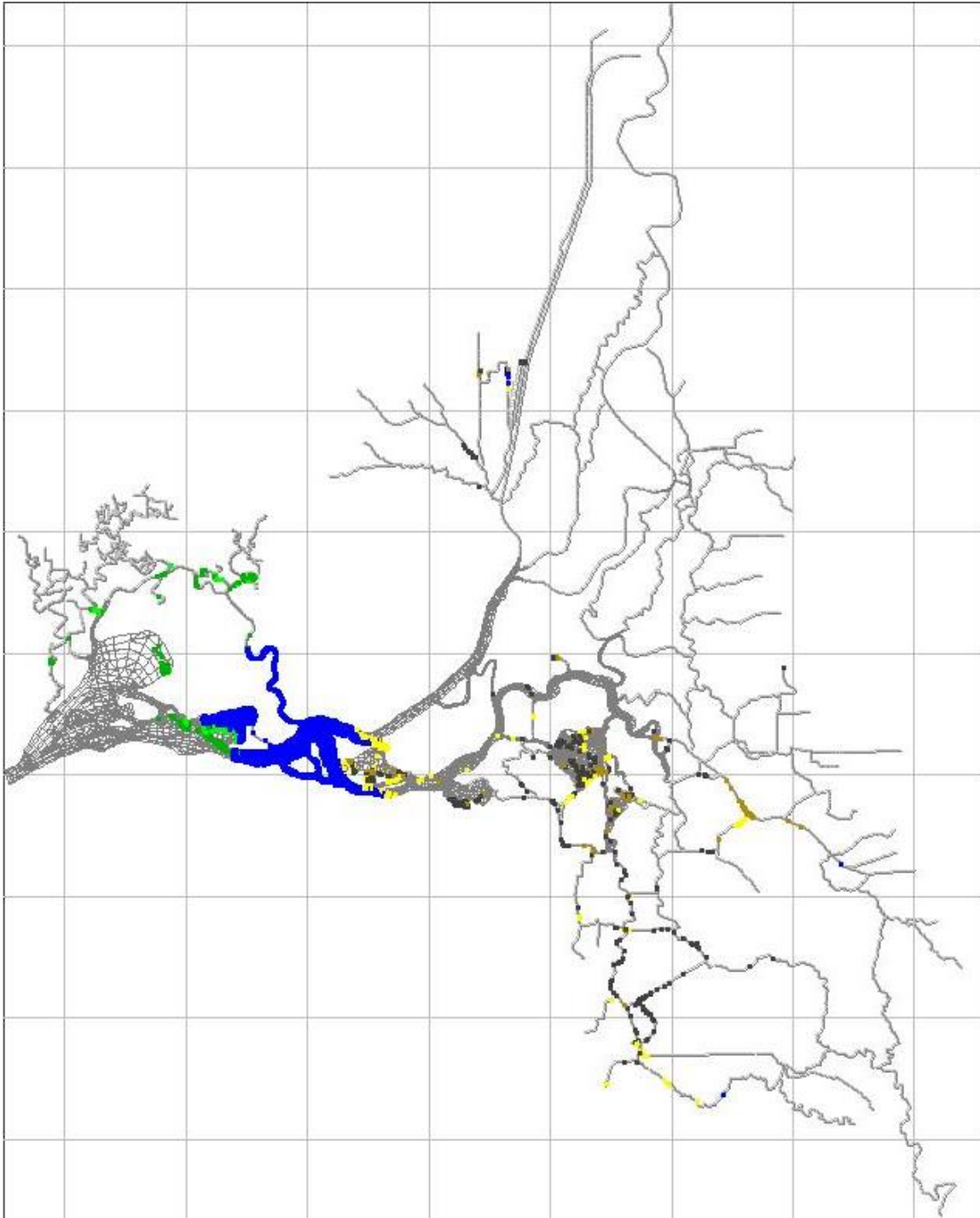


Figure 40 RMA PTRK modeled smelt distribution, January 1, 1981. For behavioral color codes, see Figure 29. Model results were driven using a smelt turbidity minimum threshold of 12 NTU and turbidity model results obtained with time variable decay coefficients. Similar distributions were produced using 10 and 14 NTU thresholds.

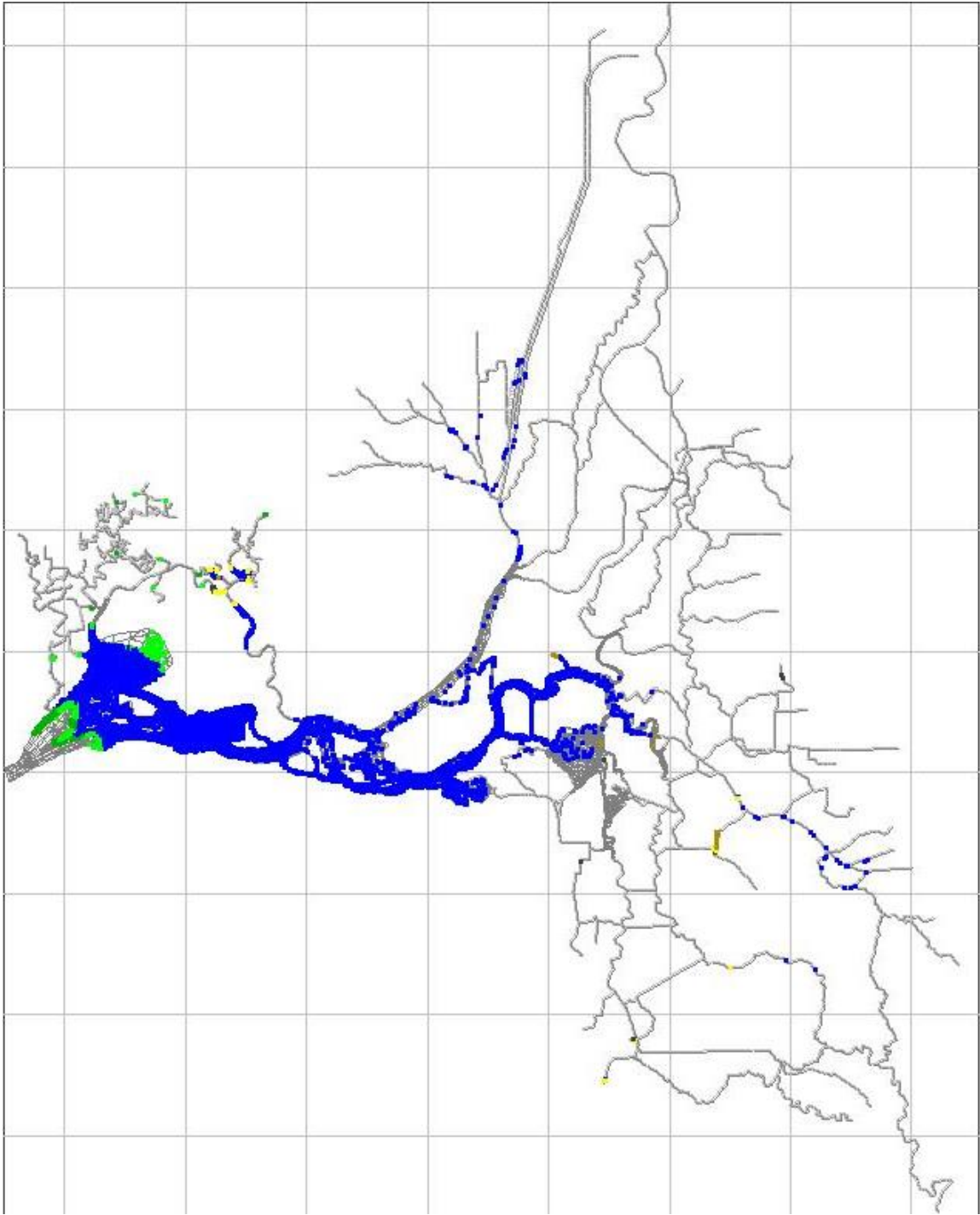


Figure 41 RMA PTRK modeled smelt distribution, February 1, 1981. For behavioral color codes, see Figure 29. Model results were driven using a smelt turbidity minimum threshold of 12 NTU and turbidity model results obtained with time variable decay coefficients. Similar distributions were produced using 10 and 14 NTU thresholds.

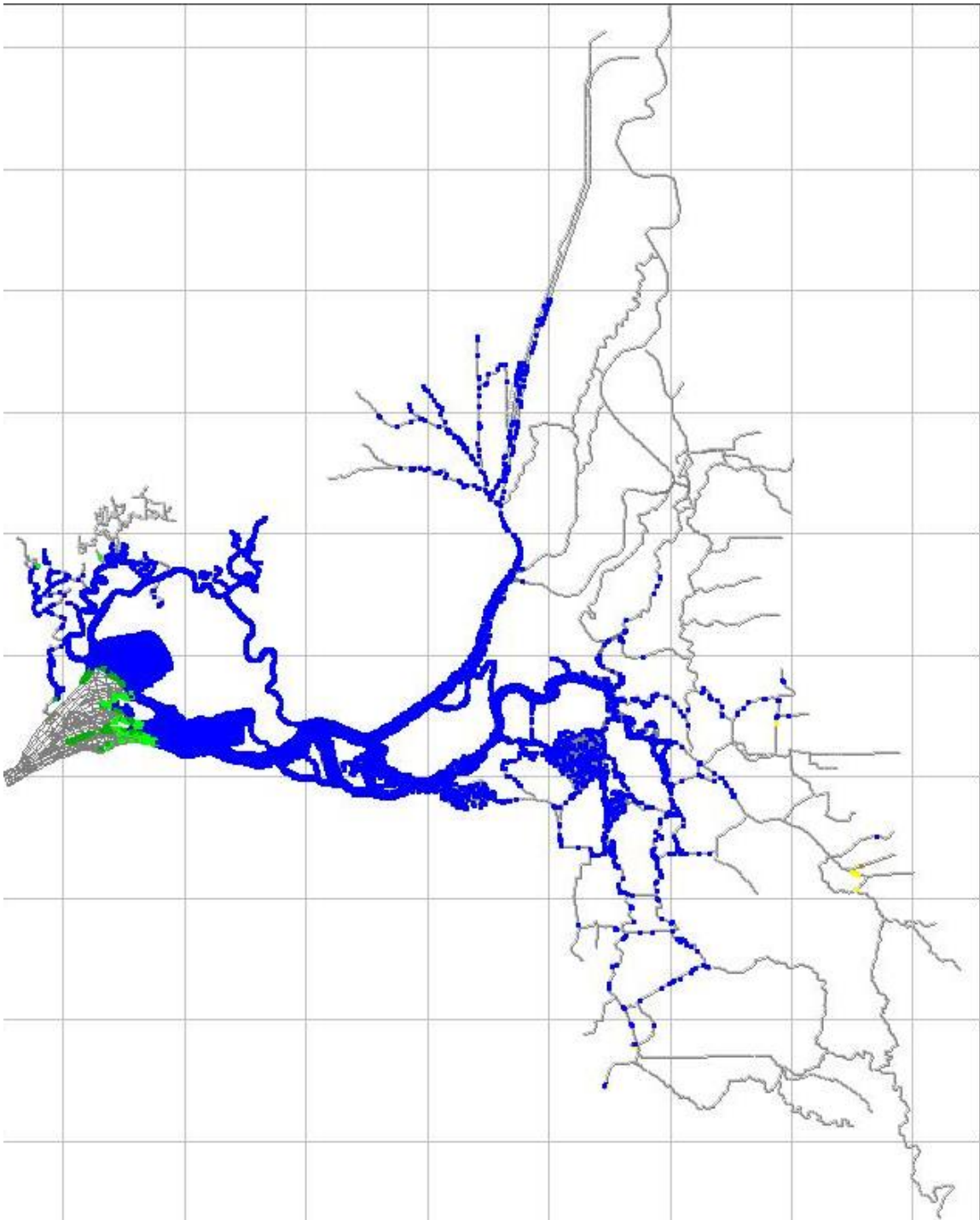


Figure 42 RMA PTRK modeled smelt distribution, March 1, 1981. For behavioral color codes, see Figure 29. Model results were driven using a smelt turbidity minimum threshold of 12 NTU and turbidity model results obtained with time variable decay coefficients. Similar distributions were produced using 10 and 14 NTU thresholds.

Water Year 1982

Water year 1982 begins with several isolated salvage events that appear uncorrelated to increased turbidity through the central Delta (Figure 43 and Figure 44). During this time the RMA smelt models shows no salvage occurring and the smelt exhibiting their typical holding pattern near the confluence region prior to migration (Figure 50 or Figure 58). FMWT smelt distributions show a similar pattern (Figure 48 and Figure 49).

The first storm event of WY1982 began in mid-November. This led to a very large salvage event measured in late November. The smelt model using the original model calibrated coefficients did not reproduce this event. However, the timing of this spike was replicated by the smelt model run with time variable turbidity decay coefficients and a smelt turbidity threshold of 10 NTU (but not in the 12 or 14 NTU simulations). This modeled salvage event occurred over a more spread out time period than the observed data. One explanation for this discrepancy may be the timing of the DWR reported removal of the Old River at head barrier which occurred in late November (Figure 3). If the barrier was removed over a period of several days (either beginning or ending with the single day listed on the website), this could change the flow down the Old and Middle River corridor, affecting the salvage patterns.

A later series of storms increased turbidity in the south and central Delta (Figure 46 and Figure 47). In the smelt model run with improved calibration coefficients, this led to a series of episodes of smelt exploring habitat into the south Delta (Figure 59) and then returning to the central Delta as turbidities decrease (Figure 60). This produced the episodic peaks in salvage patterns throughout January–March seen in both the observed and modeled data. Smelt model runs with original calibration coefficients did not reproduce high enough turbidities through the central and south Delta to cause any appreciable smelt salvage events (Figure 43). The peak in modeled March salvage only represented a very small percentage (0.02%) of the simulated particles.

High-Flow Calibrated Smelt and Turbidity Model Summary Results

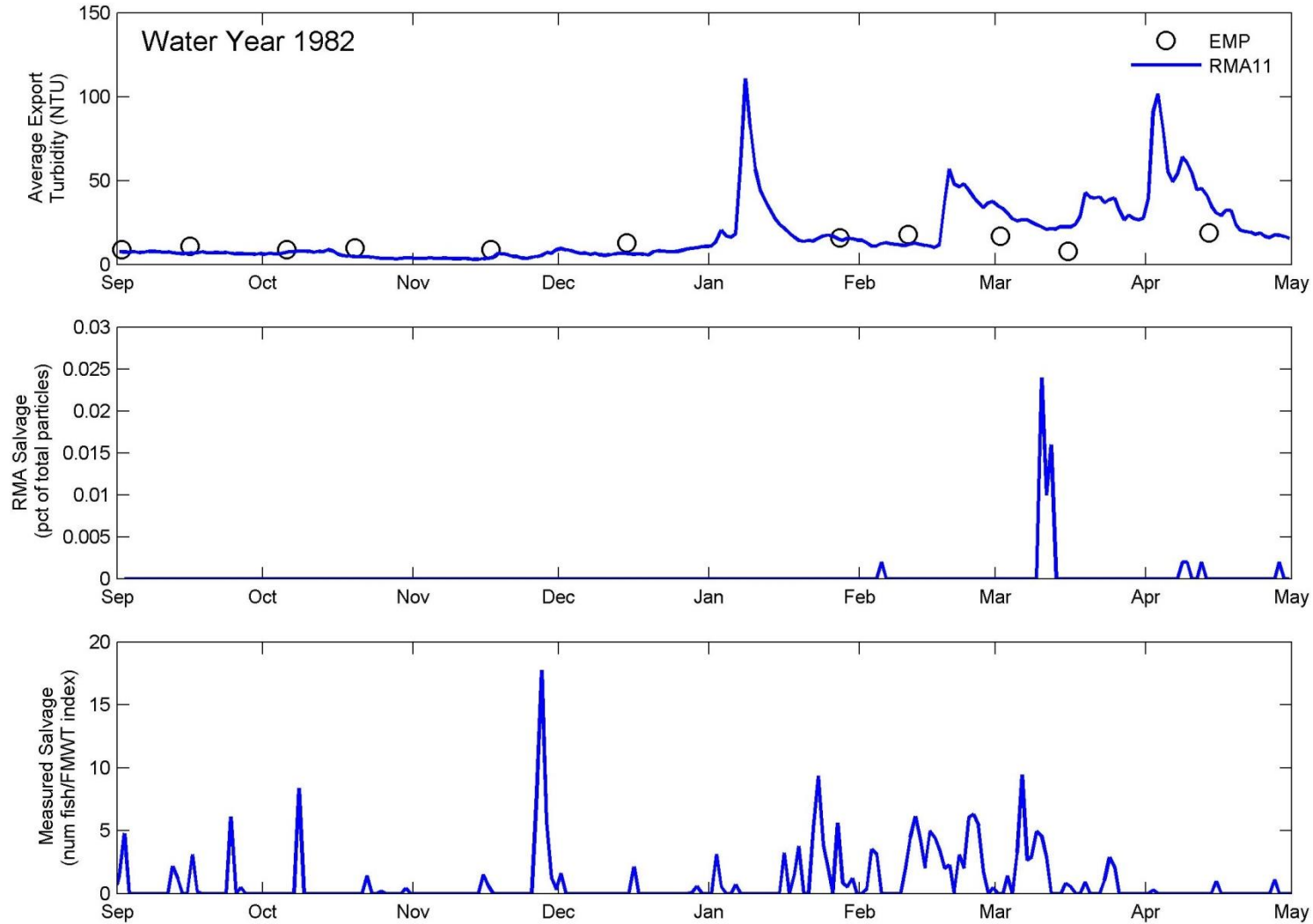
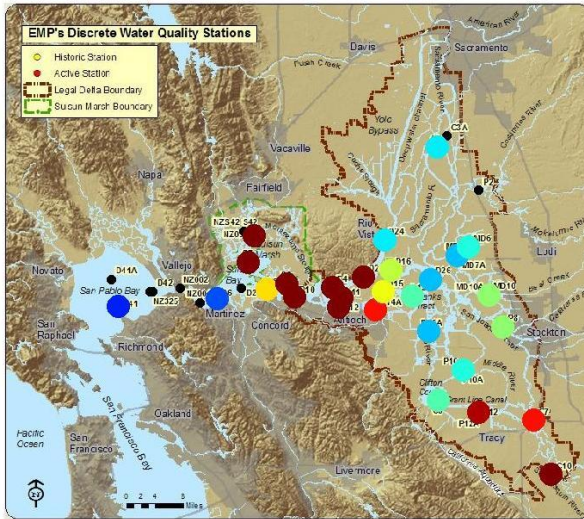


Figure 43 WY1982 modeled and observed turbidity and delta smelt salvage at the southern export locations. Original calibrated turbidity decay coefficients and smelt minimum turbidity thresholds were used. Top panel shows average modeled turbidity at the export locations along with EMP observed data. Middle panel shows RMA modeled smelt salvage (as a percent of total input particles). Bottom panel shows observed smelt salvage as number of fish divided by the water year FMWT index (a measure of the total smelt population size).

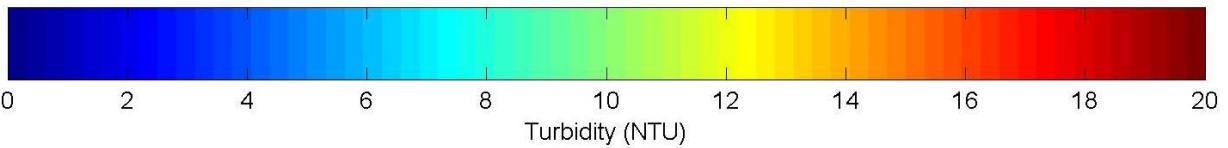
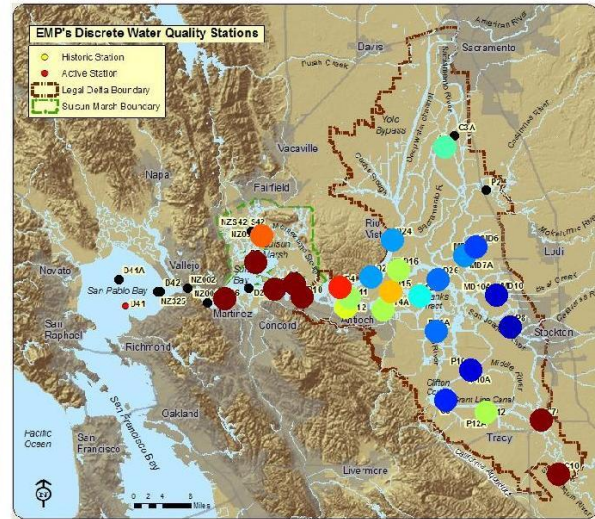
High-Flow Calibrated Model EMP Comparison Plots

03 Sep 1981

EMP Data

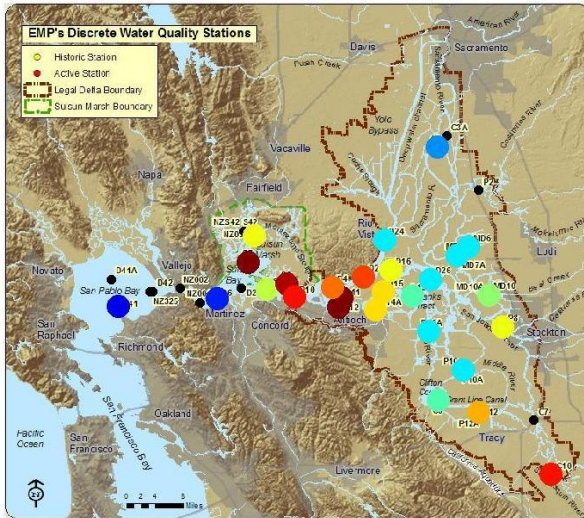


RMA11 Data



07 Oct 1981

EMP Data



RMA11 Data

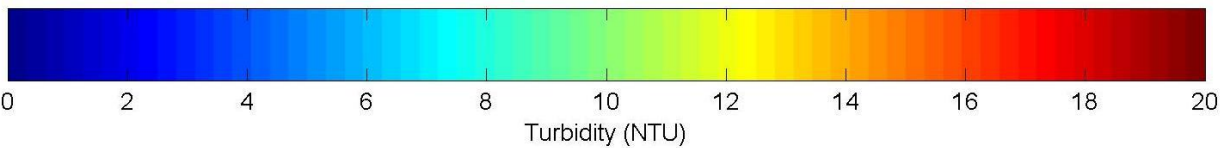
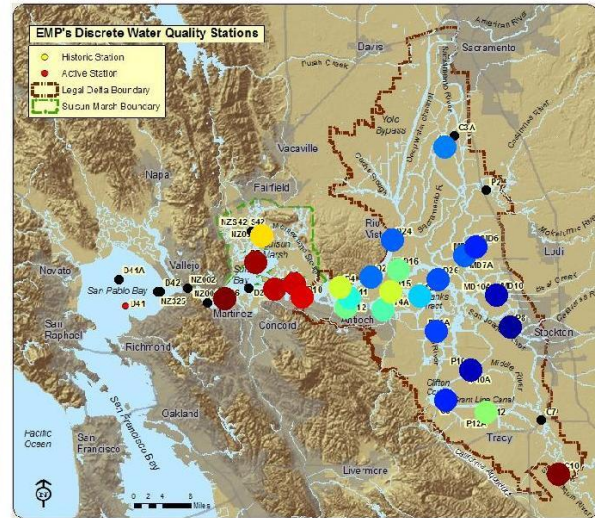
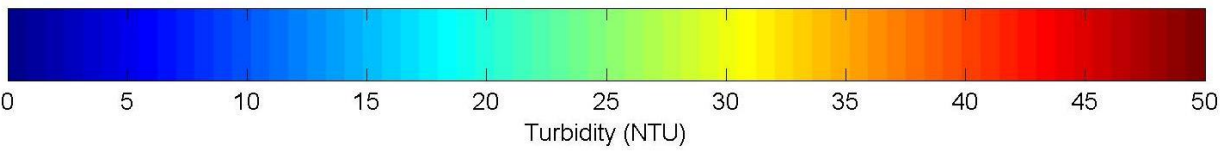
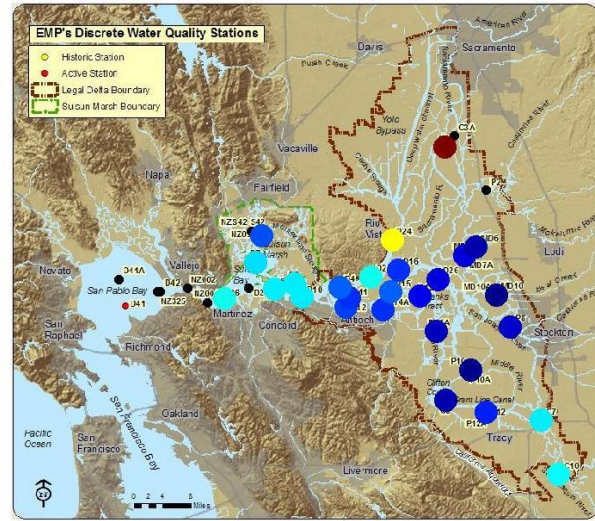
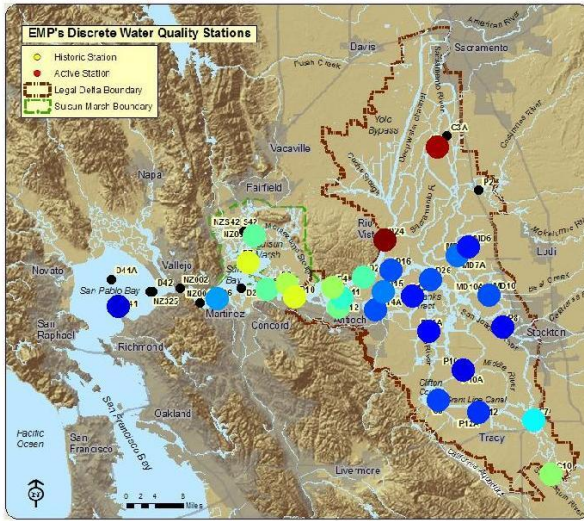


Figure 44 Turbidity distributions measured by the EMP (left panels) and modeled by RMA (right panels) for September (top panels) and October (bottom panels), WY1982. High-flow calibrated turbidity decay coefficients were used.

18 Nov 1981

EMP Data

RMA11 Data



15 Dec 1981

EMP Data

RMA11 Data

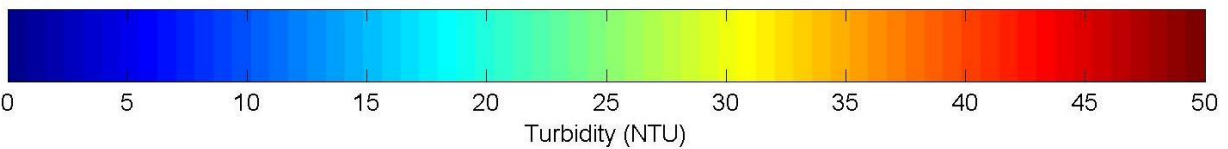
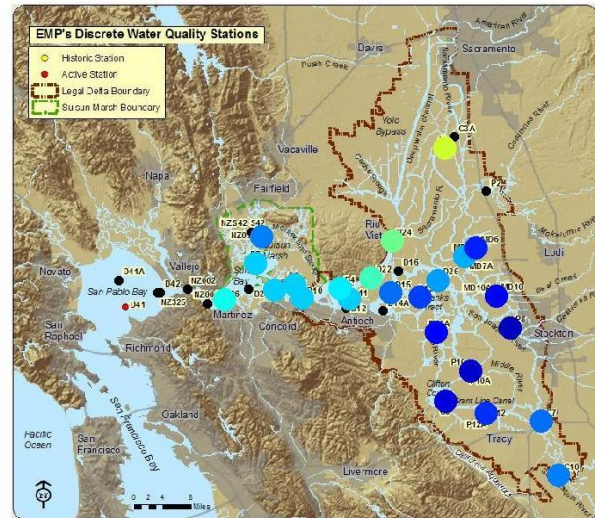
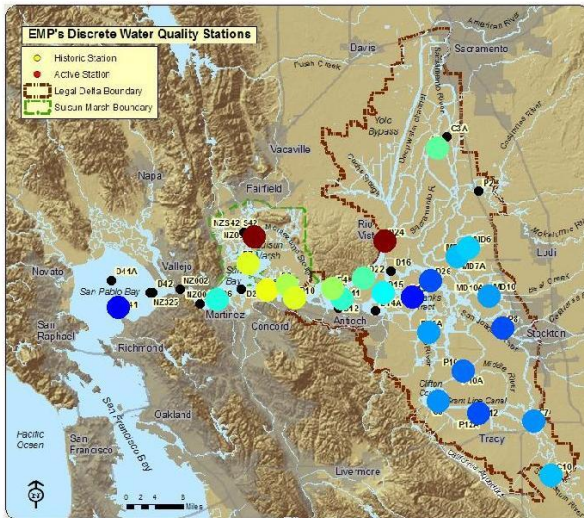
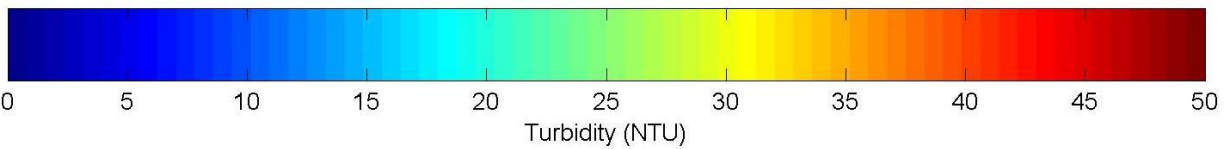
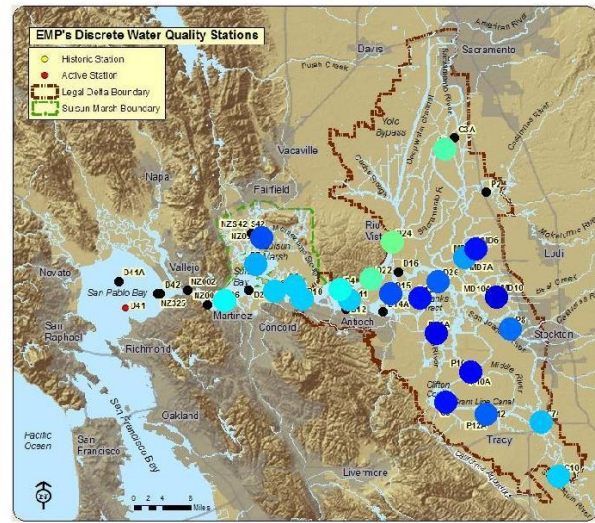
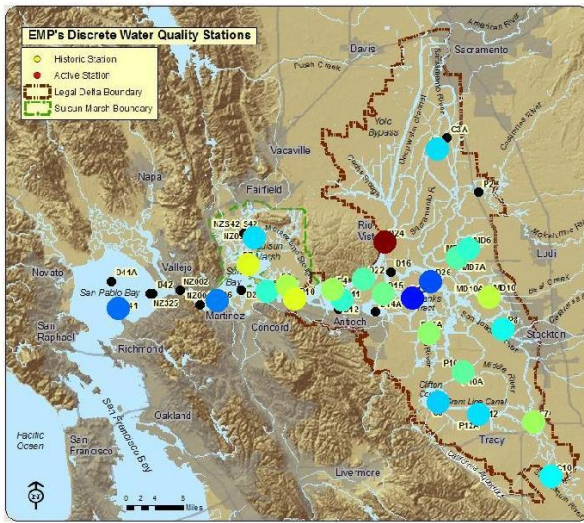


Figure 45 Turbidity distributions measured by the EMP (left panels) and modeled by RMA (right panels) for November (top panels) and December (bottom panels), WY1982. High-flow calibrated turbidity decay coefficients were used.

28 Jan 1982

EMP Data

RMA11 Data



11 Feb 1982

EMP Data

RMA11 Data

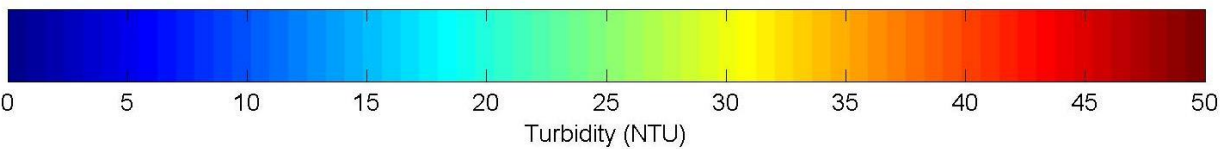
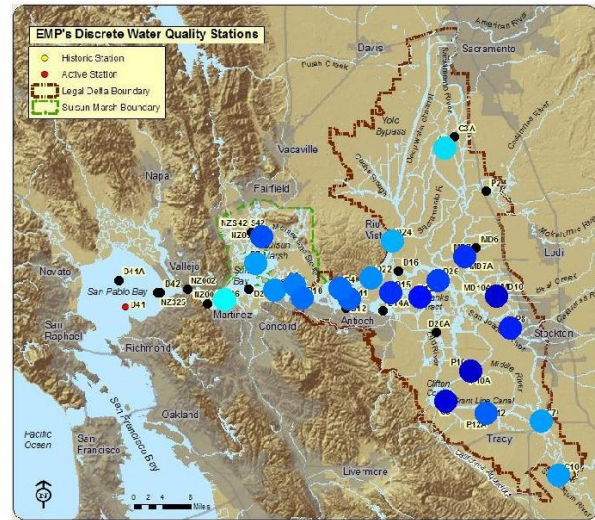
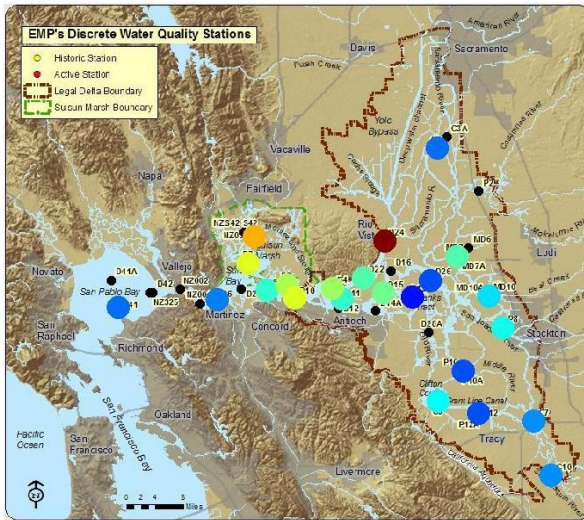
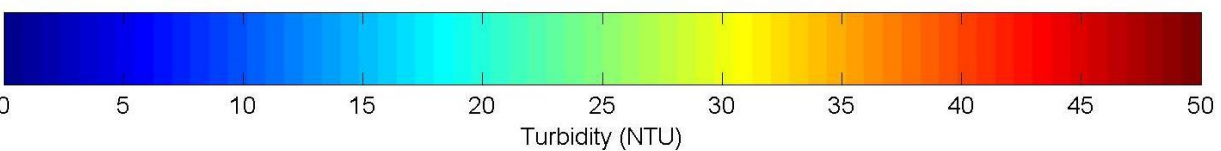
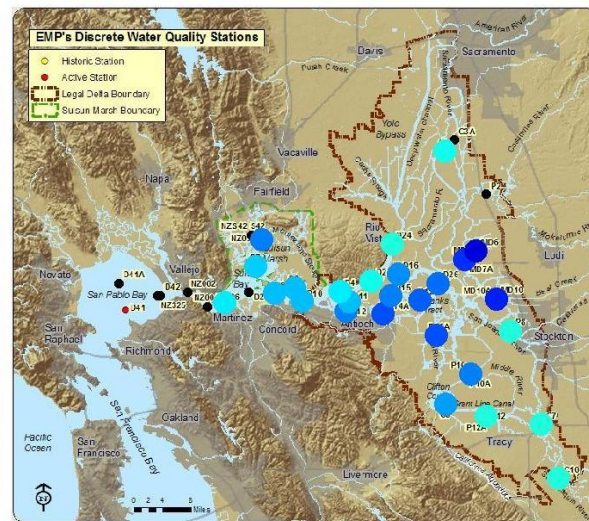
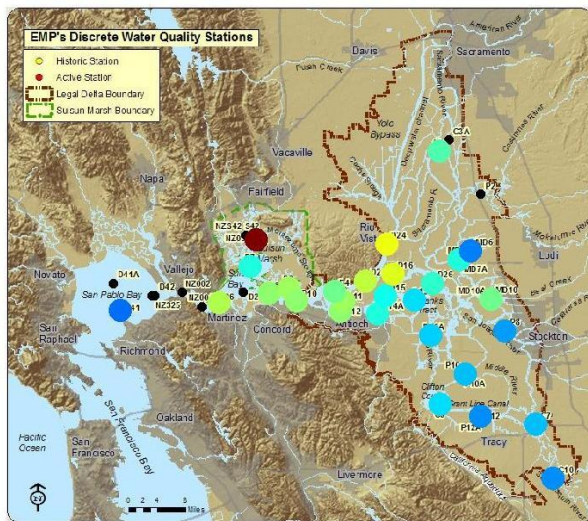


Figure 46 Turbidity distributions measured by the EMP (left panels) and modeled by RMA (right panels) for January (top panels) and February (bottom panels), WY1982. High-flow calibrated turbidity decay coefficients were used.

03 Mar 1982

EMP Data

RMA11 Data



15 Apr 1982

EMP Data

RMA11 Data

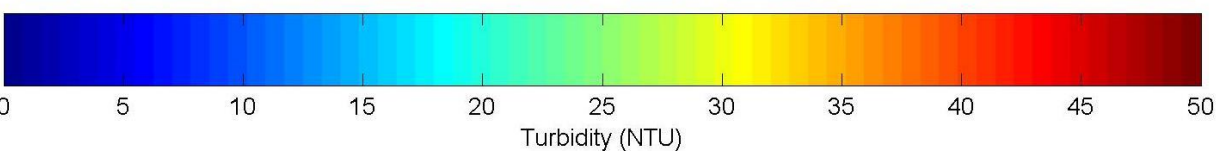
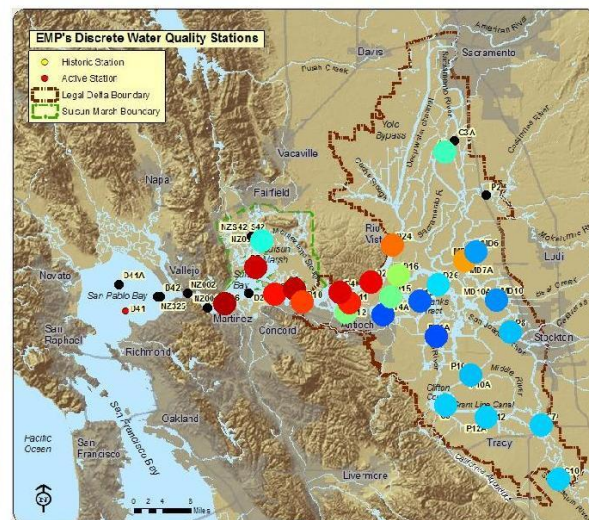
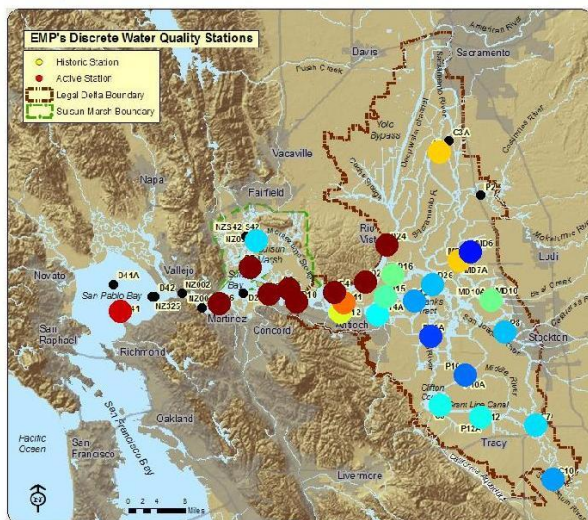


Figure 47 Turbidity distributions measured by the EMP (left panels) and modeled by RMA (right panels) for March (top panels) and April (bottom panels), WY1982. High-flow calibrated turbidity decay coefficients were used.

FMWT Smelt Distributions

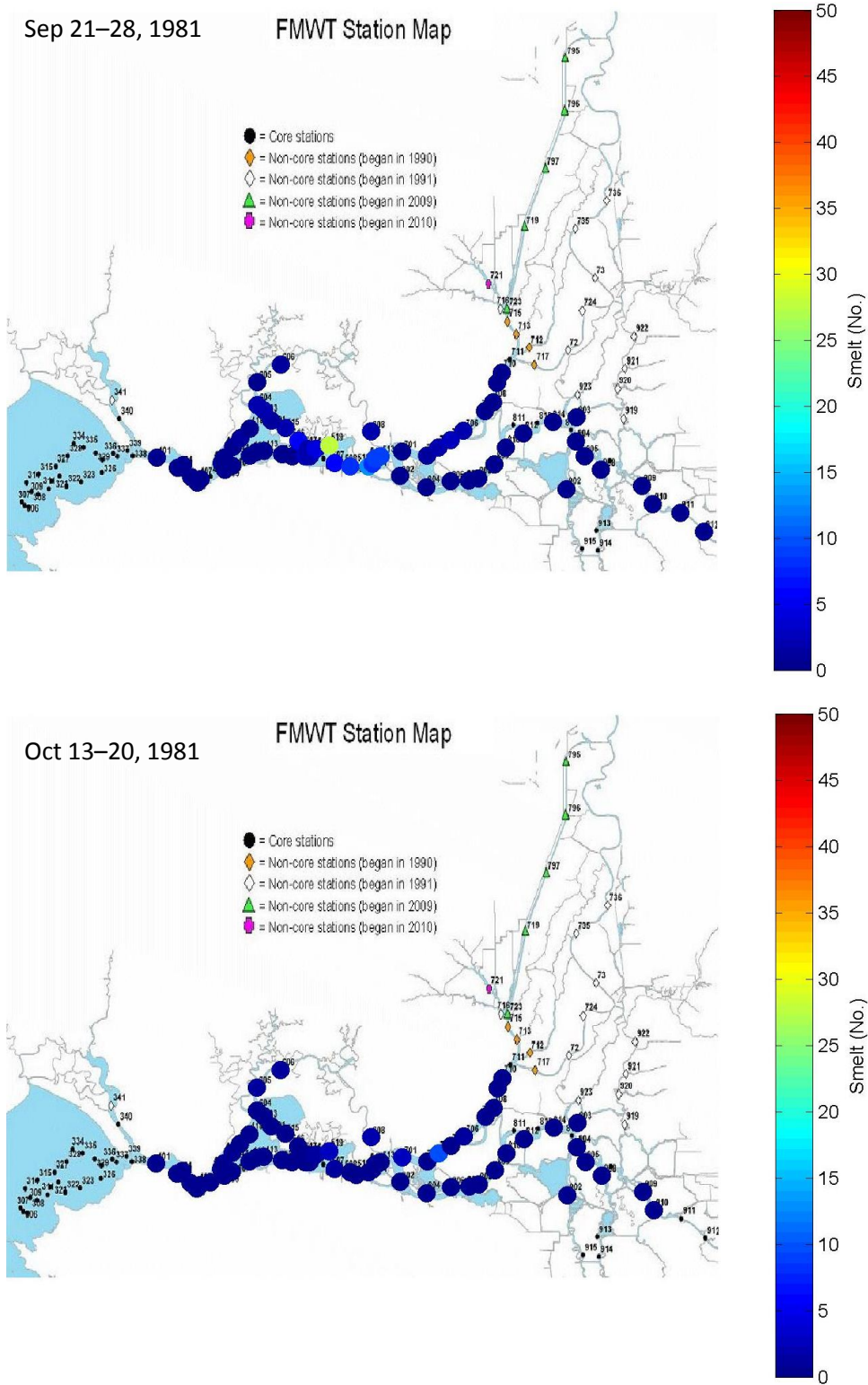


Figure 48 September and October 1981 FMWT ADS catch distributions. Dates indicate range of days catch was made over.

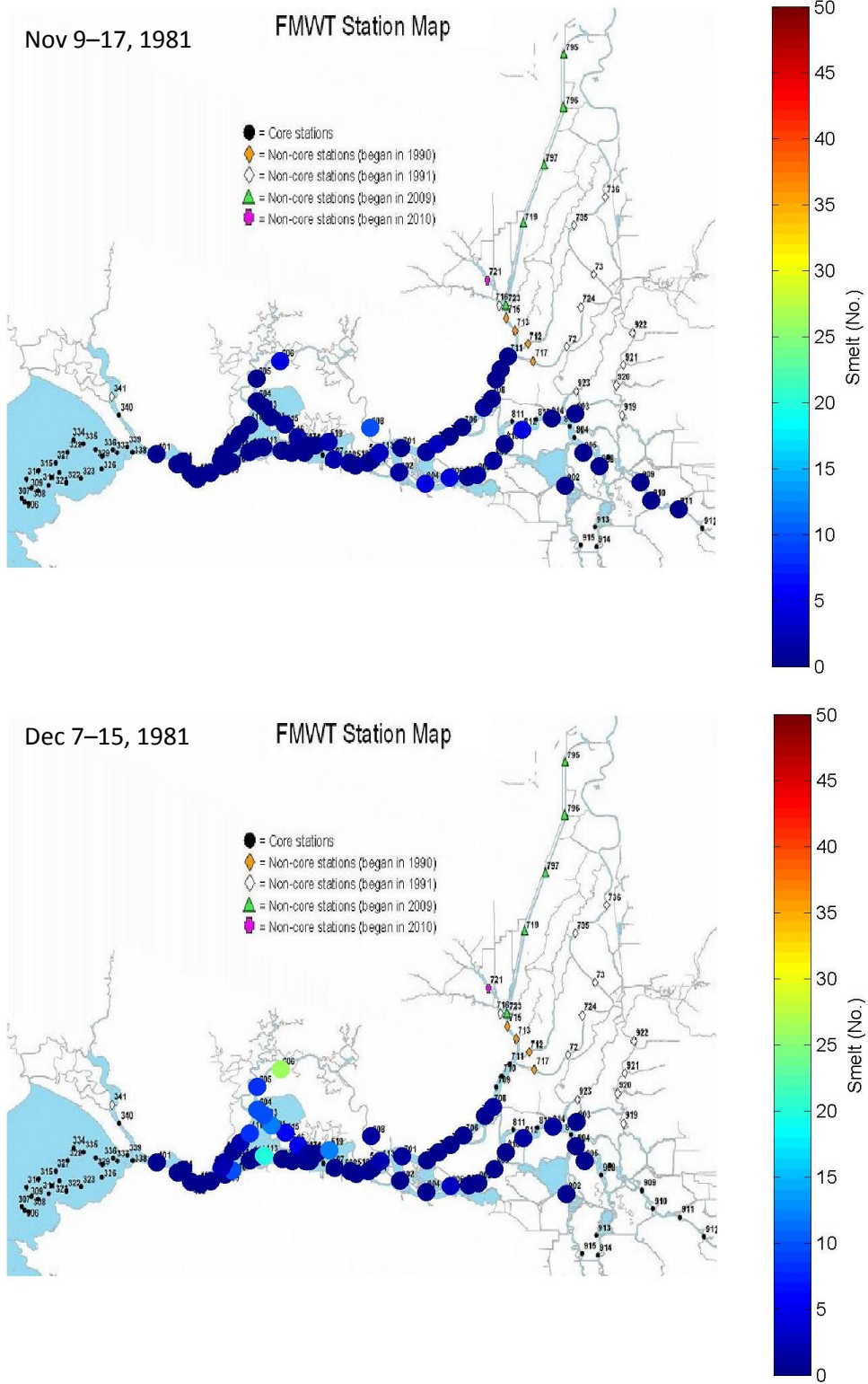


Figure 49 November and December 1981 FMWT ADS catch distributions. Dates indicate range of days catch was made over.

Original Model Calibration RMA PTRK Modeled Smelt Distributions

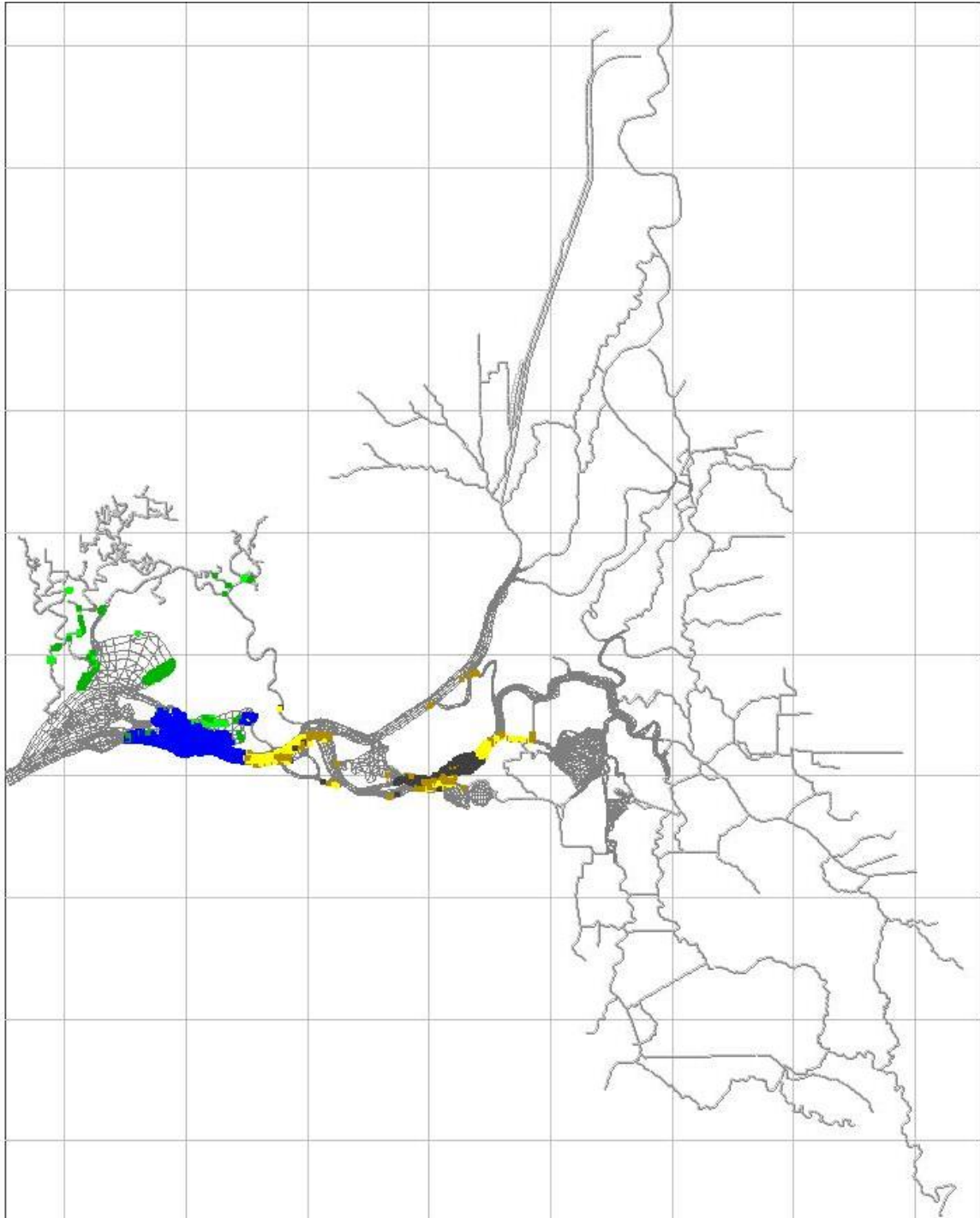


Figure 50 RMA PTRK modeled smelt distribution, November 1, 1981. For behavioral color codes, see Figure 29. Model results were driven using a smelt turbidity minimum threshold of 16 NTU and turbidity model results obtained with high-flow calibrated parameters.

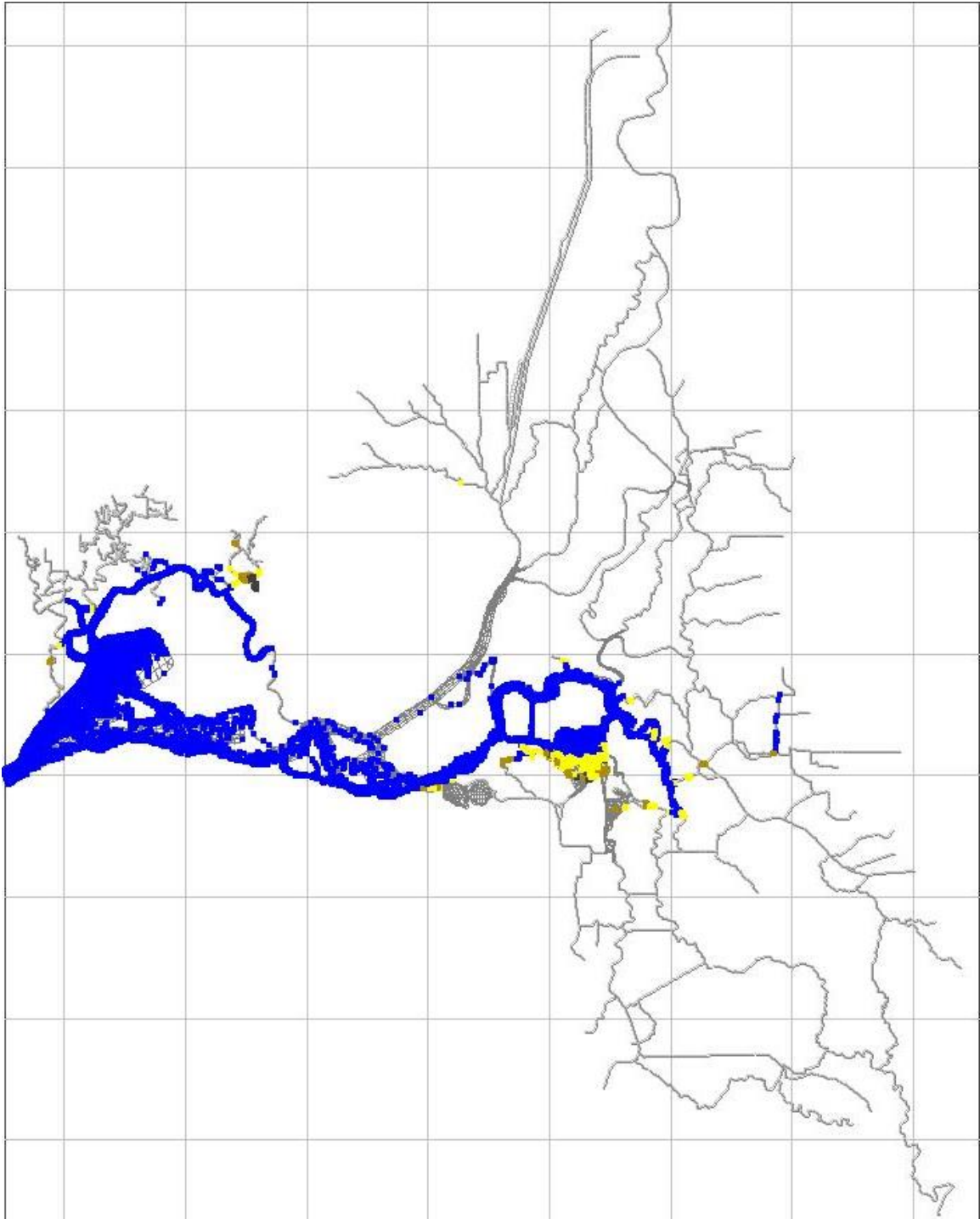


Figure 51 RMA PTRK modeled smelt distribution, January 1, 1982. For behavioral color codes, see Figure 29. Model results were driven using a smelt turbidity minimum threshold of 16 NTU and turbidity model results obtained with high-flow calibrated parameters.

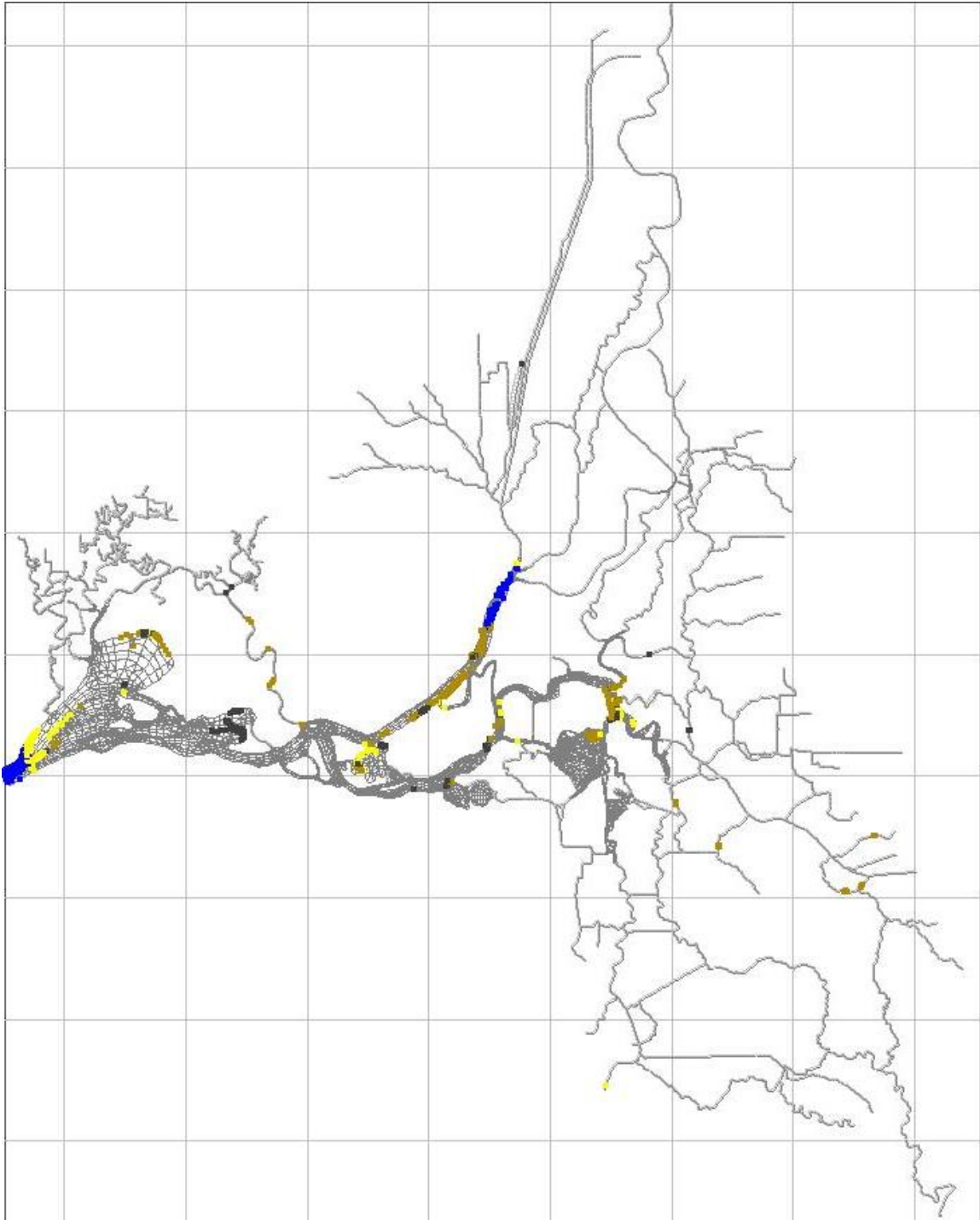


Figure 52 RMA PTRK modeled smelt distribution, February 15, 1982. For behavioral color codes, see Figure 29. Model results were driven using a smelt turbidity minimum threshold of 16 NTU and turbidity model results obtained with high-flow calibrated parameters.

Time Variable Decay Coefficient Smelt and Turbidity Model Summary Results

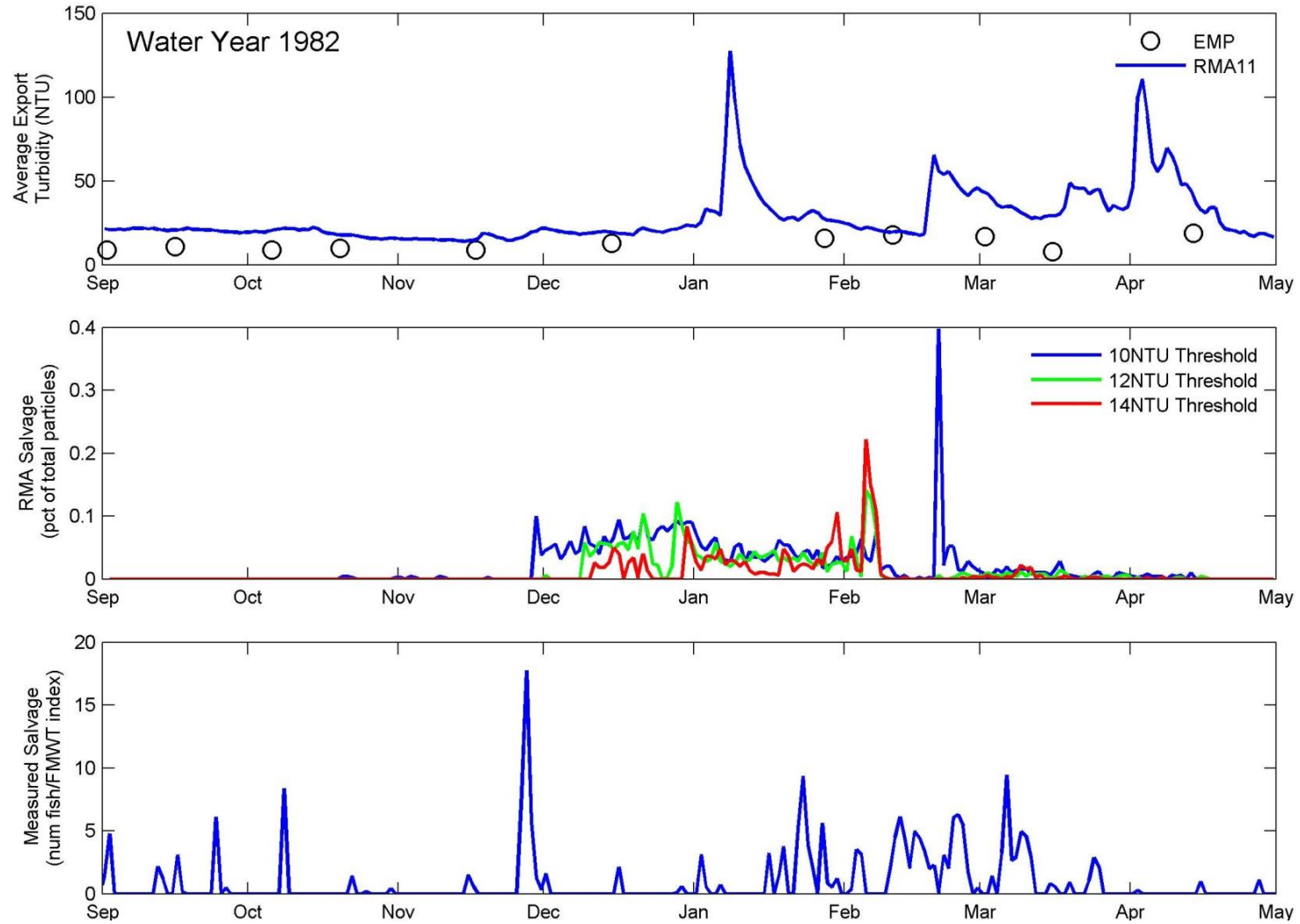


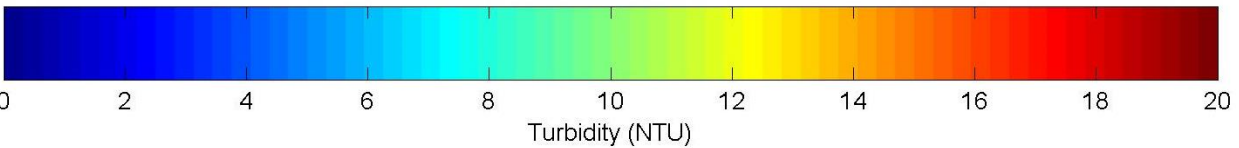
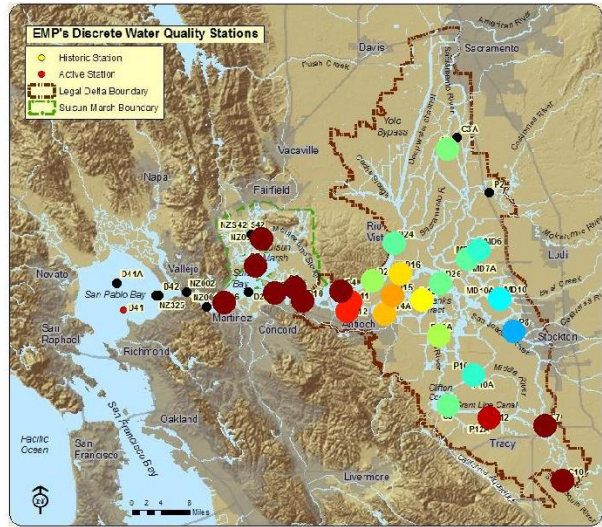
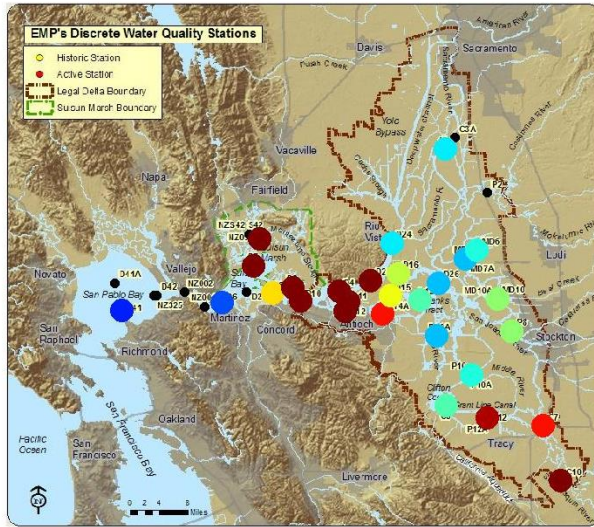
Figure 53 WY1982 modeled and observed turbidity and delta smelt salvage at the southern export locations. Time variable turbidity decay coefficients were used. Top panel shows average modeled turbidity at the export locations along with EMP observed data. Middle panel shows RMA modeled smelt salvage (as a percent of total input particles) using three different max turbidity threshold values. Bottom panel shows observed smelt salvage as number of fish divided by the water year FMWT index (a measure of the total smelt population size).

Time Variable Decay Coefficient Model EMP Turbidity Comparison Plots

03 Sep 1981

EMP Data

RMA11 Data



07 Oct 1981

EMP Data

RMA11 Data

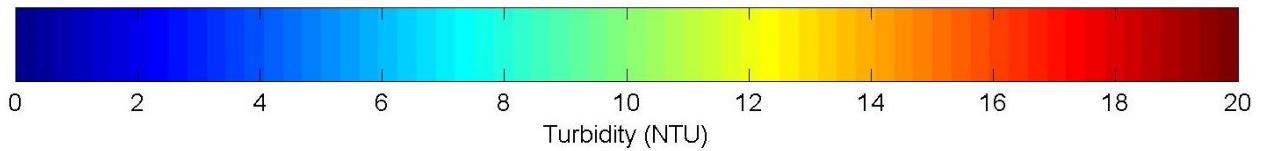
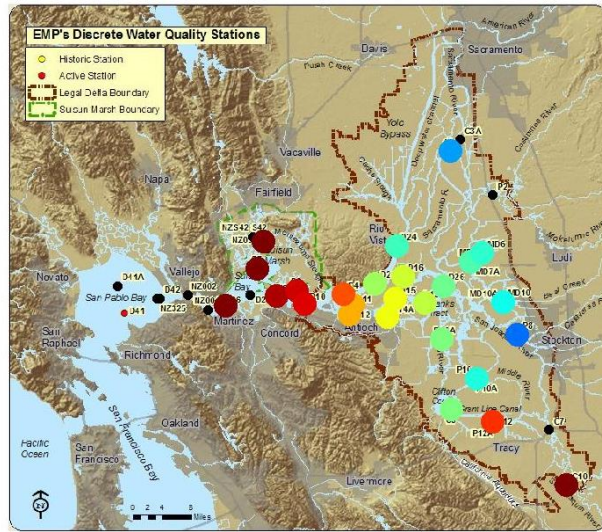
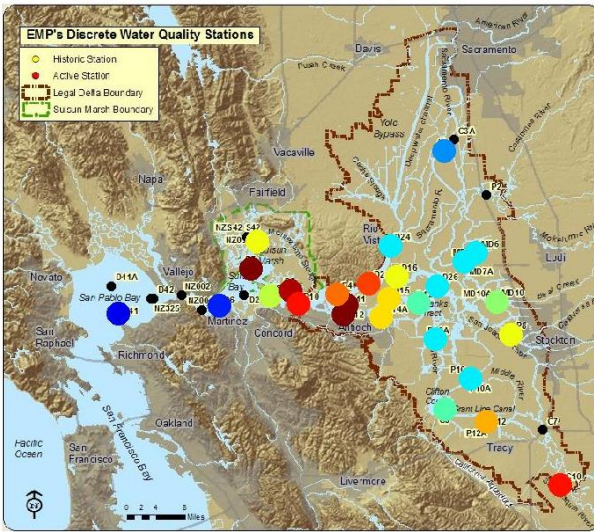
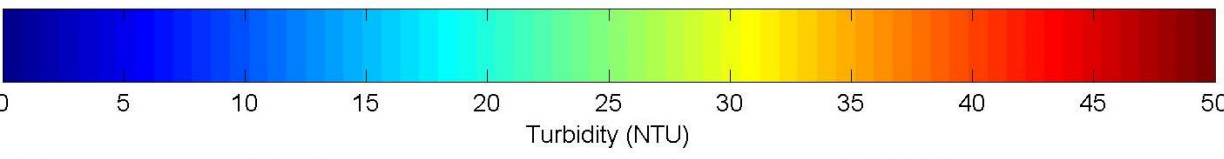
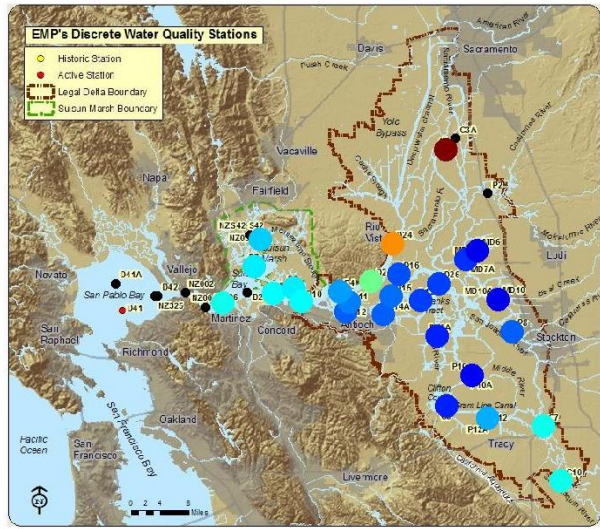
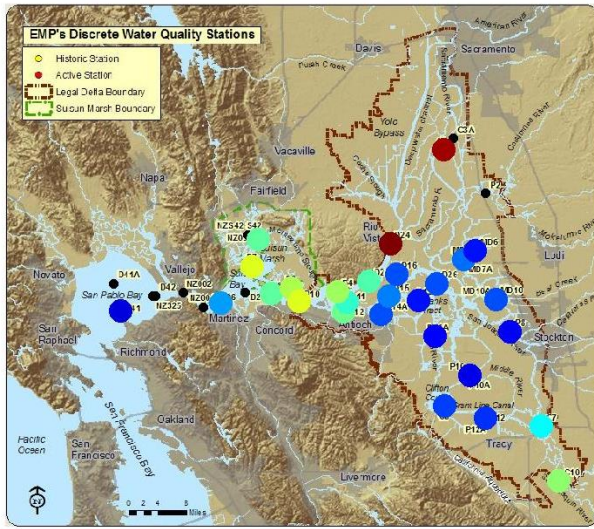


Figure 54 Turbidity distributions measured by the EMP (left panels) and modeled by RMA (right panels) for September (top panels) and October (bottom panels), WY1982. Time variable turbidity decay coefficients were used.

18 Nov 1981

EMP Data

RMA11 Data



15 Dec 1981

EMP Data

RMA11 Data

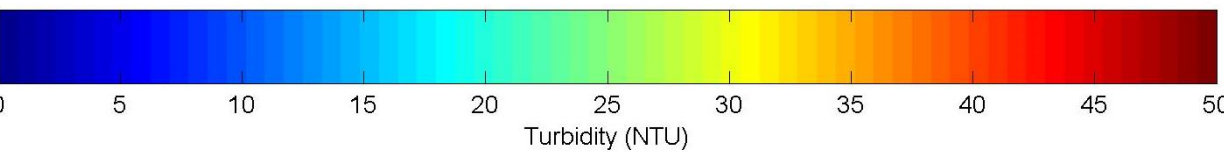
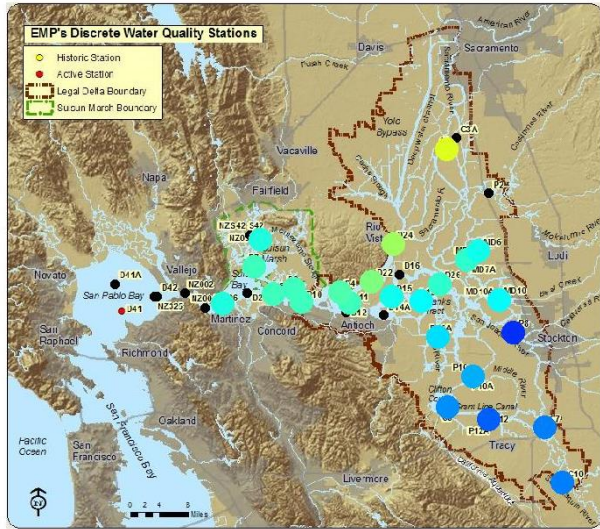
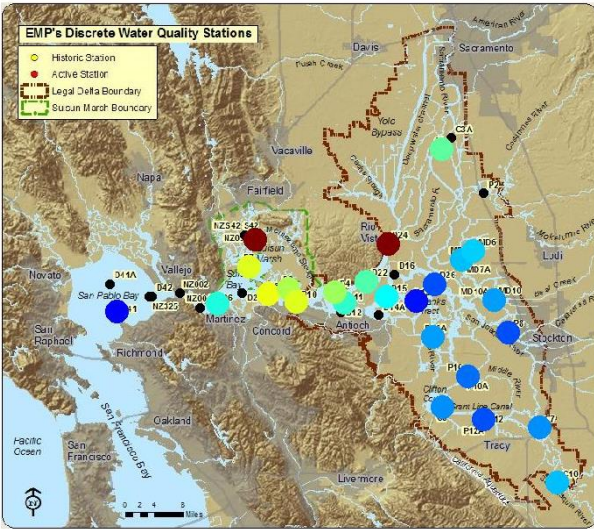
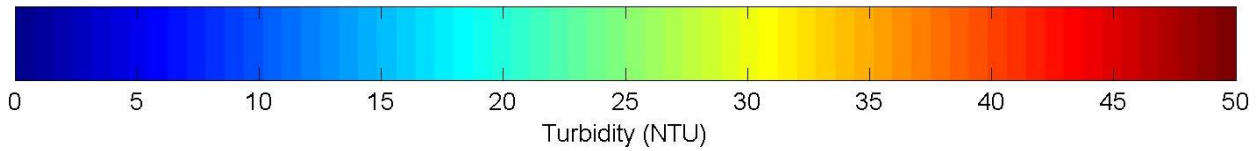
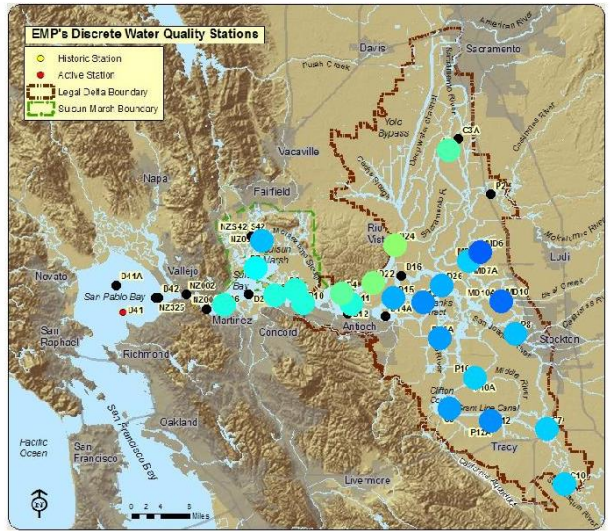
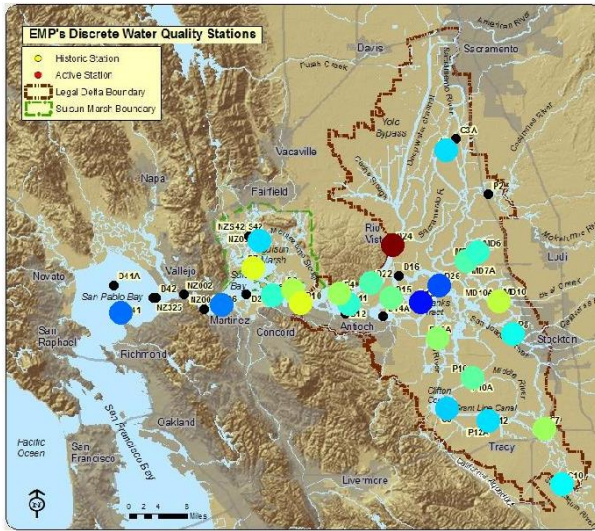


Figure 55 Turbidity distributions measured by the EMP (left panels) and modeled by RMA (right panels) for November (top panels) and December (bottom panels), WY1982. Time variable turbidity decay coefficients were used.

28 Jan 1982

EMP Data

RMA11 Data



11 Feb 1982

EMP Data

RMA11 Data

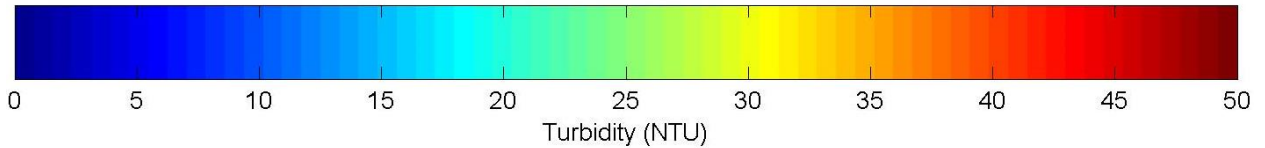
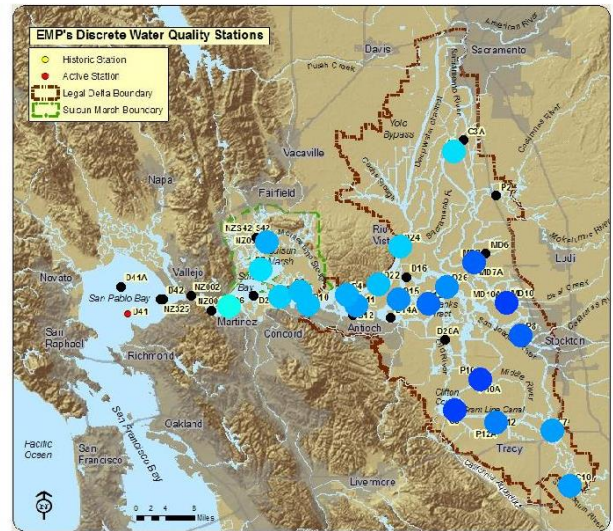
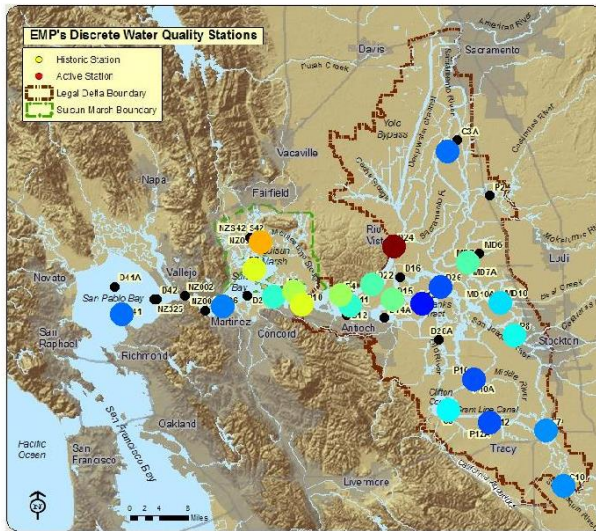
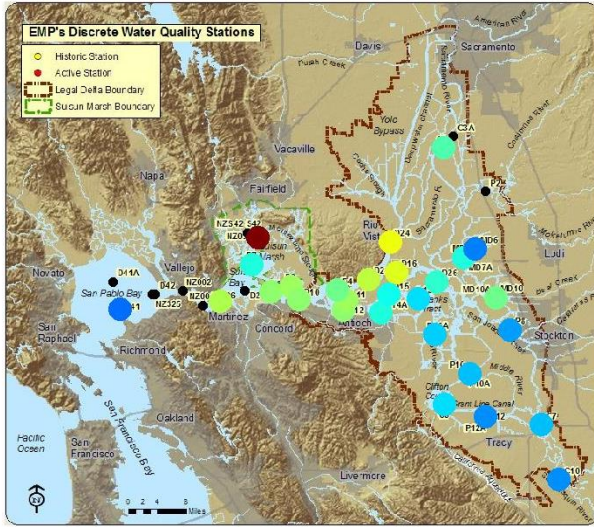


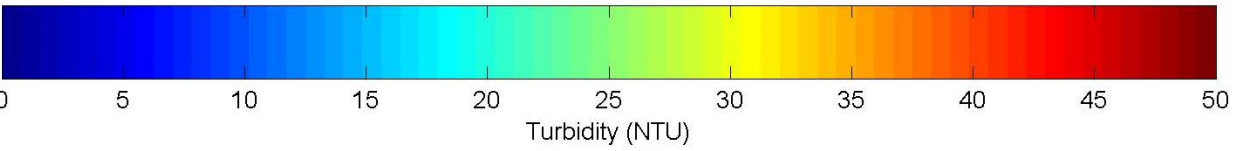
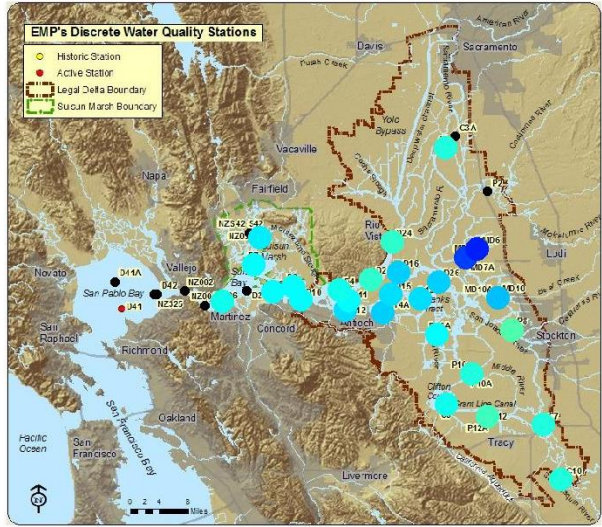
Figure 56 Turbidity distributions measured by the EMP (left panels) and modeled by RMA (right panels) for January (top panels) and February (bottom panels), WY1982. Time variable turbidity decay coefficients were used.

03 Mar 1982

EMP Data

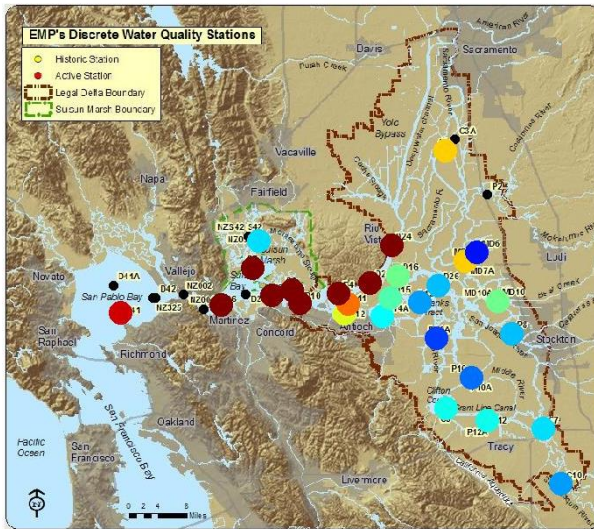


RMA11 Data



15 Apr 1982

EMP Data



RMA11 Data

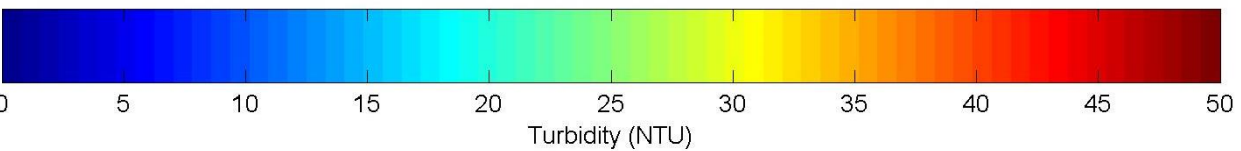
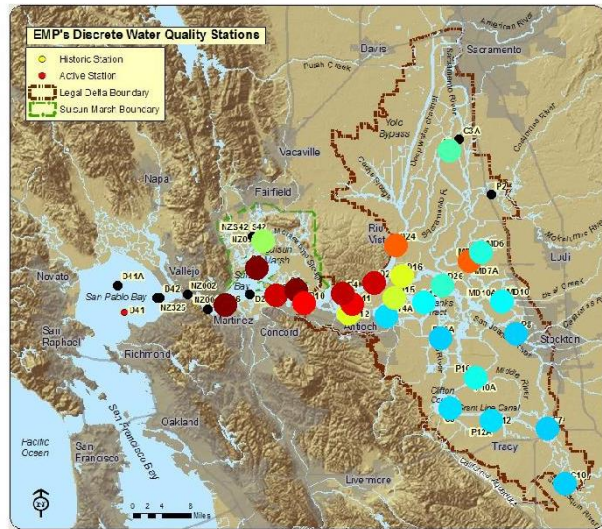


Figure 57 Turbidity distributions measured by the EMP (left panels) and modeled by RMA (right panels) for March (top panels) and April (bottom panels), WY1982. Time variable turbidity decay coefficients were used.

Time Variable Turbidity Decay RMA PTRK Modeled Smelt Distributions

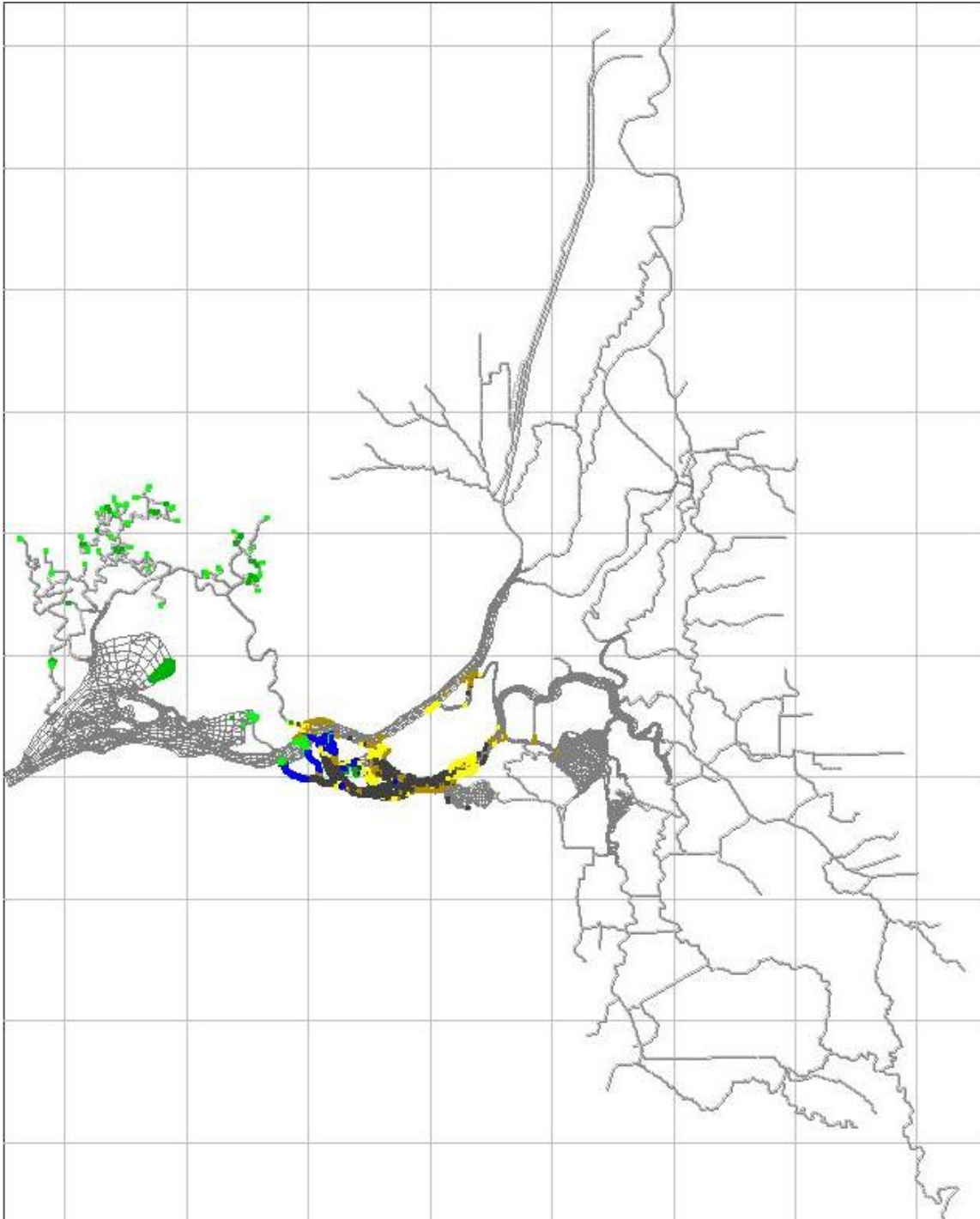


Figure 58 RMA PTRK modeled smelt distribution, November 1, 1981. For behavioral color codes, see Figure 29. Model results were driven using a smelt turbidity minimum threshold of 12 NTU and turbidity model results obtained with time variable decay coefficients. Similar distributions were produced using 10 and 14 NTU thresholds.

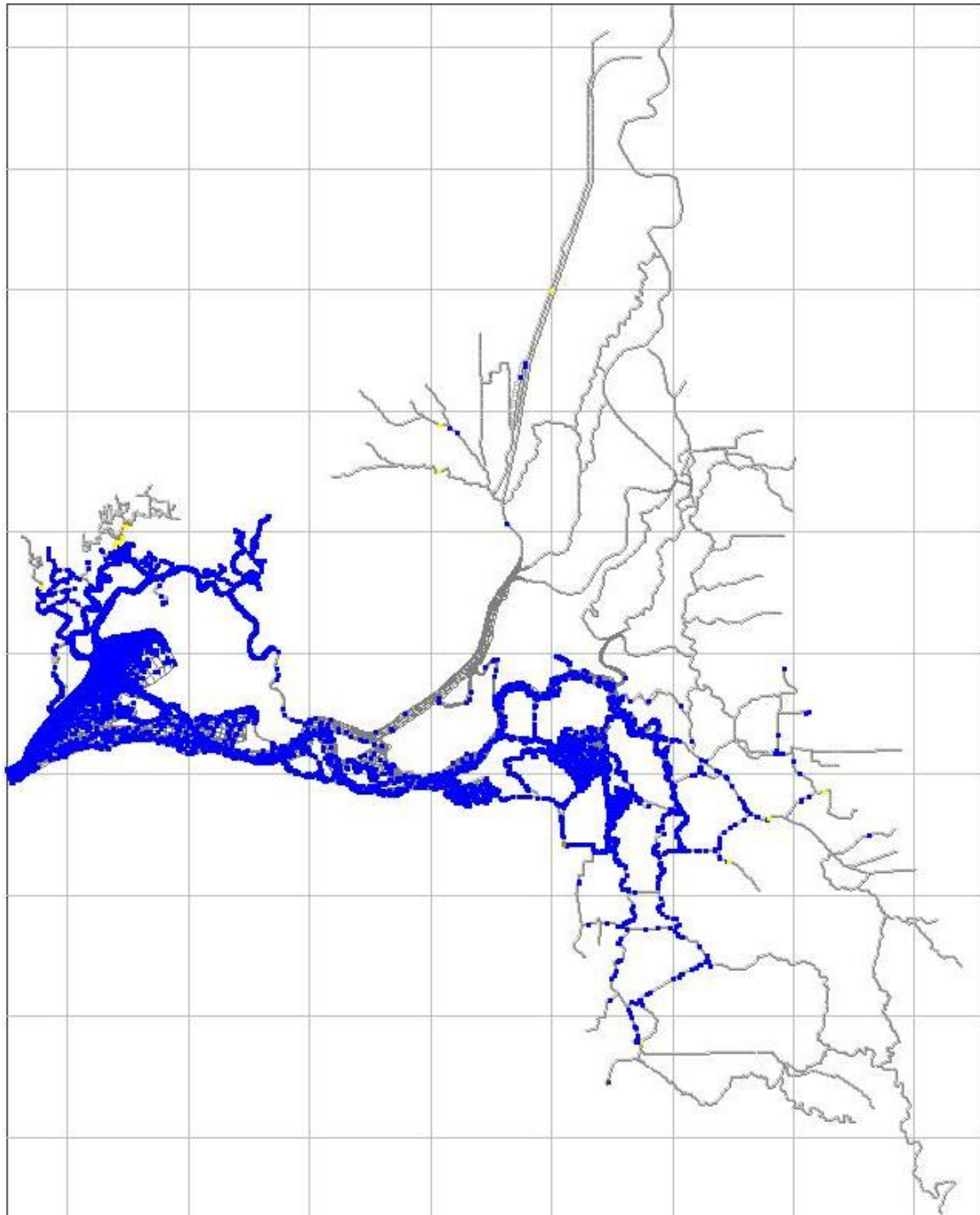


Figure 59 RMA PTRK modeled smelt distribution, January 1, 1982. For behavioral color codes, see Figure 29. Model results were driven using a smelt turbidity minimum threshold of 12 NTU and turbidity model results obtained with time variable decay coefficients. Similar distributions were produced using 10 and 14 NTU thresholds.

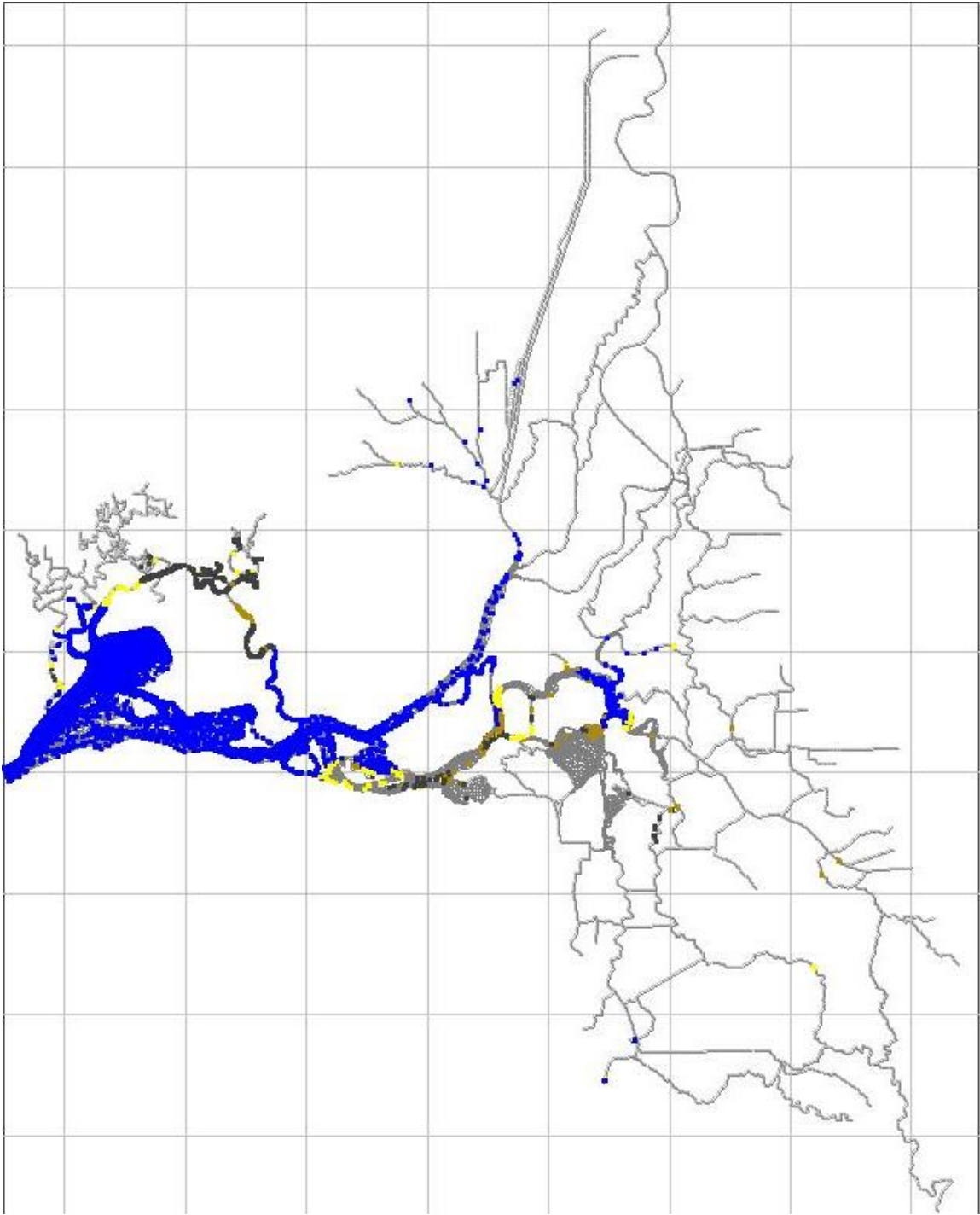


Figure 60 RMA PTRK modeled smelt distribution, February 15, 1982. For behavioral color codes, see Figure 29. Model results were driven using a smelt turbidity minimum threshold of 12 NTU and turbidity model results obtained with time variable decay coefficients. Similar distributions were produced using 10 and 14 NTU thresholds.

Water Year 1988

Water year 1988 produced a very simple salvage pattern dominated by the only two storms that impacted the basin that year, occurring in December and January. In the fall months, there was no appreciable fall salvage, which corresponded to low south and central turbidities (Figure 62 and Figure 63) and smelt distributions typical of pre-migration where smelt are concentrated near the confluence area (FMWT data in Figure 66 and Figure 67, modeled pattern in Figure 68 and Figure 76).

The large first-flush event occurring in mid-December (for which the DCC was left open) sent high turbidities through the Delta. In the smelt models run with each set of calibration coefficients, this led to simulated smelt exploring most of the south and central Delta (Figure 69 and Figure 77). High flows kept the smelt from moving significant distances up the Sacramento. The DCC was closed during the second storm event in January leading to a smaller salvage event seen in observed data. The model runs with the original calibration coefficients failed to capture this second event, but those with the updated parameters did. Modeled smelt distributions after the storm events had passed were similar to that seen in other water years, with many smelt located in the Cache Slough Complex where EC and turbidity conditions are optimal.

High-Flow Calibrated Smelt and Turbidity Model Summary Results

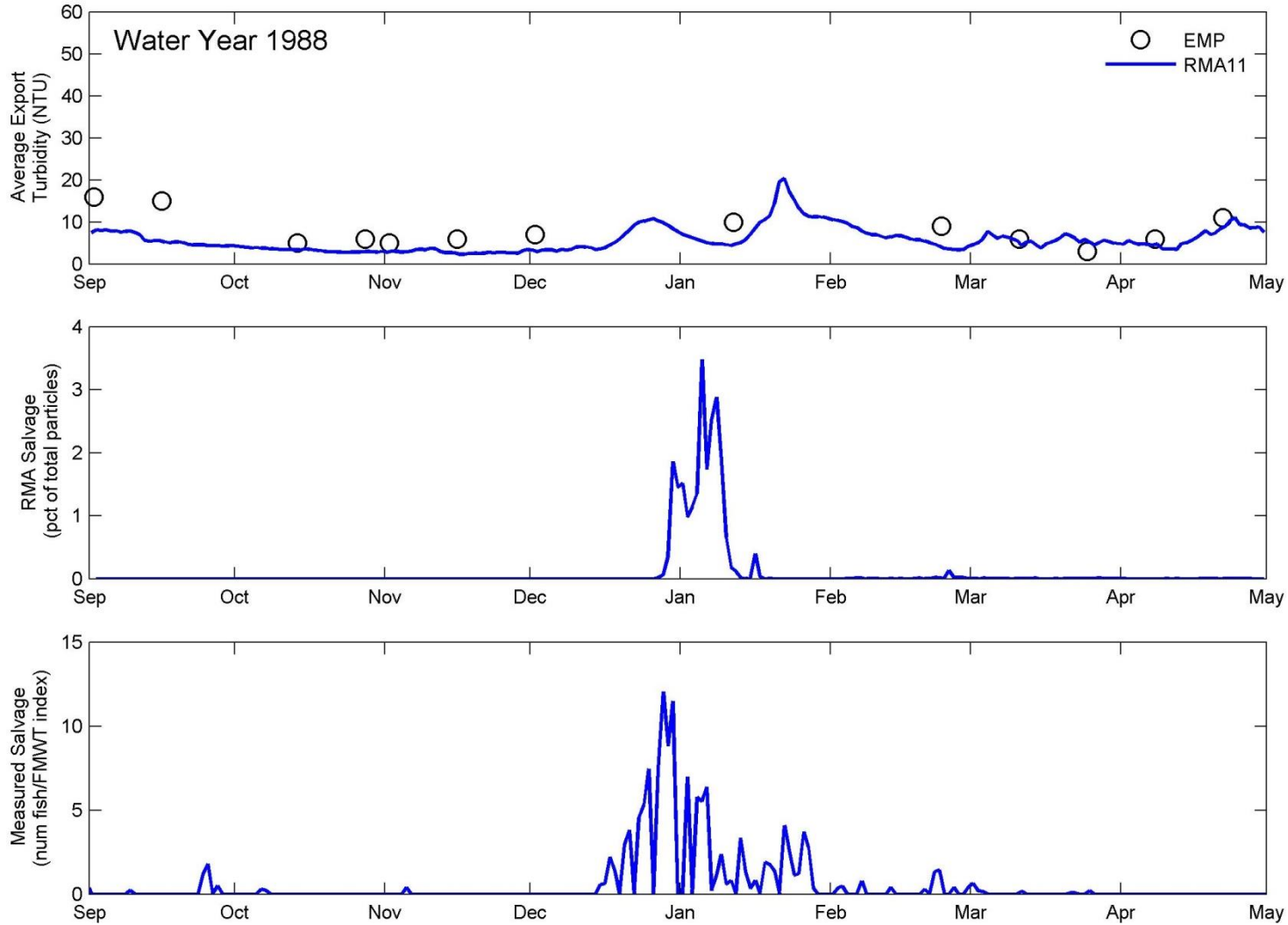
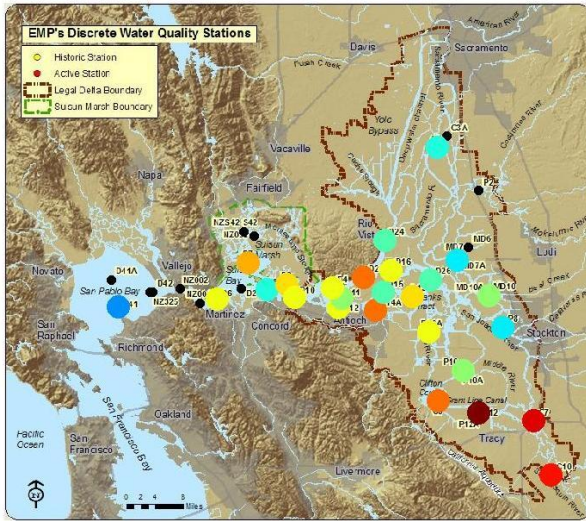


Figure 61 WY1988 modeled and observed turbidity and delta smelt salvage at the southern export locations. Original calibrated turbidity decay coefficients and smelt minimum turbidity thresholds were used. Top panel shows average modeled turbidity at the export locations along with EMP observed data. Middle panel shows RMA modeled smelt salvage (as a percent of total input particles). Bottom panel shows observed smelt salvage as number of fish divided by the water year FMWT index (a measure of the total smelt population size).

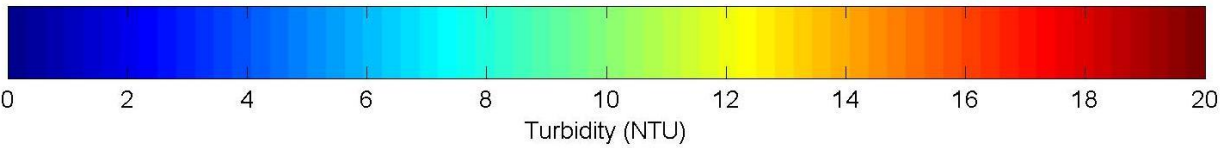
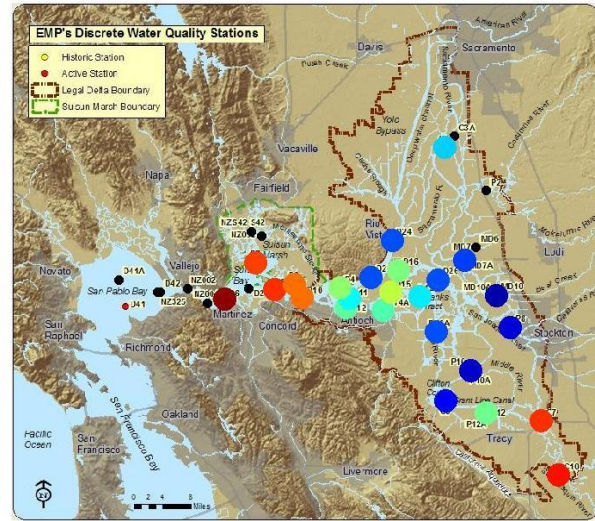
High-Flow Calibrated Model EMP Comparison Plots

17 Sep 1987

EMP Data

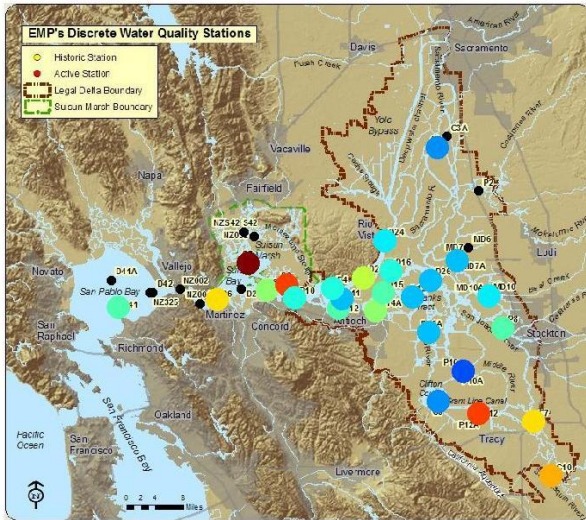


RMA11 Data



15 Oct 1987

EMP Data



RMA11 Data

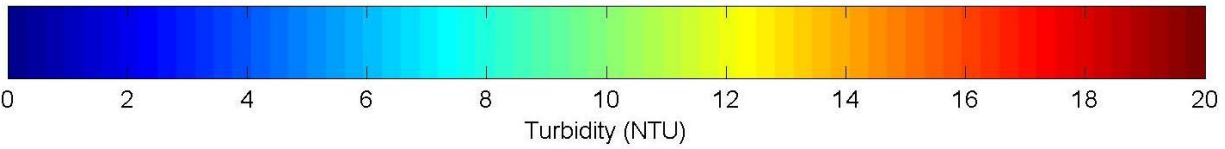
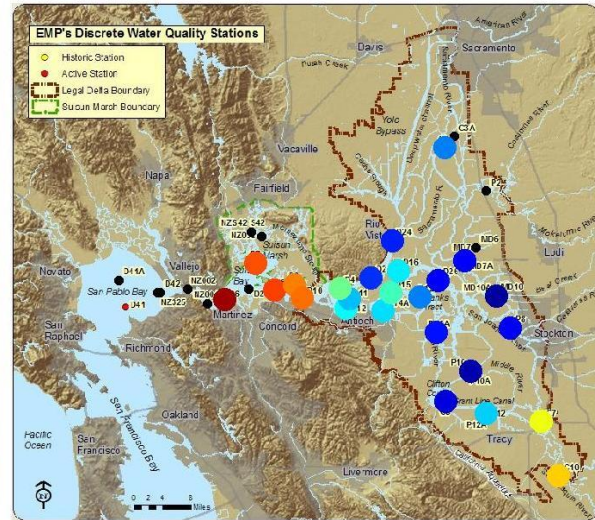
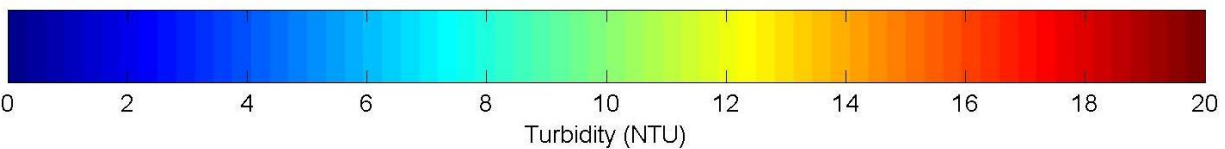
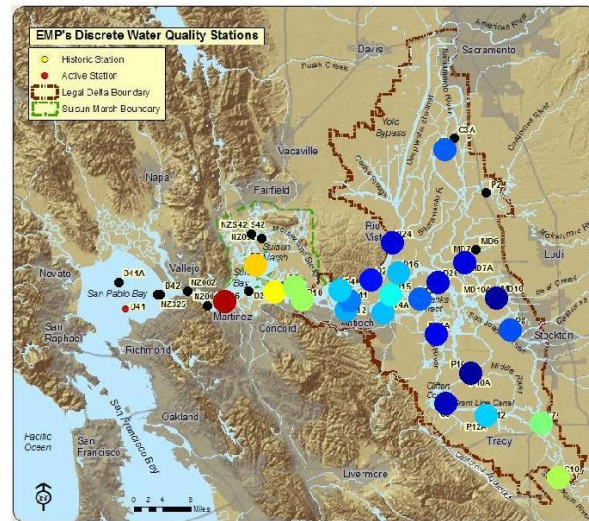
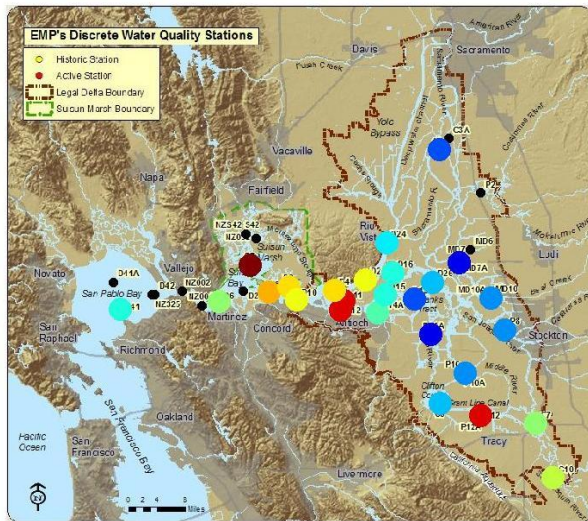


Figure 62 Turbidity distributions measured by the EMP (left panels) and modeled by RMA (right panels) for September (top panels) and October (bottom panels), WY1988. High-flow calibrated turbidity decay coefficients were used.

19 Nov 1987

EMP Data

RMA11 Data



03 Dec 1987

EMP Data

RMA11 Data

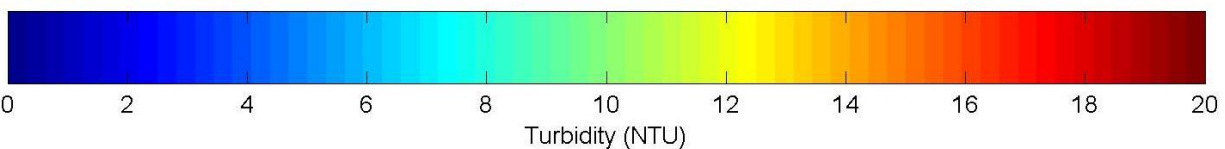
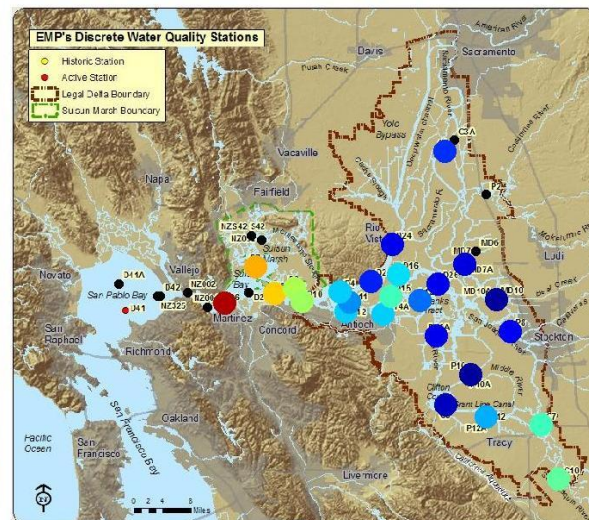
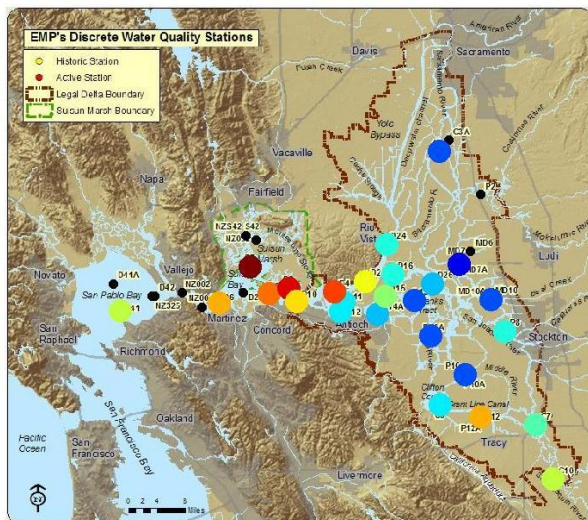
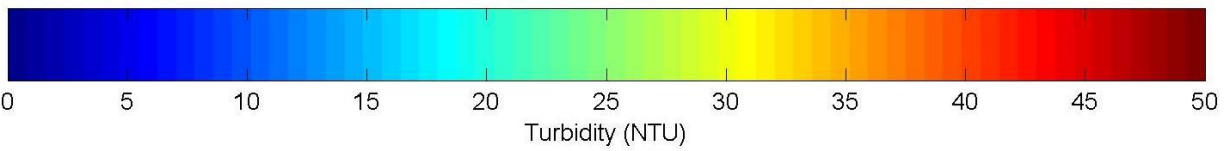
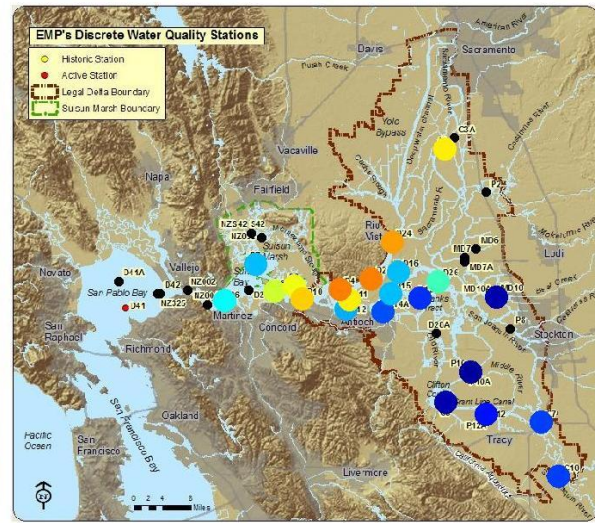
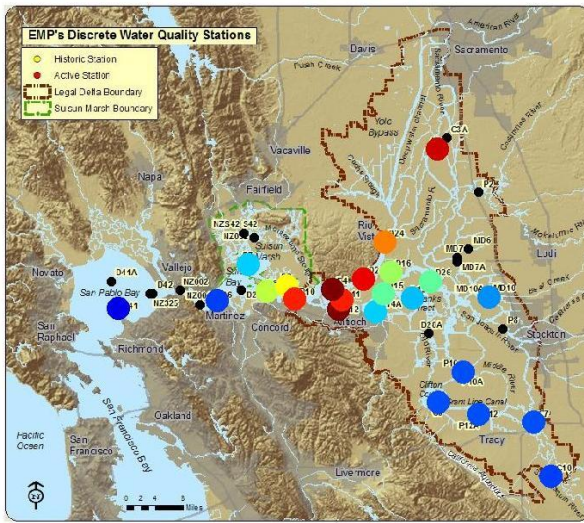


Figure 63 Turbidity distributions measured by the EMP (left panels) and modeled by RMA (right panels) for November (top panels) and December (bottom panels), WY1988. High-flow calibrated turbidity decay coefficients were used.

13 Jan 1988

EMP Data

RMA11 Data



26 Feb 1988

EMP Data

RMA11 Data

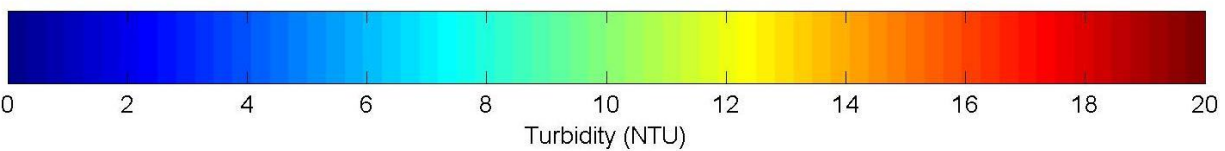
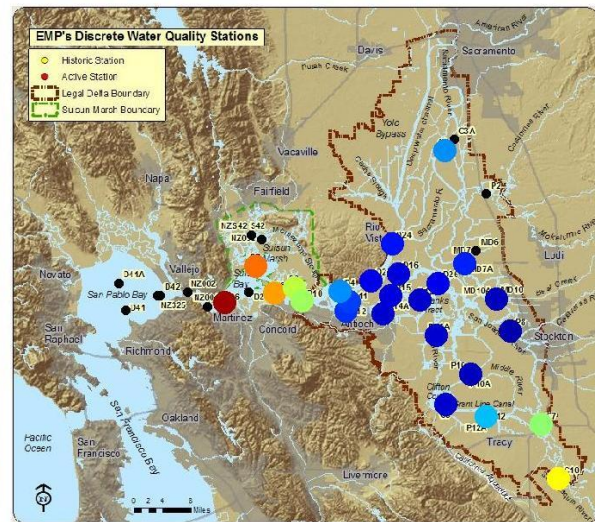
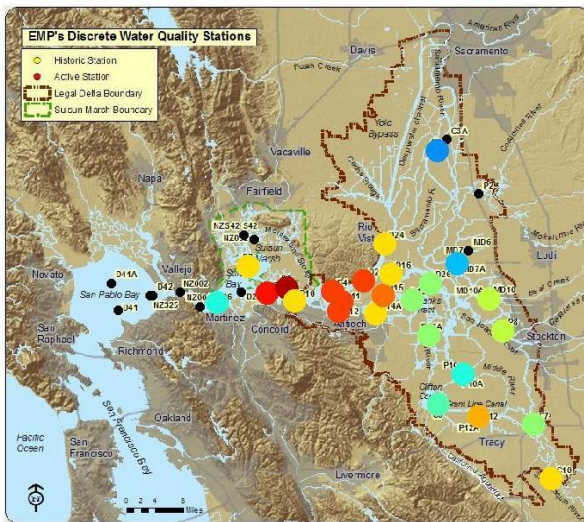
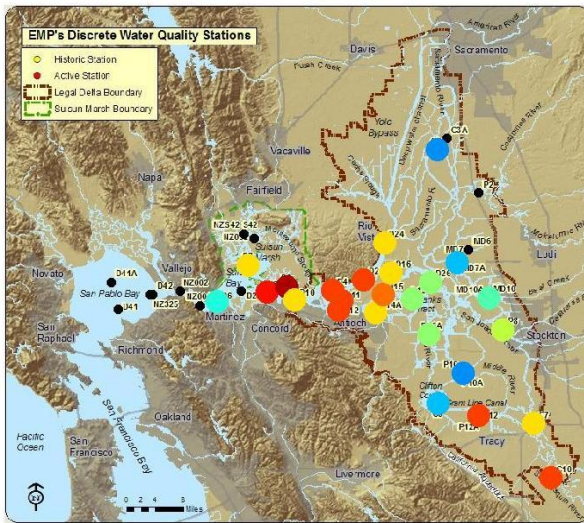


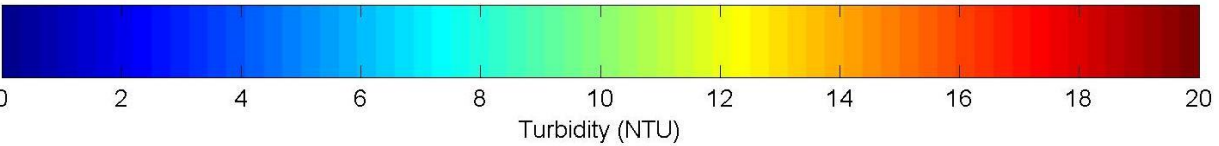
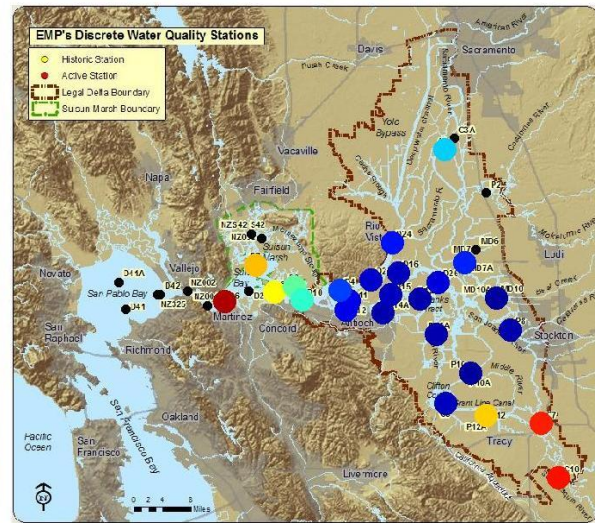
Figure 64 Turbidity distributions measured by the EMP (left panels) and modeled by RMA (right panels) for January (top panels) and February (bottom panels), WY1988. Note difference in color scales between top and bottom plots. High-flow calibrated turbidity decay coefficients were used.

11 Mar 1988

EMP Data

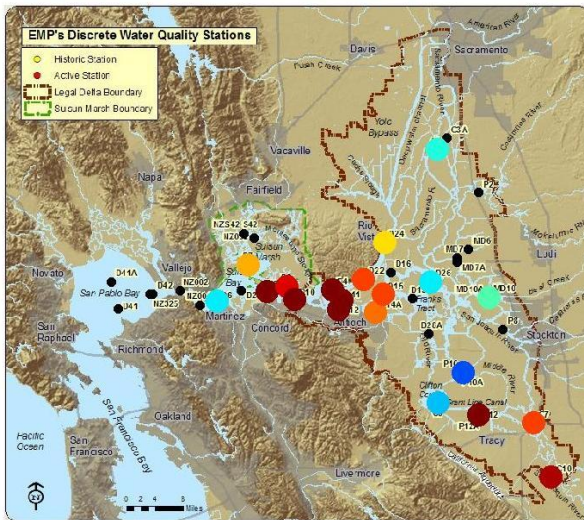


RMA11 Data



08 Apr 1988

EMP Data



RMA11 Data

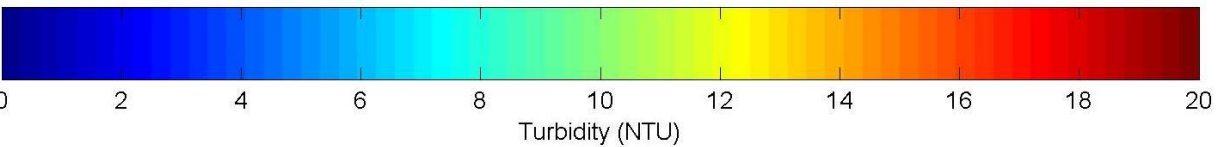
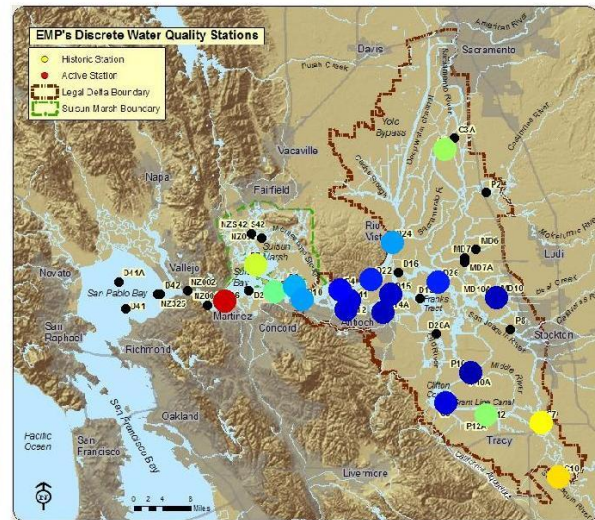


Figure 65 Turbidity distributions measured by the EMP (left panels) and modeled by RMA (right panels) for March (top panels) and April (bottom panels), WY1988. High-flow calibrated turbidity decay coefficients were used.

FMWT Smelt Distributions

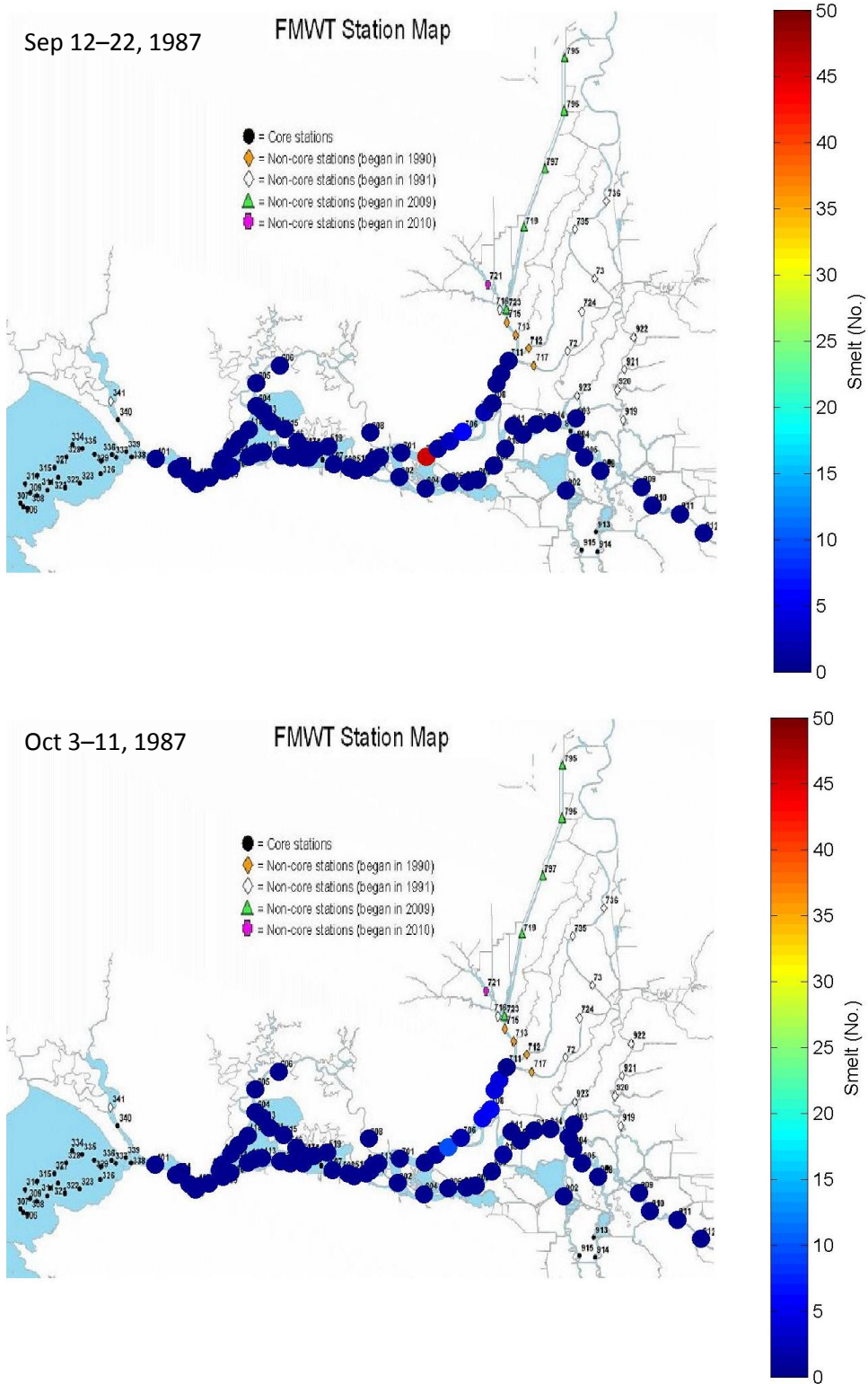


Figure 66 September and October 1987 FMWT ADS catch distributions. Dates indicate range of days catch was made over.

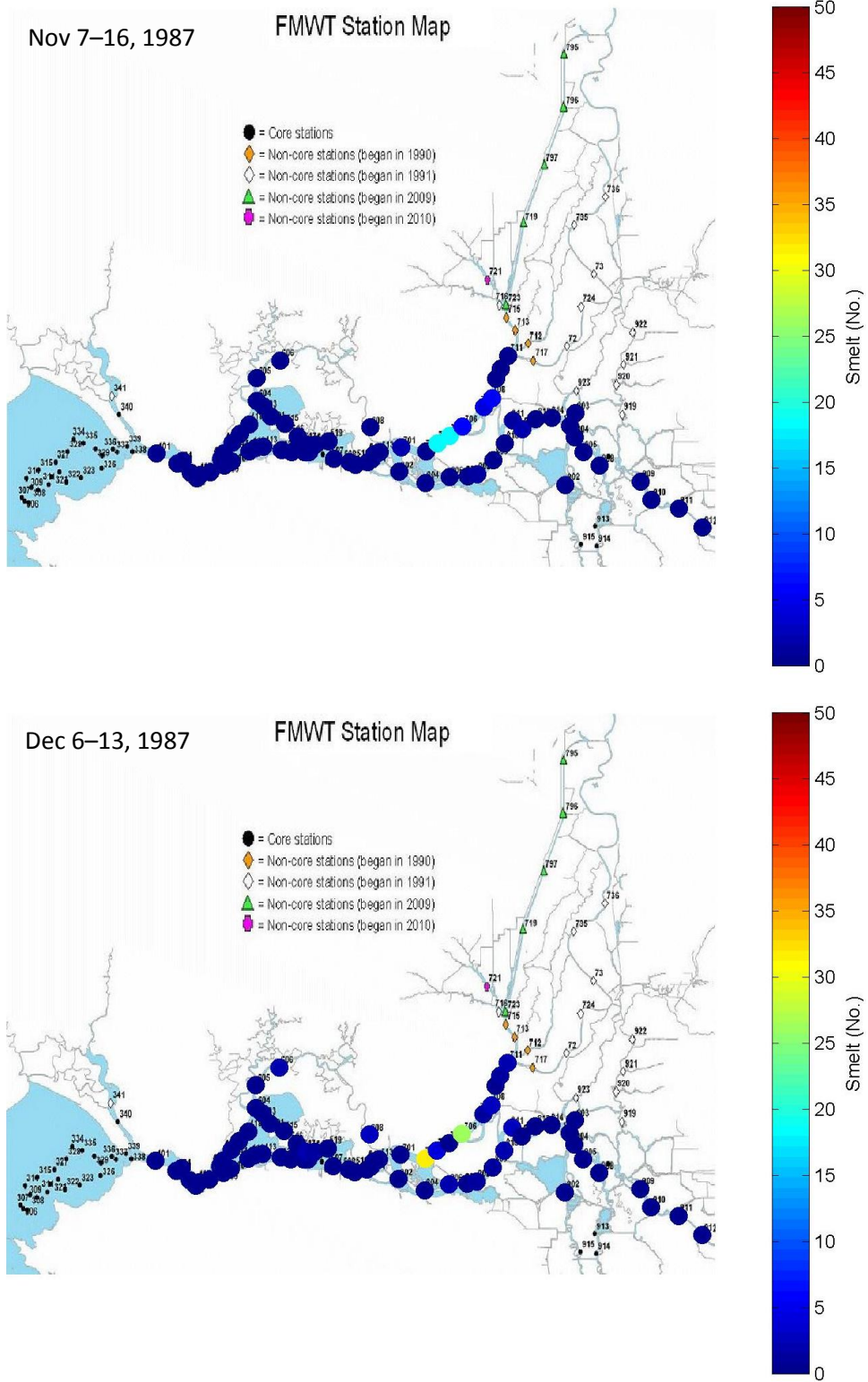


Figure 67 November and December 1987 FMWT ADS catch distributions. Dates indicate range of days catch was made over.

Original Model Calibration RMA PTRK Modeled Smelt Distributions

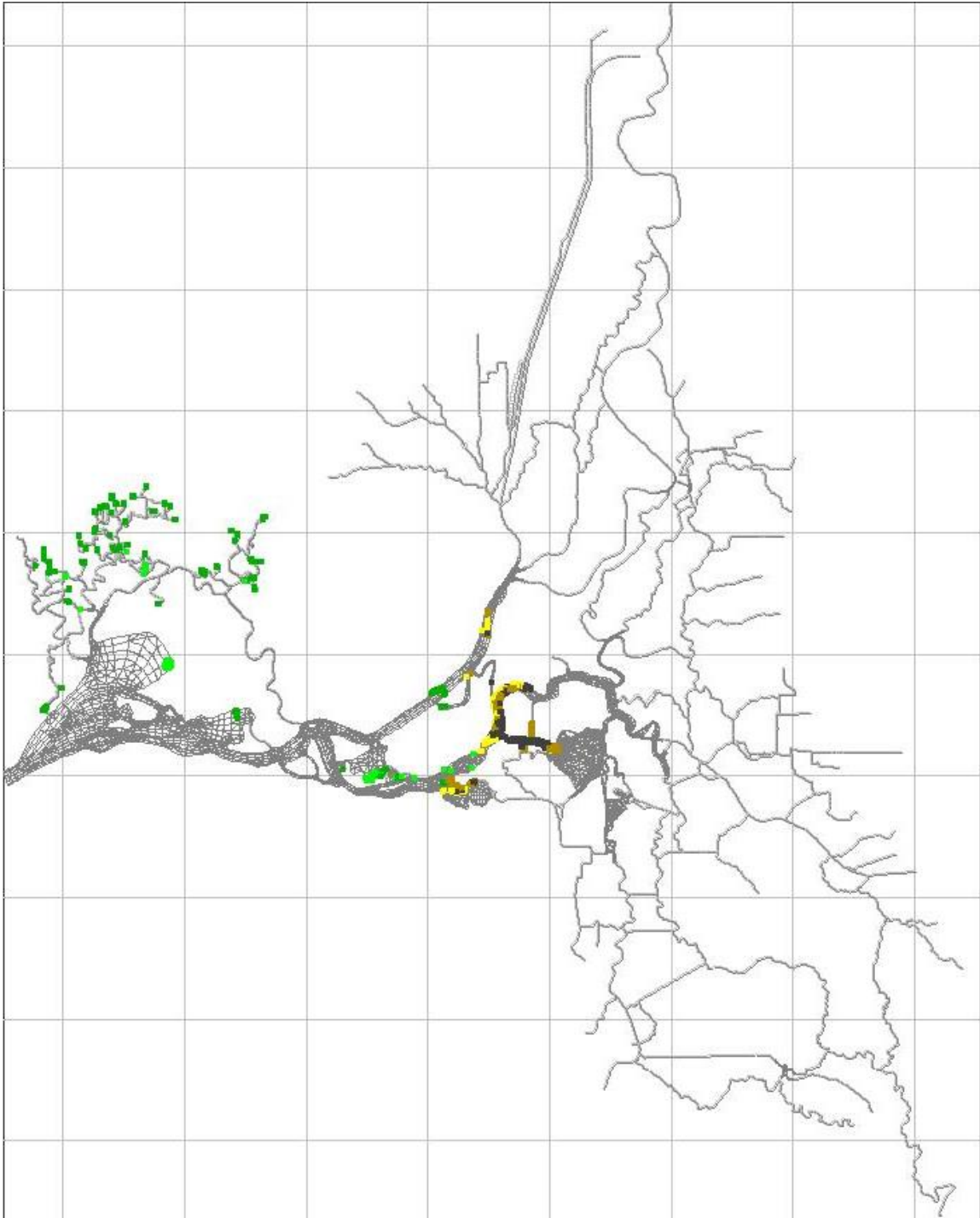


Figure 68 RMA PTRK modeled smelt distribution, November 1, 1987. For behavioral color codes, see Figure 29. Model results were driven using a smelt turbidity minimum threshold of 16 NTU and turbidity model results obtained with high-flow calibrated parameters.

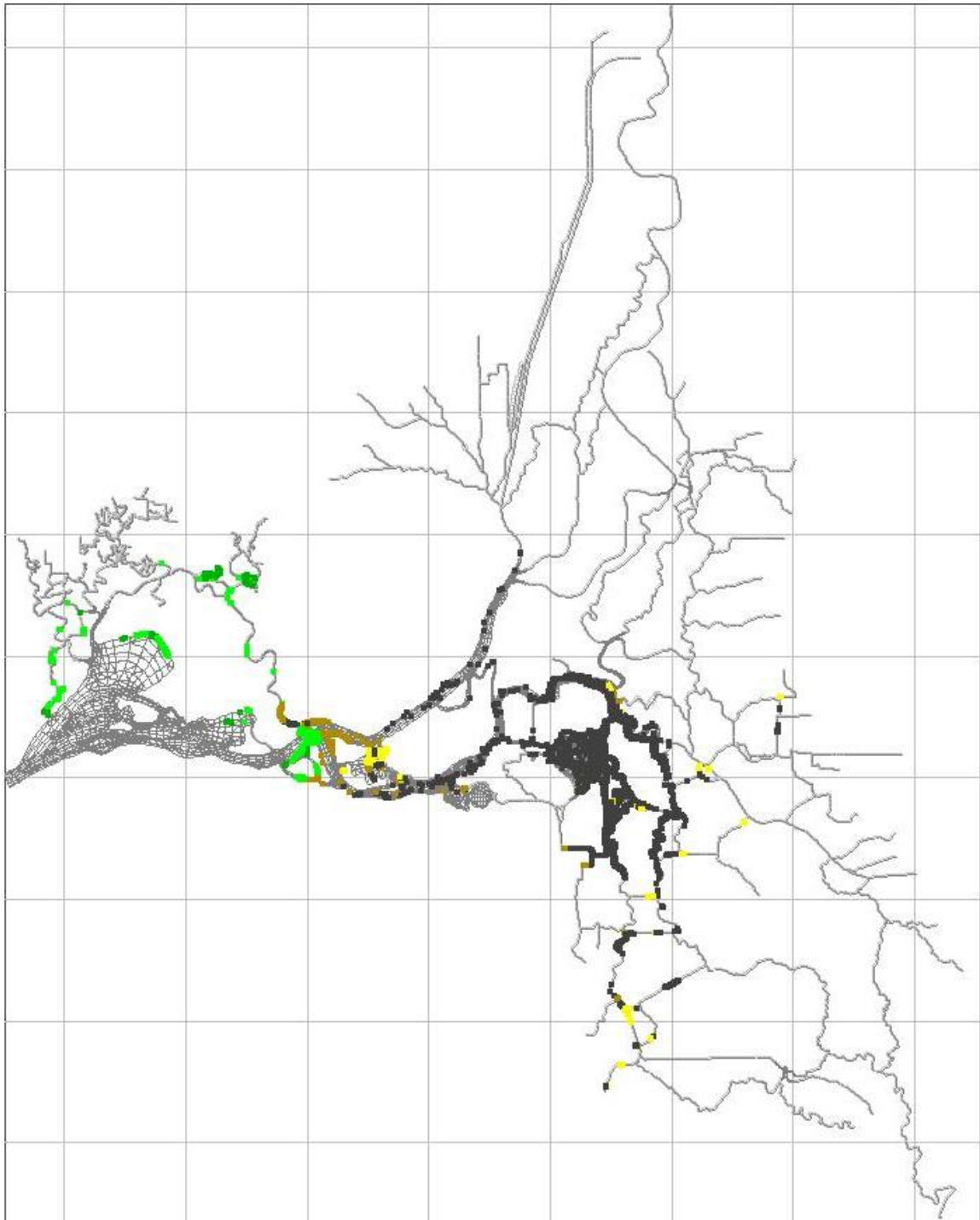


Figure 69 RMA PTRK modeled smelt distribution, January 1, 1988. For behavioral color codes, see Figure 29. Model results were driven using a smelt turbidity minimum threshold of 16 NTU and turbidity model results obtained with high-flow calibrated parameters.

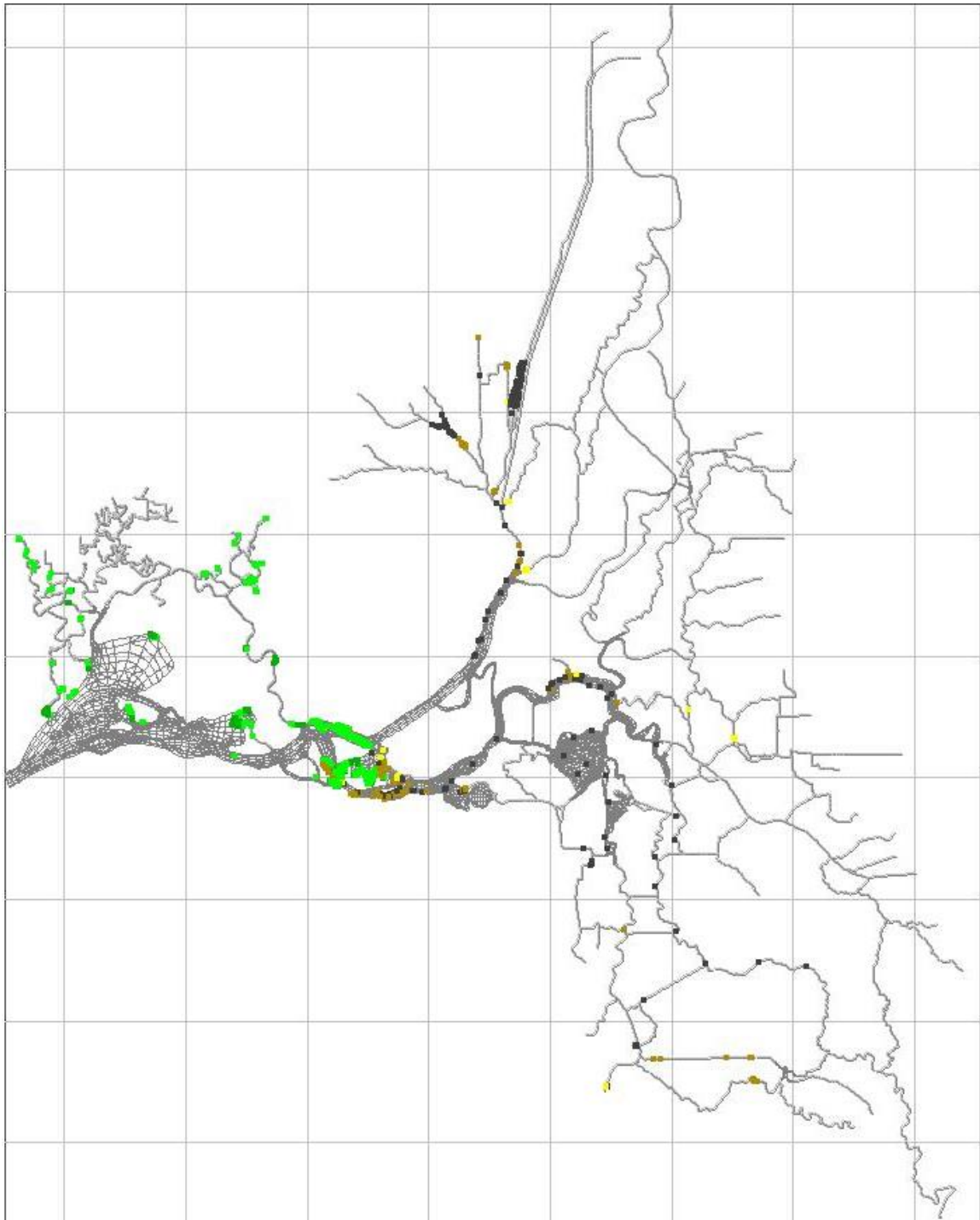


Figure 70 RMA PTRK modeled smelt distribution, March 1, 1988. For behavioral color codes, see Figure 29. Model results were driven using a smelt turbidity minimum threshold of 16 NTU and turbidity model results obtained with high-flow calibrated parameters.

Time Variable Decay Coefficient Smelt and Turbidity Model Summary Results

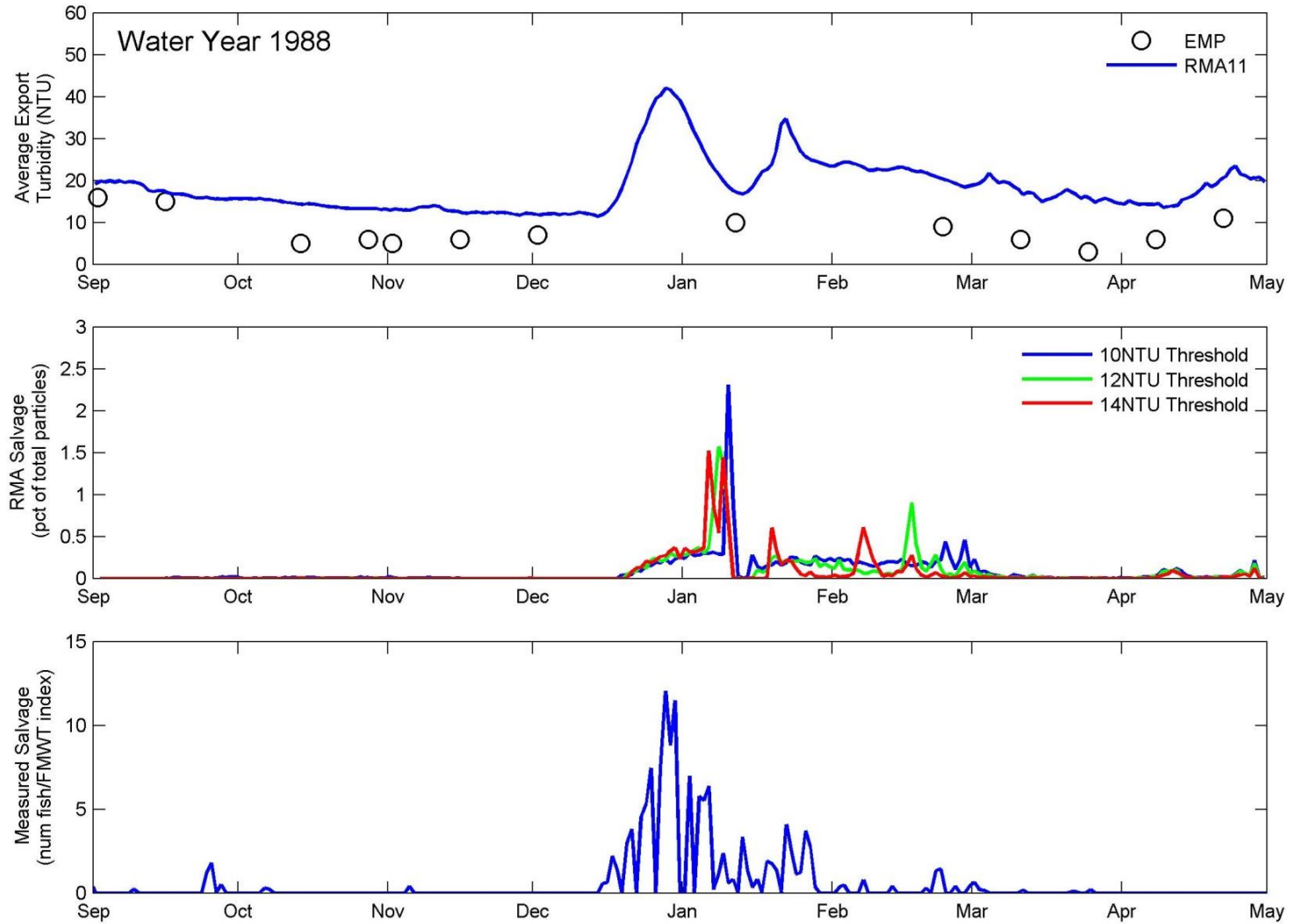


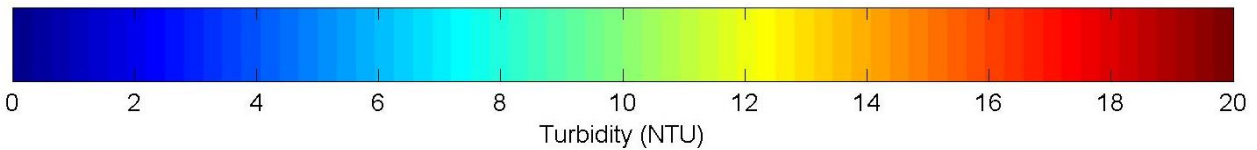
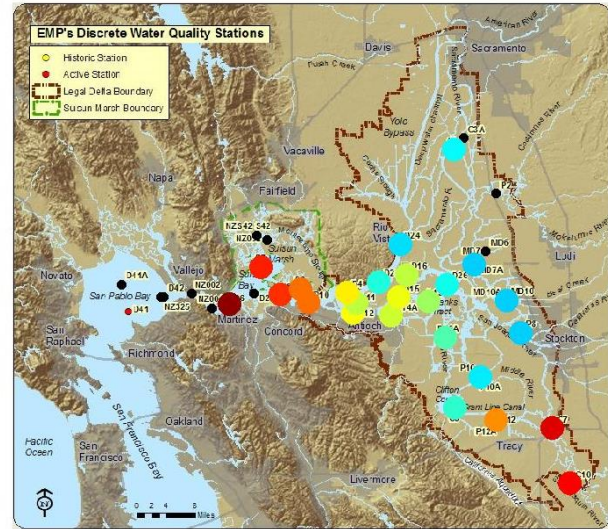
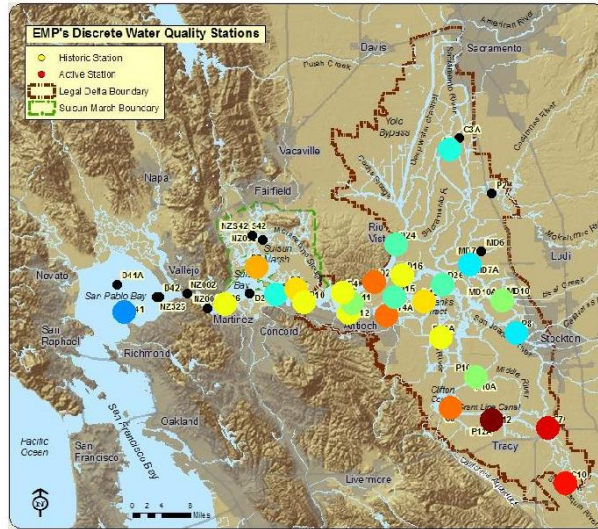
Figure 71 WY1988 modeled and observed turbidity and delta smelt salvage at the southern export locations. Time variable turbidity decay coefficients were used. Top panel shows average modeled turbidity at the export locations along with EMP observed data. Middle panel shows RMA modeled smelt salvage (as a percent of total input particles) using three different max turbidity threshold values. Bottom panel shows observed smelt salvage as number of fish divided by the water year FMWT index (a measure of the total smelt population size).

Time Variable Decay Coefficient Model EMP Turbidity Comparison Plots

17 Sep 1987

EMP Data

RMA11 Data



15 Oct 1987

EMP Data

RMA11 Data

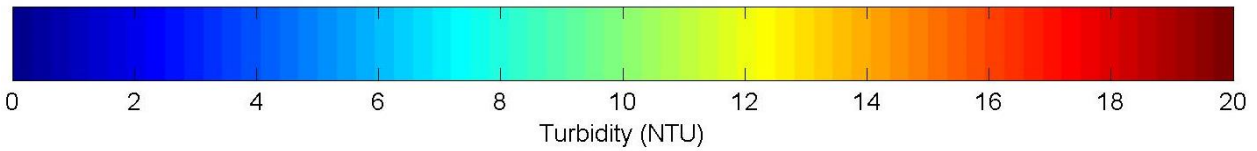
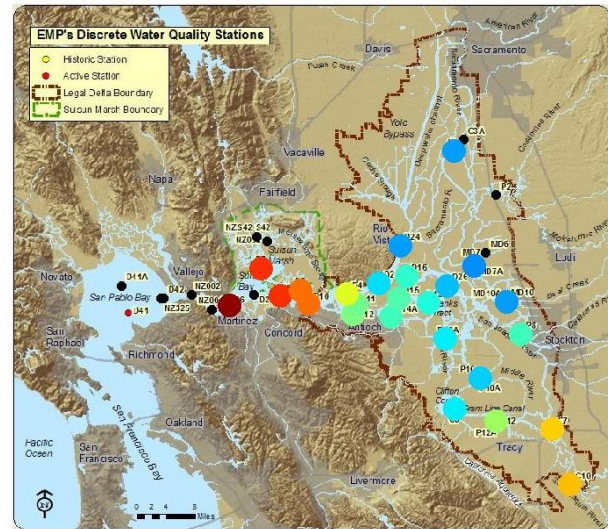
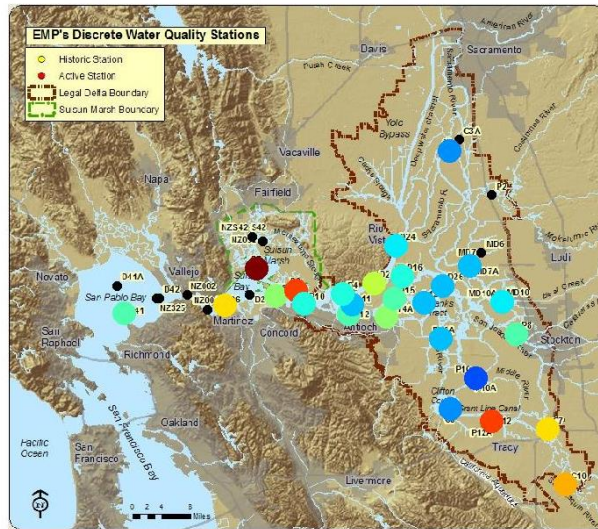
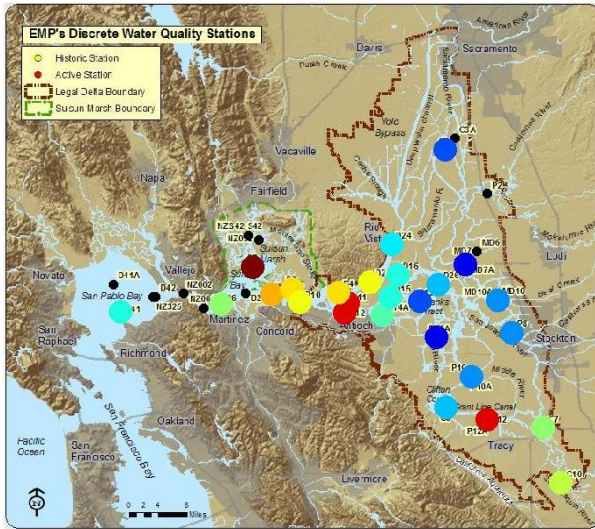


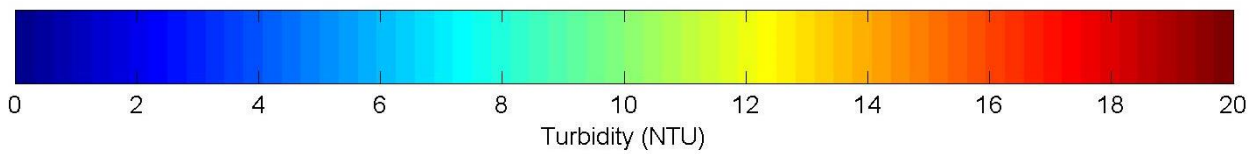
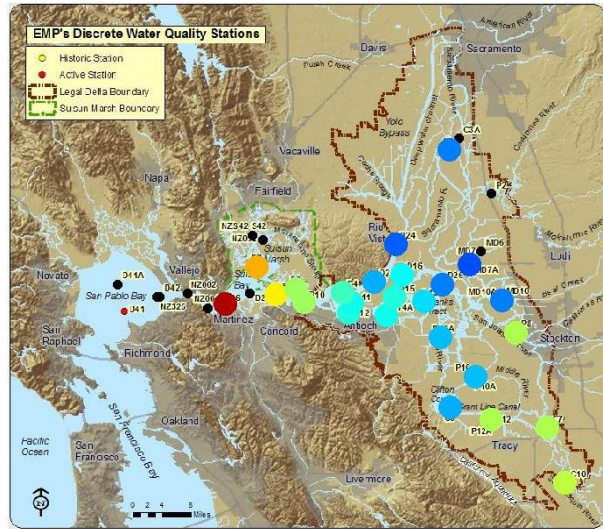
Figure 72 Turbidity distributions measured by the EMP (left panels) and modeled by RMA (right panels) for September (top panels) and October (bottom panels), WY1988. Time variable turbidity decay coefficients were used.

19 Nov 1987

EMP Data

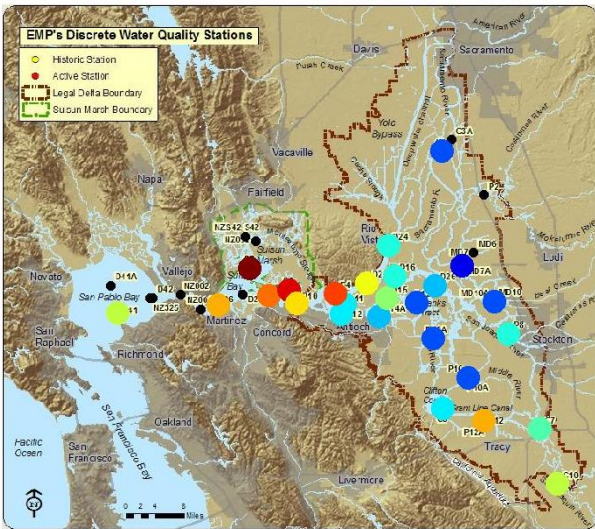


RMA11 Data



03 Dec 1987

EMP Data



RMA11 Data

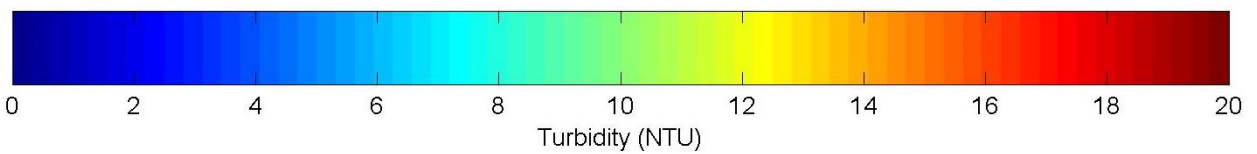
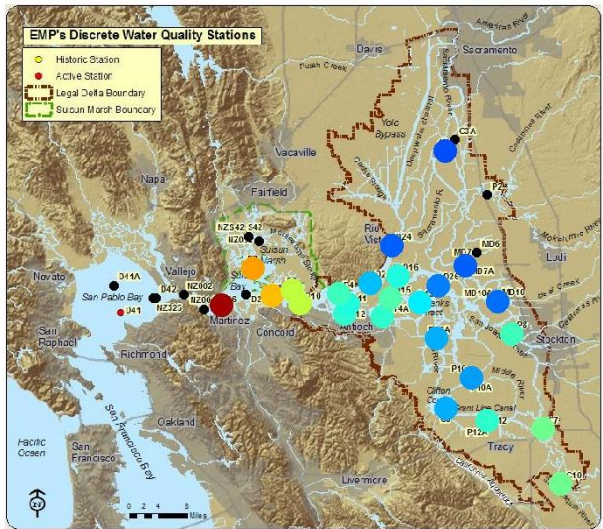
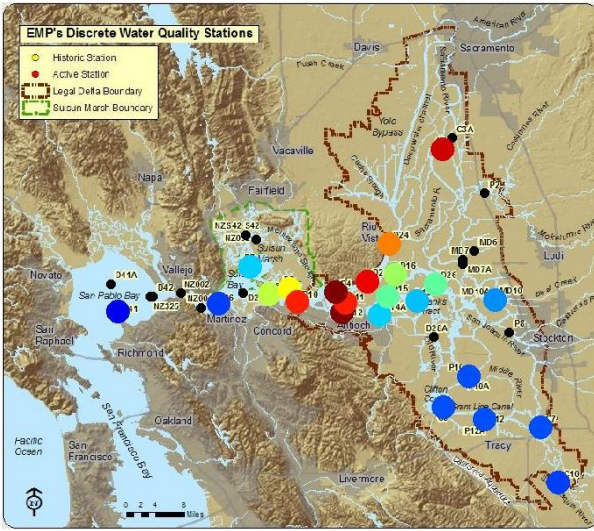


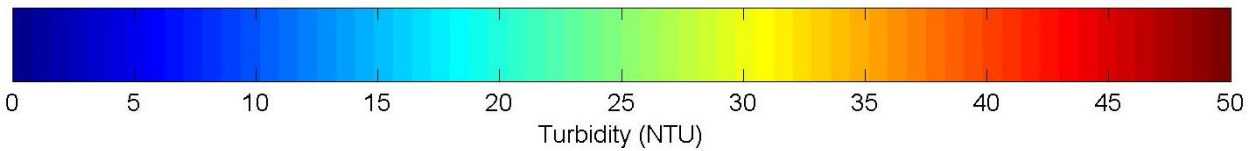
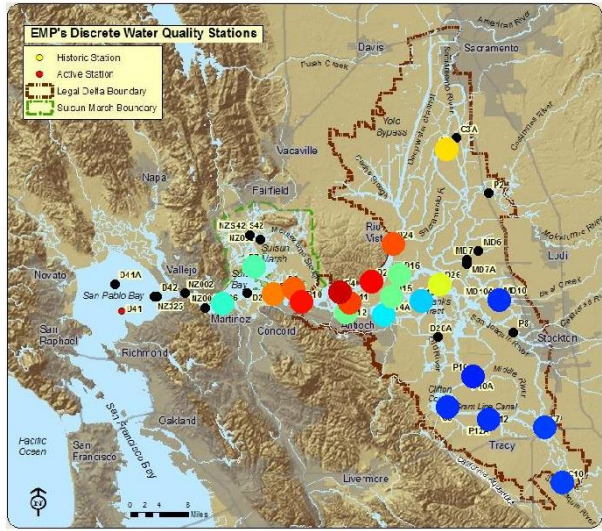
Figure 73 Turbidity distributions measured by the EMP (left panels) and modeled by RMA (right panels) for November (top panels) and December (bottom panels), WY1988. Time variable turbidity decay coefficients were used.

13 Jan 1988

EMP Data

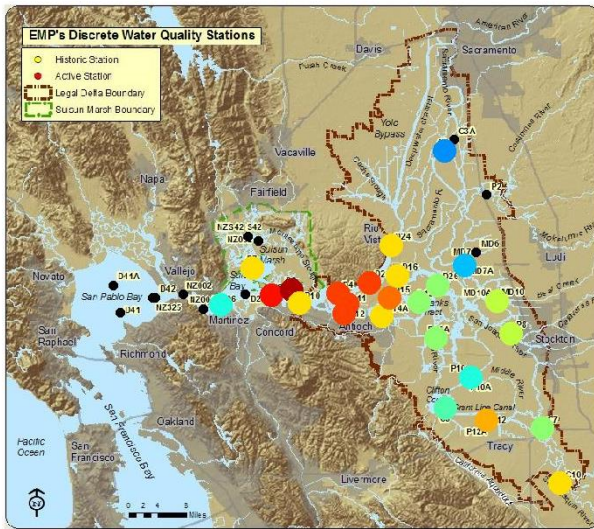


RMA11 Data



26 Feb 1988

EMP Data



RMA11 Data

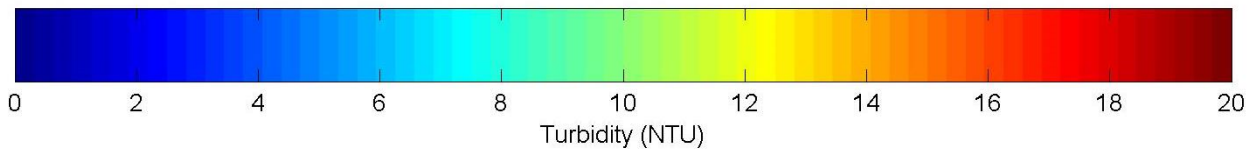
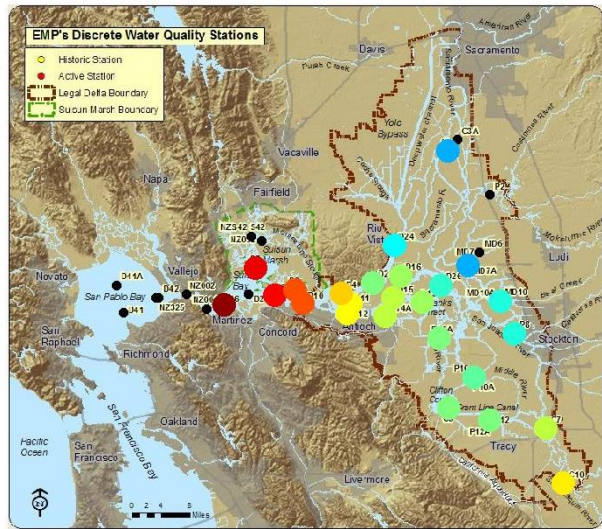
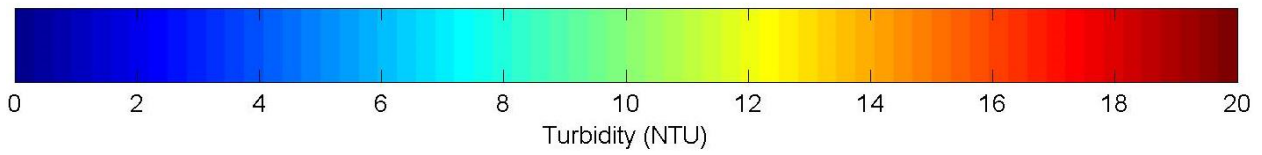
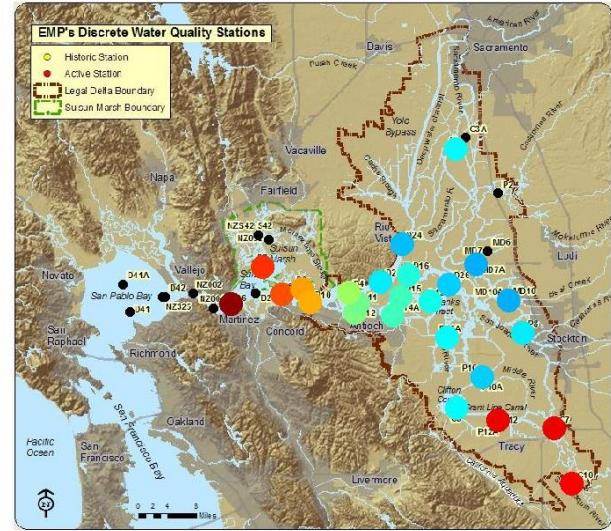
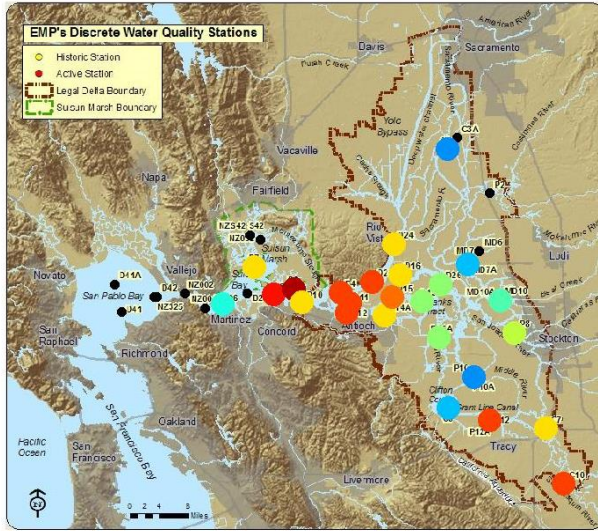


Figure 74 Turbidity distributions measured by the EMP (left panels) and modeled by RMA (right panels) for January (top panels) and February (bottom panels), WY1988. Note difference in color scales between top and bottom plots. Time variable turbidity decay coefficients were used.

11 Mar 1988

EMP Data

RMA11 Data



08 Apr 1988

EMP Data

RMA11 Data

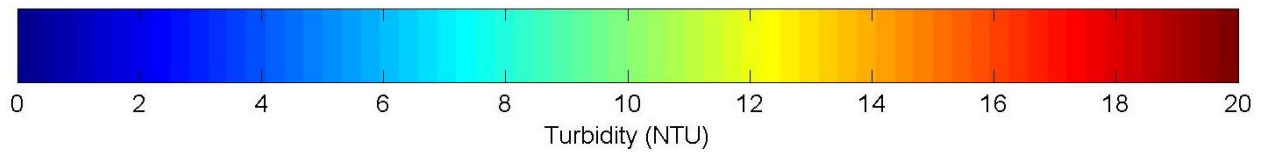
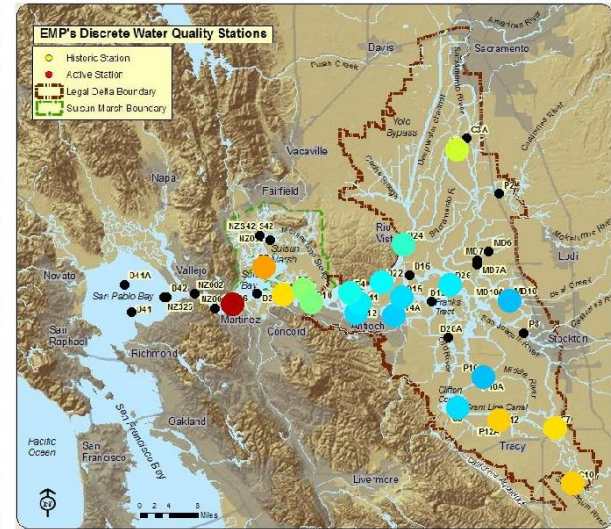
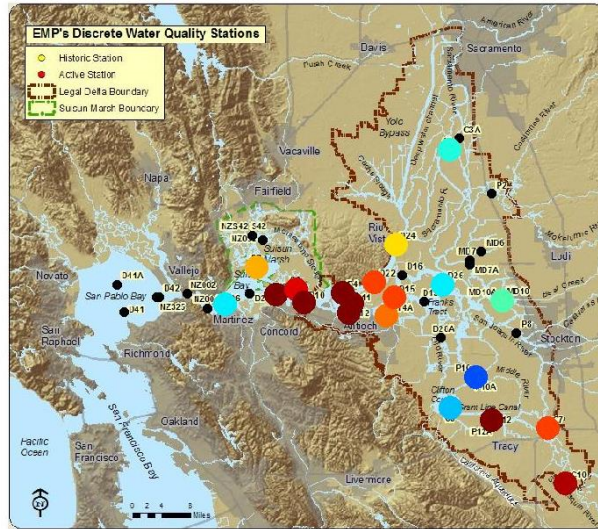


Figure 75 Turbidity distributions measured by the EMP (left panels) and modeled by RMA (right panels) for March (top panels) and April (bottom panels), WY1988. Time variable turbidity decay coefficients were used.

Time Variable Turbidity Decay RMA PTRK Modeled Smelt Distributions

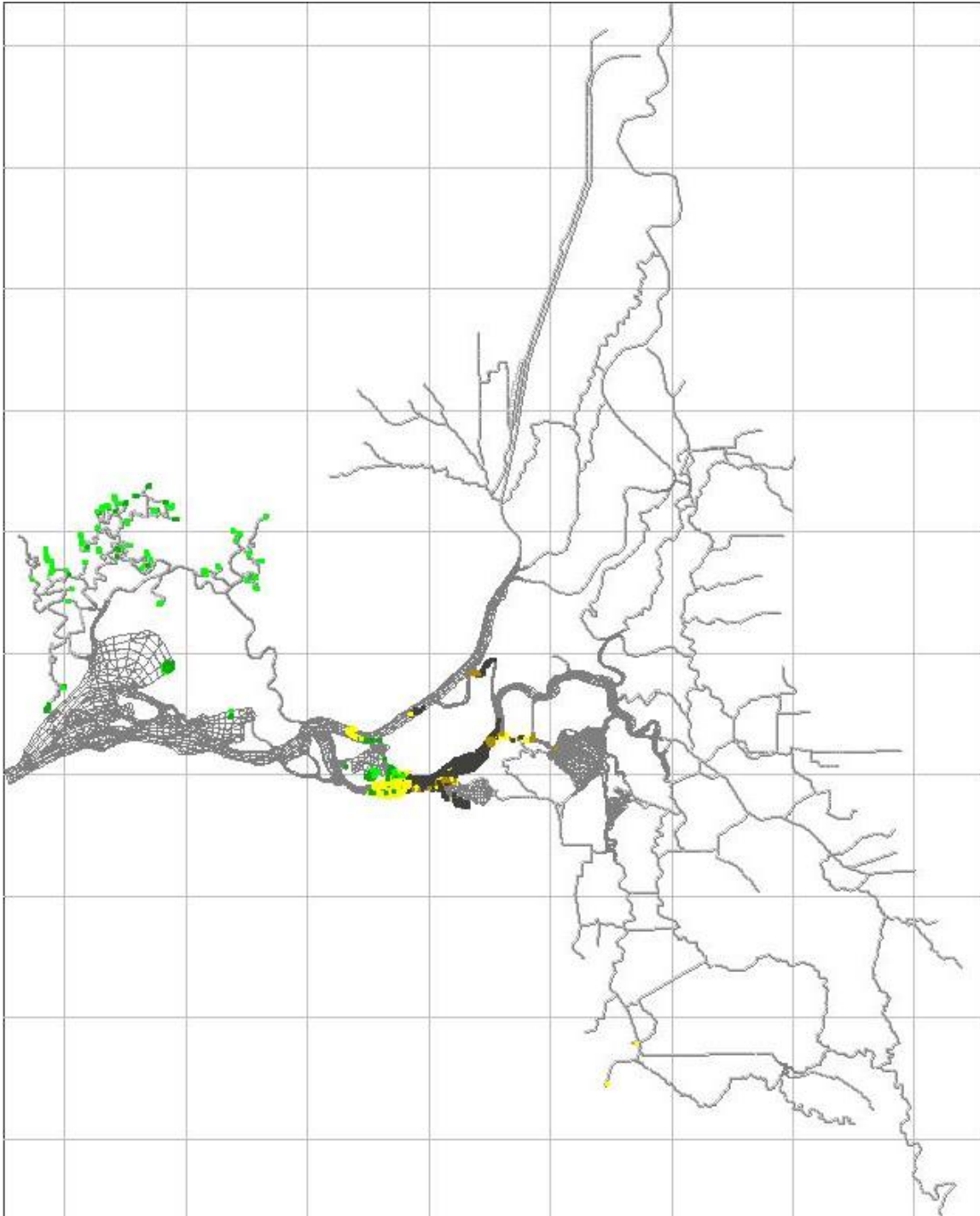


Figure 76 RMA PTRK modeled smelt distribution, November 1, 1987. For behavioral color codes, see Figure 29. Model results were driven using a smelt turbidity minimum threshold of 12 NTU and turbidity model results obtained with time variable decay coefficients. Similar distributions were produced using 10 and 14 NTU thresholds.

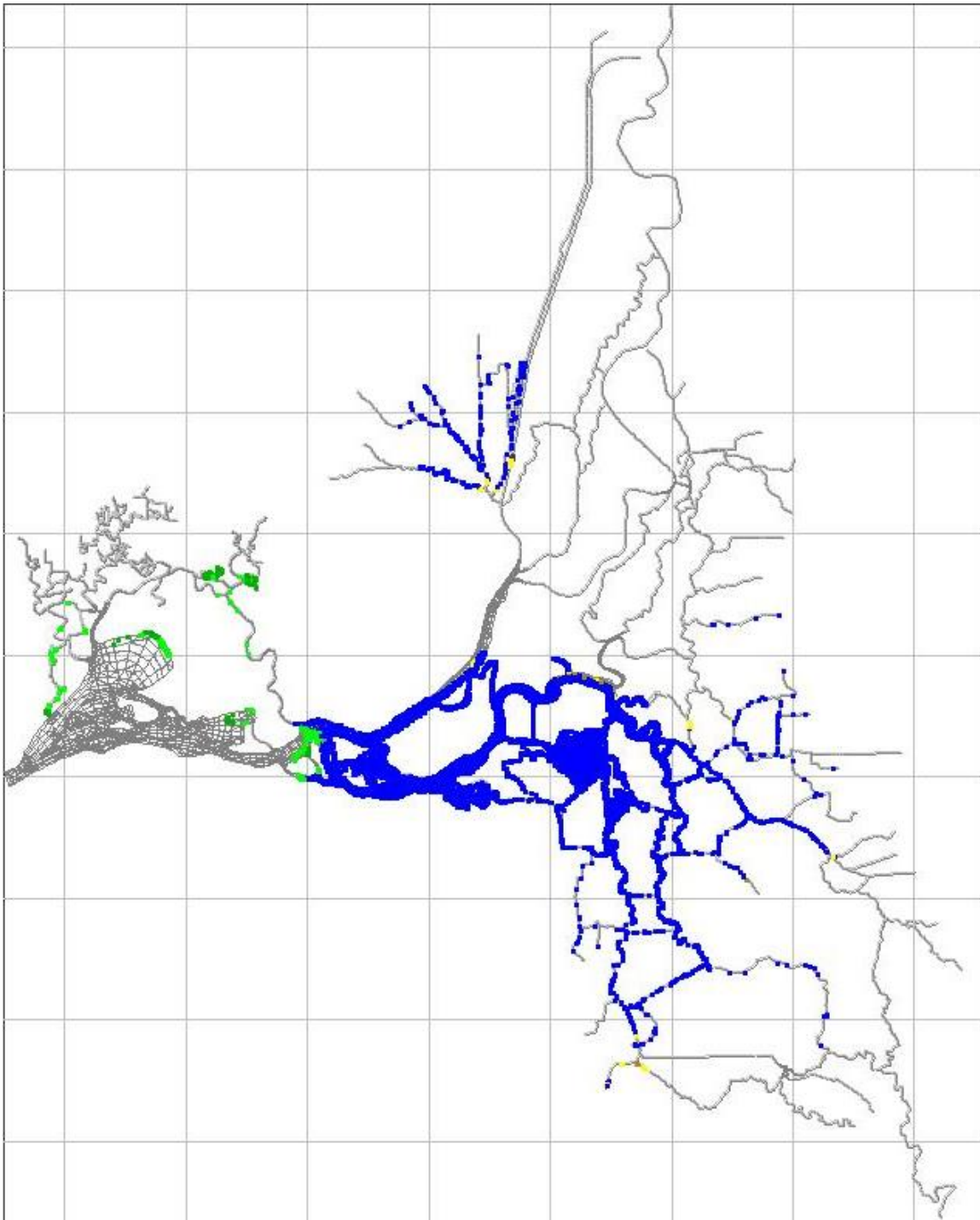


Figure 77 RMA PTRK modeled smelt distribution, January 1, 1988. For behavioral color codes, see Figure 29. Model results were driven using a smelt turbidity minimum threshold of 12 NTU and turbidity model results obtained with time variable decay coefficients. Similar distributions were produced using 10 and 14 NTU thresholds.

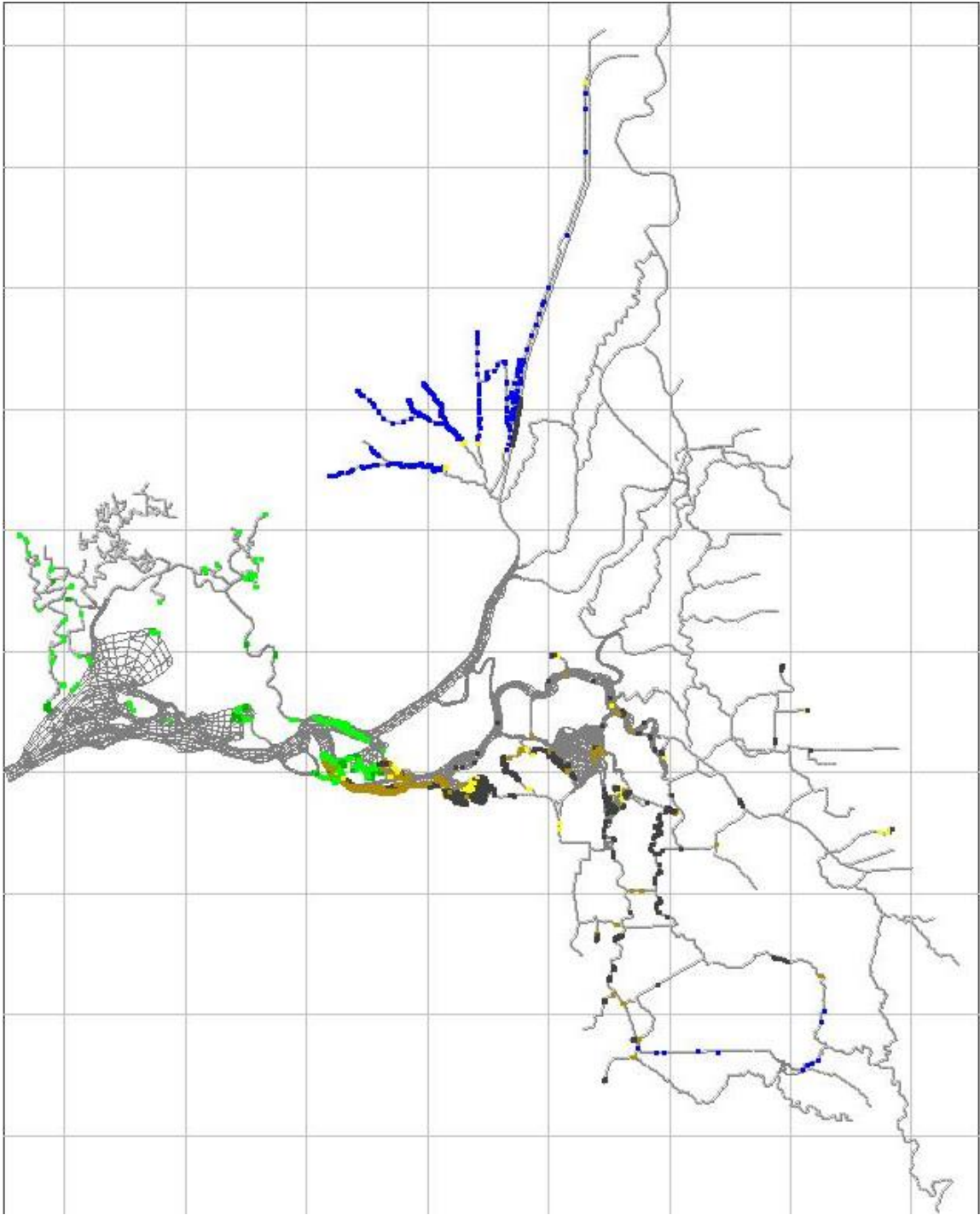


Figure 78 RMA PTRK modeled smelt distribution, March 1, 1988. For behavioral color codes, see Figure 29. Model results were driven using a smelt turbidity minimum threshold of 12 NTU and turbidity model results obtained with time variable decay coefficients. Similar distributions were produced using 10 and 14 NTU thresholds.

Conclusions

- Modeled smelt migratory movement and salvage patterns at the southern export locations are very sensitive to the modeled turbidity fields. This is especially true through the central Delta where turbidities are often near behavioral thresholds (10–16 NTU).
- There is a lot of uncertainty associated with modeling turbidity in historical water years where observed turbidity data is sparse.
- The decay coefficient approach to modeling turbidity is sufficient for high flows and works well for predicting salvage patterns in water years with well-defined first flush events. However, it does not perform as well during complex hydrological time periods, where turbidities in the central Delta are affected by resuspension during low-flow and periodic storm events.
- Fall salvage events in WY1981 and WY1982 appear to be disconnected from the high turbidities in the south central Delta needed to drive smelt migration from the confluence area toward the south Delta. These salvage patterns may either be due to errors in the facility identification, counting, or reporting procedures, or may be a result of incorrect smelt behavioral model assumptions.
- When turbidity and smelt model coefficients from previous calibration efforts were used, model predicted salvage at the export locations matched observed patterns in only one out of the three years tested. Updates to the model coefficients to account for time-variable turbidity decay constants and lower minimum smelt turbidity thresholds improved model fit in all three years.
- In spite of the difficulties associated with modeling smelt movement in these historic water years, the model reproduced observed salvage data reasonably well in water years 1982 and 1988. The model did not perform as well in water year 1981.

References

- California Department of Water Resources (DWR). 2009. "Flood Management." Appendix A in California Water Plan Update 2009, Volume 3: Regional Report for Sacramento-San Joaquin Region.
- Merz, J.E., Hamilton S., Bergman P.S, and B. Cavallo. 2011. Spatial perspective for delta smelt: a summary of contemporary survey data. *California Fish and Game*, 97(4):164–189.
- Resource Management Associates (RMA). 2005. "Flooded Islands Pre-Feasibility Study: RMA Delta Model Calibration." Technical Report prepared for CA Department of Water Resources.
- Resource Management Associates (RMA). 2008. "San Francisco Bay-Delta Turbidity Modeling." Technical Report prepared for Metropolitan Water District of Southern California.
- Resource Management Associates (RMA). 2009. "Particle Tracking and Analysis of Adult and Larval/Juvenile Delta Smelt for 2-Gates Demonstration Project." Technical Report prepared for Metropolitan Water District of Southern California.
- Resource Management Associates (RMA). 2010. "Turbidity and Adult Delta Smelt Forecasting with RMA 2-D Models: December 2009 – May 2010." Technical Report prepared for Metropolitan Water District of Southern California.
- Resource Management Associates (RMA). 2011a. "Turbidity and Adult Delta Smelt Modeling with RMA 2-D Models: December 2010 – February 2011." Technical Report prepared for Metropolitan Water District of Southern California.
- Resource Management Associates (RMA). 2011b. "Turbidity and Adult Delta Smelt Modeling with the RMA Delta Models: Simulations for Water Years 2002, 2004, 2008 and 2009." Technical Report prepared for Metropolitan Water District of Southern California.
- Resource Management Associates (RMA). 2012. "Turbidity and Adult Delta Smelt Modeling with RMA 2-D Models: November 2011 – February 2012." Technical Report prepared for Metropolitan Water District of Southern California.
- Sommer, T., Mejia, F., Nobriga, M., Feyrer, F., and L. Grimaldo. 2011. The spawning migration of delta smelt in the Upper San Francisco Estuary. *San Francisco Estuary and Watershed Science*, 9(2). <http://www.escholarship.org/uc/item/86m0g5sz>
- United States Bureau of Reclamation (USBR), Mid-Pacific Region. 2008. Basic biology and life history of delta smelt and factors that may influence delta smelt distribution and abundance. Chapter 7 in *Biological Assessment on the Continued Long-term Operations of the Central Valley Project and the State Water Project*. Sacramento, CA.